Pontificia Universidad Católica de Chile
Facultad de Medicina
Doctorado en Neurociencia

Tesis Doctoral

INTRINSIC CORTICAL DYNAMICS IN THE HIPPOCAMPUS-PFC SYSTEM AND SOCIAL INTERACTIONS DURING COLLECTIVE NAVIGATION IN A DECISION-MAKING TASK

Por

ARIEL FERNANDO LARA VÁSQUEZ

Julio 2020

Pontificia Universidad Católica de Chile
Facultad de Medicina
Doctorado en Neurociencia

Tesis Doctoral

INTRINSIC CORTICAL DYNAMICS IN THE HIPPOCAMPUS-PFC SYSTEM AND SOCIAL INTERACTIONS DURING COLLECTIVE NAVIGATION IN A DECISION-MAKING TASK

Tesis presentada a la Pontificia Universidad Católica de Chile como parte de los requisitos para optar al grado de Doctor en Neurociencias

Por

ARIEL FERNANDO LARA VÁSQUEZ

Director de Tesis: Pablo Fuentealba D.
Codirector de Tesis: Pablo Billeke B.
Comisión de Tesis: Diego Cosmelli S.
Jaime Campusano A.
Pablo Henny V.
Rodrigo Vásquez S.

PONTIFICIA UNIVERSIDAD CATÓLICA DE CHILE
Doctorado en Neurociencia

El Comité de Tesis, constituido por los Profesores abajo firmantes, aprueba la Defensa Pública de la Tesis Doctoral titulada:

"Intrinsic cortical dynamics in the hippocampus-PFC system and social interactions during collective navigation in a decision-making task"

Aprobación Defensa:
ARIEL FERNANDO LARA VASQUEZ
Calificándose el trabajo realizado, el manuscrito sometido y la defensa oral, con nota

(……..)

Dr. Felipe Heusser
Decano
Escuela de Medicina
Pontificia Universidad Católica de Chile

Dr. Mauricio Cuello
Director de Investigación y Doctorado
Facultad de Medicina
Pontificia Universidad Católica de Chile

Dra. Claudia Sáez
Sub-directora
Dirección de Investigación y Doctorado
Escuela de Medicina
Pontificia Universidad Católica de Chile

Dr. Francisco Aboitiz
Jefe Programa Doctorado en Neurociencias
Centro Interdisciplinario de Neurociencias
Facultad de Medicina
Pontificia Universidad Católica de Chile

Dr. Pablo Fuentealba
Director de Tesis
Escuela de Medicina
Pontificia Universidad Católica de Chile

Dr. Pablo Billeke
Codirector de Tesis
Escuela de Medicina
Universidad del Desarrollo

Dr. Diego Cosmelli
Profesor Evaluador Interno
Escuela de Psicología
Pontificia Universidad Católica de Chile

Dr. Jaime Campusano
Profesor Evaluador Interno
Facultad de Ciencias Biológicas
Pontificia Universidad Católica de Chile

Dr. Pablo Henny
Profesor Evaluador Interno
Facultad de Medicina
Pontificia Universidad Católica de Chile

Dr. Rodrigo Vasquez
Profesor Evaluador Externo
Facultad de Ciencias
Universidad de Chile

Santiago, 10 de septiembre 2020

In memory of my father

ACKNOWLEDGMENTS

I want to thank all the people involved in this work. First, I would like to express my sincere thanks to my supervisor, Dr. Pablo Fuentealba, for the opportunity to do science, also for his patience and help during my stay in his laboratory. I would also like to thank Nelson Espinosa, Cristian Morales, and Constanza Moran for being there to help me in behavioral experiments, technical support, and data analyses. The rest of the PF lab team members Gonzalo, Mauricio, and Trinidad for the daily discussions about contingency and science.

Equally important, I want to thank my co-supervisor, Dr. Pablo Billeke, for their vital help in the discussion and analysis during the thesis. Besides, I would like to thank the rest of my thesis committee: Prof. Diego Cosmelli, Prof. Jorge Campusano, Prof. Pablo Henny, and Prof. Rodrigo Vásquez for their comments and discussion. Each meeting helped me to improve this research.

I am very grateful to my funding, Vicerrectoría de Investigación and Colegio de Programas Doctorales of the Pontificia Universidad Catolica de Chile, and programa de apoyo a tesis doctoral, facultad de medicina, Pontificia Universidad Católica de Chile during all my PhD. To my friends from the Ph.D. program

I want to thank my family, brothers, and all my childhood friends. My parents Ana and Abraham, uncles Sonia and Jorge, and my grandparents Luis and María, who raised me and formed me into who I am.

Finally, I want to express my gratitude to my wife Anita and my son Agustín and my daughter Isidora, to make me happy and for their infinite patience and unconditional love that I receive every day.

TABLE OF CONTENTS

FUNDING

This work was supported by Fondecyt Regular grant 1190375; CONICYT, PIA Anillos ACT 1414, PIA Anillos ACT 172121 and PMD-03/17 of facultad de medicina, Pontificia Universidad Católica de Chile.

ANIMAL WELFARE

All experimental procedures related to animal experimentation are approved by the Institutional Animal Ethics Committee of the Pontificia Universidad Católica de Chile (protocol code: CEBA 150914003 and CEBA 151223006).

INDEX OF FIGURES

INDEX OF TABLES

Table 10. Multiple linear models for social (collective – individual) task latency (n = 21 animals used for electrophysiological experiments).

Table S1. P-values of linear regressions between pairs of neural and behavioral parameters.

Table S2. Univariate tests of significance for firing rate (n = 22 animals used for acute recordings).

Table S3. Summary of statistical tests per figure.

LIST OF ABBREVIATIONS

Abbreviations in the text:

ACC: anterior cingulate cortex

AID: dorsal agranular insular cortex

AIV: ventral agranular insular cortex

ASD: autism spectrum disorders

BLA: basolateral amygdala

CA: Cornu Ammonis areas

CA1: Cornu Ammonis area one

CA2: Cornu Ammonis area two

CA3: Cornu Ammonis area tree

Cg1: anterior cingulate cortex

dHIP: dorsal hippocampus area

dlPFC: dorsolateral prefrontal cortex

DRN: dorsal nuclei raphe

fMRI: functional magnetic resonance imaging

Hz: Hertz

IL: infralimbic cortex

LFP: local field potential

LC: locus coeruleus

LO: lateral orbital cortex

lPFC: lateral prefrontal cortex

MO: medial orbital cortex

mPFC: medial prefrontal cortex

ms: millisecond

NR: raphe nuclei

NAc: nucleus accumbens core area

OFC: orbitofrontal cortex

PAG: periaqueductal gray

PFC: prefrontal cortex

PL: prelimbic cortex

PrC: precentral cortex

rACC: anterior rostral cingulate cortex

REM: rapid eye movement

STC: superior temporal cortex

STS: superior temporal sulcus

SWM: spatial working memory

SWRs: sharp-wave ripples

SWS: slow-wave sleep

TPJ: temporoparietal junction

vHIP: ventral hippocampus area

VLO: ventral lateral orbital cortex

vlPFC: ventrolateral prefrontal cortex

VO: ventral orbital cortex

VTA: ventral tegmental area

ABSTRACT

Environmental sensory inputs and previously learned information to guide decision-making during complex behaviors such as foraging or navigation. Social mammals forage collectively, yet little is known about the influence of social interactions in decision-making during collective spatial navigation. To achieve efficient decision-making, social animals engaging in collective behavior must balance inherent and contingent factors, yet this process is not well understood. Here, I implemented a simplified spatial navigation task in rodents to assess the role of social interactions and found that they exert a powerful influence on individual decision-making. Indeed, instead of prioritizing memory-based pertinent information, mice shifted their decisions according to contingent social interactions arising during collective navigation. Dominance hierarchy, a form of a social ranking system, was an intrinsic social interaction relevant to organize the timing of behavior during collective navigation. Thus, individual task accuracy was dependent on the density of animals collectively moving during spatial navigation. Finally, dominance hierarchy correlated with brain-state specific coordinated activity expressed as larger hippocampal sharp-wave ripples associated with higher prefrontal firing rates, suggesting reinforced synaptic cortical coupling. These results suggest that both contingent and intrinsic social interactions modulate behavioral performance and are correlated with enhanced activity and connectivity patterns in the hippocampo-prefrontal circuit.

CHAPTER 1

INTRODUCTION

1.1. SOCIAL CONTEXT AND DECISION-MAKING

In our daily life, we tend to make decisions based on experience or the contingent information, and most of the decisions are influenced by various factors such as sex, age, and genotype (Crone and van der Molen, 2004; Van den Bos et al., 2013). Surprisingly, although everyday decisions are often strongly affected by the social environment and involve direct and indirect social interaction, the influence of the social context on individual preferences has not received much attention in the literature. Indeed, subjects can adjust their decisions according to whom they consider their reference at the time of the decision (Morgan and Laland, 2012). For example, individuals can often adjust their behavior to match the group, which is referred to as "compliance behavior" (Morgan and Laland, 2012).

In animals, the social environment can affect decision-making in different ways. For example, rats can induce olfactory clues in conspecifics to change their food preferences (Galef et al., 2007). Also, in guppies (Poecilia reticulata), a previously observed route is preferred over an equally valid available alternative when choosing food (Laland et al., 1997). This means that animals approaching other individuals or larger groups infer indicative signs of greater foraging success without having to pay the cost of sampling the environment directly (Coolen et al., 2005; Lachlan et al., 1998; Day et al., 2001).

Even though mammalian social behaviors occur in the context of extended groups, most social behaviors are generally investigated in pairs of individuals, given the technical limitations of data collection and analysis (Insel and Fernald, 2004; Shemesh et al., 2013). Nevertheless, the study of dyads presents limitations because animal groups commonly rely on more complex social structures. Moreover, different types of social interaction arise in animal groups. Indeed, social interactions can be contingent, such as when individuals randomly meet during environment exploration, courting a mating partner, or during collective movements. However, although this type of contingent interaction and decision-making is relevant to the social behavior of individuals, they have not yet been fully examined.

1.1.1. Contingent social interactions and decision-making

Both humans and animals show group behavioral patterns that are complex and coordinated, such as pedestrian flows in human crowds or movements of fish shoals (Couzin and Krause, 2003; Helbing and Molnar, 1995). A typical property of these phenomena is self-organization, suggesting that much of the complex group behavior can be coordinated through relatively simple interactions between group members (Couzin and Krause, 2003). Behavioral studies have suggested that collective decision-making mechanisms between animal species – insects, birds, and even humans – share comparable operational features with regards to the contingency (Couzin and Krause, 2003; Conradt and Roper 2003; Sumpter, 2006). For instance, simple rules such as "try to minimize travel time," "avoid collisions," and "move in the same direction as other people" would explain pedestrian movements on busy streets or during life-threatening situations (Helbing and Molnar, 1995). Similar patterns have been proposed for non-human animals, including the traces left by ants along food-seeking routes (Couzin and Franks, 2003), collective starling movements (Ballerini et al., 2008), and social interactions in fish (Day et al., 2001).

Group decisions result from a consensus achieved by individuals in the social group (Conradt and Roper, 2003). In many situations, however, there may be conflicts between the preferences of different individuals, resulting in a disadvantage of living in a group (Couzin et al., 2005). Individuals have to decide on the same action because the group will fall apart unless a consensus is achieved (Conradt and Roper, 2003). It has been shown that only a small proportion of individuals is needed to decide the direction of the entire group's movement. In social insect colonies, specifically bees and ants, group decisions depend on a few informed individuals or explorers for nest-site choice. (Seeley and Visscher, 2004; Pratt et al., 2005;). Thus, through collective action, individuals can improve their ability to detect and respond to outstanding characteristics of the environment, resulting in more precise decision-making with non-explicit signals or complex communication (Couzin et al., 2002; Couzin, 2005).

1.1.2. Cortical areas involved in individual decision-making

The decision-making process requires top-down and bottom-up neural processes to command several neural operations in a flexible and coordinated manner. A critical region in decision-making is the prefrontal cortex (PFC). The PFC is in the most rostral region of the frontal lobe (Uylingns et al., 1990; Fuster et al., 1997).). The PFC region as a whole shows considerable variation between species in terms of established anatomical criteria, such as cytoarchitectural and connectivity, especially the presence or absence of a granular area and the existence of strong reciprocal connections from the mediodorsal nucleus of the thalamus (Uylings, 1990; Groenewegen and Uylings, 2000; Ongur and Price, 2000). In primates and rodents, a common characteristic observed is the mutual connectivity with the mediodorsal thalamic nucleus (Rose et al., 1948; Fuster et al., 1997). In rodents, the anatomical PFC structures can be divided into three main areas (Fig S1). First, a lateral region that includes the dorsal and ventral agranular insular (AID, AIV) and lateral orbital (LO) cortices. Second, an orbital region (located ventral to the corpus callosum) that

includes the ventral orbital (VO) and ventral lateral orbital (VLO) cortices. Finally, a medial frontal division, namely medial prefrontal cortex (mPFC), which can be sub-divided into a dorsal region that includes precentral (PrC) and anterior cingulate (ACC) cortices and a ventral component that includes the prelimbic (PrL), infralimbic (IL), and medial orbital (MO) cortices (Watson et al., 2012) (**Fig. S1**). Although the role of these cortical subdivisions is not fully entirely clear, studies infer that the projections from the ventral regions, including the ventral prelimbic and infralimbic cortex, are specialized for autonomic/emotional control and dorsal regions, including the anterior cingulate and dorsal prelimbic cortex, which are specialized for the control of actions (Heidbreder and Groenewegen, 2003).

In this thesis, PFC is used to denote the prelimbic and infralimbic regions of the medial PFC cortex, as well as the anterior cingulate cortex. Anatomically, PFC interacts with other brain areas in a reciprocal manner. That is, the PFC receives and provides inputs mainly from and to the thalamus, the aminergic nuclei, basal amygdaloid complex, hypothalamus, and the hippocampus (Vertes et al., 2004). Thus, the PFC has the role of integrative information center par excellence. It comprises a set of interconnected neocortical areas that send and receive projections to virtually all cortical sensory systems, motor systems, and many subcortical structures (Groenewegen and Uylings, 2000). Therefore, the convergence of this extensive and intricate network and the broad distribution of mostly excitatory (glutamatergic) efferents indicate how its strategic positioning contributes to learning new tasks, goal-oriented behaviors, social motivation, environmental status and decision-making (Baddeley, 1996; Fuster, 2000; Passetti et al., 2000; Groenewegen and Uylings, 2000; Ongur and Price, 2000).

As previously described, the PFC has many anatomical connections with cortical, limbic, and subcortical structures (Petrides and Pandya, 1994; Fuster, 2015). Thus, through these connections, in a simple decision-making task, the PFC can monitor and control the functioning of these areas of the brain, such as activating or inhibiting

specific networks and integrating communication between networks. In humans, lesions in areas of the PFC have led to a decrease in several skills required in decision-making. These include learning from reward and punishment, making transitive decisions and making future-oriented decisions (Bechara et al., 1994; Fellows et al., 2007; Peters et al., 2016; Vaidya et al., 2015). Specifically, patients with damage to the ventromedial regions of the PFC, which covers the orbitofrontal cortex (OFC) and the ventral aspects of the AAC, showed impaired decision-making and more high-risk choices (Bechara et al., 1994; Bechara et al., 1998). These initial findings generated a marked increase in research that attempts to elucidate the neural circuits that mediate decision-making. With the development of new tasks, evaluation of patients, and the exploitation of functional brain images, cognitive neuroscience has made remarkable progress in identifying some of the neural circuits that mediate different aspects of decision-making. Currently, different behavioral, physiological and neuroimaging studies, such as those quantitating Blood Oxygen Level Dependent (BOLD) signals, have demonstrated the participation of different PFC areas in various decision-making tasks (Buckley et al., 2009; Daw et al., 2006; Lee, 2007; Wallis, 2007; Rushworth et al., 2008). Specifically, these results show functional differences within the PFC; for example, in humans and nonhuman primates, OFC and ACC seem to play a particularly important role in coding and updating the values of expected results (Rushworth et al., 2008). Also, other regions like the lateral PFC (including PL and IL) seem to be necessary to maintain, in the working memory, the representation of the situation necessary for identifying optimal options in any given environment (Buckley et al., 2009; Lee et al., 2007). In rodents, PFC areas, such as OFC, PL, and IL, have different roles in decision-making. For example, lesions in the cortex PL and IL alter the behavior of choice when animals choose food rewards of different values (Cardinal et al., 2001). Also, the OFC lesions show that this region plays a prominent role in updating the values of the expected results of the chosen actions (Hoon et al., 2010).

There is abundant literature regarding decision-making in humans and animal models based on tasks involving only one subject. Thanks to the progress of new imaging

techniques and data processing, it has been possible to study the brain areas involved in decision-making in the presence of other subjects that will be described below.

1.1.3. Cortical brain areas involved in social decision-making

Many efforts have been devoted to studying decision-making in the social context where, in addition to considering individual characteristics, both prior and contingent interactions based on memory must be taken into account. Recent research in humans with functional magnetic resonance imaging (fMRI) has discovered a set of brain regions that participate in decision-making and social context. It has been reported that the identification of the social context is strongly associated with brain activity in the medial temporal lobes and the fusiform gyrus (an area involved in facial recognition, located in the basal face of the temporal lobe (Tsao et al.; 2006; Behrens et al., 2009). On the other hand, there is a process known as the theory of mind or mentalization, in which a person can infer the mental states of him/herself and others. It has been described that mentalization involves brain areas, such as the posterior superior temporal sulcus (STS), the temporoparietal junction (TPJ), the anterior rostral cingulate cortex (rACC), and the mPFC (Yoshida et al., 2010; Coricelli et al., 2009; Carter et al., 2012). Also, there are areas of the brain involved in personal assessment at the level of personal preferences and internal state, and mainly include the ventromedial PFC, orbitofrontal cortex, and ventral striatum (Bartra et al., 2013). Despite the use of functional images to predict individual variation in social behavior, there are temporal and structural limitations that prevent understanding the neuronal mechanisms that develop at the cellular and molecular scale. Besides, there are practical and ethical considerations that make it difficult to functionally test neuronal populations with temporal and spatial specificity in humans. Thus, animal models of social interactions represent an opportunity to develop a mechanistic explanation of human social behavior.

Given the large amount of literature that addresses the roles of different neuronal systems in rodents' social behavior, it is necessary to focus literature on PFC as a central brain region implicated in the context of social behaviors, specifically inherent social dynamics.

1.1.4. PFC and social cognition

Convergent research in animal models implicates the PFC in social behaviors and as a crucial neural substrate of behavior and social cognition (complex cognitive behavior as well as the regulation of goal-directed social behaviors) (Bicks et al., 2015). Although it is challenging to assume a conserved neuronal mechanism across different social species, human patients with lesions in PFC exhibit several social impairments and minimal behavioral flexibility (Eslinger et al., 2004). In mice, PFC is activated during social interaction, and social stress induces a reduction in neural activity (Covington et al., 2010; Kim et al., 2015). Besides, PFC shows elevated firing rates when the animal approaches an unfamiliar mouse, compared to when mice approach an inanimate object (Kaidanovich-Beilin et al., 2011). On the other hand, a synaptic imbalance within neural micro circuitry between excitatory/inhibitory transmission and social dysfunction has been observed in mouse models of psychiatric disorders, such as autism spectrum disorders (ASD) (Yizhar et al., 2011). Social cognition is an intricate process that requires the integration of a wide variety of behaviors, including the pursuit of a reward, motivation, knowledge of oneself and others, and flexible adjustment of behavior in social groups (Bicks et al., 2015).

PFC is a crucial regulator of social cognition and is a structural domain in several pathophysiological disorders that share social impairment, including schizophrenia and ASD (Bicks et al., 2015). The use of etiologically relevant behavioral models is essential because it provides the natural insight required when evaluating social processing such as social motivation, social memory, and dominance hierarchy. Recognition and social memory are vital aspects of social cognition, and its normal

functioning is a requirement for the formation of long-term attachment behaviors. The evidence of the role of PFC areas in rodents for social recognition has not been fully established. A few studies have demonstrated that the ACC participates in social recognition, as ACC is necessary to acquire a conditioned contextual fear by observing conspecifics, and its lesion alters social recognition in rats (Rudebeck et al., 2007). Besides, the hippocampus and medial amygdala are other areas that participate in social recognition, specifically, in the formation of social memory and processing odor cues (Kogan et al., 2000; Noack et al., 2015).

On the other hand, the establishment of social hierarchies across dominance hierarchy are complex social strategies in animals and occurs among different animal taxa, including insects, fish, rodents, primates, and humans (Sapolsky, 2005; Wang et al., 2014). In mice, social hierarchies develop when living in high-density conditions, and this probably allows for a decrease in aggressive behavior and, thus, an increase in social tolerance (Anderson, 1961). The specific neuronal circuit implied in social hierarchies is currently unknown. However, it has been shown that PFC participates in this circuit as a critical modulator of hierarchical behavior, which will be described in more detail below.

1.1.5. Establishment of social hierarchy

The concept of a hierarchical structure in a social group was first described by Thorleif Schjelderup-Ebbe in 1921, when he described a hierarchical order in a group of domestic birds and proposed that the structure formed avoids or reduces conflicts and injuries between them, thus minimizing energy costs and promoting social stability (Schjelderup-Ebbe, 1922).

Currently, "hierarchy" as a concept is defined as the categorization of the members of a social group based on objective characteristics such as the influence or superiority they exhibit, giving rise to subordinate and dominant members in a social

group (Fiske, 2010; Mazur, 1985; Chase and Seitz., 2011;). Another term used is "rank," often used to objectively refer to the position or place in which a member is found within the hierarchy (conceptually similar to a sequence of ordinal numbers) (Chiao et al., 2008). Moreover, the term "status" can be measured through social opinion or reputation and is generally associated with admiration and respect (Chase and Seitz., 2011). Consequently, the terms "status" and "rank" are often used indistinctively, as both represent the highest position in a social hierarchy in mammals. Thus, the rank order determines, for example, access to resources, places of rest, and sexual partners for courtship (Chase and Seitz., 2011).

Likewise, "dominance" is associated with an asymmetry in aggressive behaviors from one animal to another, establishing a state of interaction between individuals (Chase, 1982). The interaction state also generates a dominance hierarchy, which refers to the extensive collection of interactions, or network of domain relationships between the pairs of individuals within a group. For example, in many groups of low numbers of animals and human children of about eight members or less, dominance hierarchies often acquire a linear order form (Hausfater et al., 1982; Savin-Williams, 1980).

In a linear hierarchy, there is an individual who dominates all other members of the group, a second who dominates all but the superior individual, and so on, until the last individual who exhibits no behavior of dominance with another (transitive relationship). There are exceptions to linearity, for example, in those cases in which there are no interactions between some pairs, especially those that seem distant in range. Thus, in hierarchies that are non-linear, there may be inconsistencies in the range that shows intransitive relationships (by example, A dominates B, B dominates C, but C dominates A) (Chase and Seitz., 2011).

Studies in human and animal models have begun to identify brain areas that are activated during the formation of social hierarchies. A critical brain area is the PFC, since it would act as a central regulator with subcortical brain areas transmitting

information about the social position to execute a domination behavior (Wang et al., 2014; Zhou et al.,2018).

1.1.5.1. PFC areas involved in social hierarchy

Behaviors based on social hierarchies lead to the use of a series of cognitive operations that involve the recognition of the social state, the learning of social norms, the detection of alterations of the social norm, the interpretation of the intentions of others, the monitoring of the reciprocal obligation, and perhaps competing with a conspecific (Wang et al., 2014). Sensory inputs provide the animal with information about social hierarchy in different species. For example, many social mammals use odor marks, tail rise, mounting, or vocalization to express dominance (Bicks et al., 2015). In primates, facial expressions are common: direct gaze or eyebrow raises are often used to signal domination, while subordinates use the "fear grimace" to appease or redirect aggression (Ghazanfar and Santos, 2004).

In human neuroimage studies, it has been reported that subjects can rapidly form a coherent understanding of the whole hierarchy by pooling the result of different game interactions between subjects within an interactive simulated social context. The subjects selectively activate the dorsolateral PFC (dlPFC) when seeing the face of a superior player versus a lower player (Zink et al., 2008). Besides, it has been described that dlPFC participates in attentional control, interpersonal judgments, compliance with social norms, moral and social judgment (Miller and Cohen, 2001). Other frontal cerebral areas like the mPFC are involved in processing the current context and comparing it with experience, in order to predict and execute the most adaptive behavioral response, and include prediction errors, recognition of intentions, and even the formation of judgments towards people (Amodio and Frith, 2006; Matsumoto et al., 2007). Likewise, the ventrolateral PFC (vlPFC) has been reported to be activated by non-verbal signals in people, such as body posture. In particular, it is important to note that vlPFC receives information from the temporal lobes, such as

the superior temporal cortex (STC), a brain region that responds to face and body movements (Allison et al., 2000). In non-human primates, during social engagement in a food-grabbing task, PFC activity increased in the dominant monkey and was suppressed in the submissive monkey (Fujii et al., 2009).

Furthermore, neurons in the lateral prefrontal cortex (lPFC) of macaque monkeys showed response sensitivity to winning and losing in competitive video games (Hosokawa et al., 2012). Consistent with these correlative studies, selective lesions in regions of PFC areas have also impacted social hierarchy behavior. For example, monkeys with lesions in their anterior cingulate cortex (ACC) showed less social interest towards other macaques (Rudebecket al., 2006).

In rats with mPFC lesions, animals behaved as subordinates in agonistic encounters, attended fewer daily feeding sessions, and acted more timidly, consistent with a reduced social rank (Holson, 1986). A more detailed study on the different areas of the PFC showed that the ACC participates in the codification of competitive effort. Neurons of the ACC fire much more often when the rats are on a route leading them to food competition with a subordinate rat than when it leads to a dominant rat (Hillman and Bilkey, 2012). In mice, the PrL cortex is activated during social interaction with the presence of a conspecific, and a lesion changes their behavior during social interaction (Avale et al., 2011). Also, an augmented amplitude of spontaneous postsynaptic currents in the PrL and IL cortex increases social dominance behaviors (Anacker et al., 2019).

Similarly, a seminal work for this thesis examines the functional consequence of social dominance by promoting or blocking synaptic plasticity selectively in PFC (includes ACC, PL, and IL areas) (Wang et al., 2011). Furthermore, this study demonstrates that molecular manipulations based on viruses show that the synaptic efficacy of mPFC pyramidal neurons increases or decreases in mice, causing a gradual change in their dominance hierarchy, in a reversible manner (Wang et al., 2011). Other work showed that the activation of the PFC (includes ACC, Pl, and IL

areas) is both necessary and sufficient to quickly induce winning in the social competition dominance test (Zhou et al., 2017). Thus, the PFC is identified as a prominent mediator in the regulation and processing of social hierarchy.

1.1.5.2. PFC areas modulate social hierarchy

The regulation of the PFC in social dominance can occur across modulation of the downstream subcortical nuclei, and its potential participation in different features of social behavior are related to dominance hierarchy. For example, lesions in the reciprocal projection of the mPFC to the basolateral nucleus of the amygdala (BLA) in animal models produce different outcomes with respect to the dominance hierarchy, such as increased aggression, loss of dominance and competitive behaviors (Lukaszewska et al., 1984). Another target of the PFC implicated in dominance hierarchy behavior is the dorsal raphe nucleus (DRN), the main serotonergic nucleus in the brain which is implicated in impulsive and aggressive behavior (Audero et al., 2013). Also, the hypothalamus, periaqueductal gray (PAG), and striatum are cerebral areas with reciprocal connectivity with the PFC (Hoover and Vertes, 2007). These areas are implicated in the regulation of agonistic behavior in mice (Wang et al., 2014), while in humans they are associated with reward events and social status (Bault et al., 2011).

Although the neural circuits that control the dominance hierarchy are only starting to be elucidated, the PFC can be recognized as a mediator in the regulation and processing of social hierarchy. Studies of hierarchy dominance show that it might be regulated by the activity of specific neural circuits, especially circuits in higher cerebral areas of the central nervous system, in particular cortical areas. Moreover, the cortical areas, including PFC, are implicated in many cognitive processes associated with the domain of social cognition. However, few studies describe the neural activity involved in hierarchy dominance. Besides, synaptic activity in the medial PFC is also required for the control of decision-making and spatial navigation. An essential cortical region

that communicates with PFC in the cognitive process is the hippocampus (associated with memory and spatial navigation). The hippocampus and the PFC are reciprocally connected, and their interplay is essential in regulating individual spatial navigation and decision-making (Euston et al., 2012). This topic will be examined in a separate section of this thesis (see next section 1.2.).

1.2. CORTICAL INTERACTIONS DURING SPATIAL NAVIGATION AND DECISION-MAKING

During spatial navigation, the decision process can be interpreted as an internal process where various known navigation routes are evaluated on a cognitive map (Tolman, 1948). This process would require the formation and recollection of memories created previously during navigation to deliberate on its options (Euston et al., 2012; Yu and Frank., 2015). Thus, decision-making recruits brain regions such as the hippocampus and PFC. Indeed, activity patterns of the hippocampus are tightly related to memory formation and consolidation (Anderson et al., 2006). In contrast, patterns found in the PFC are responsible for the collection and evaluation of options or contexts based on memory selection during an individual's goal-directed spatial behavior (Euston et al., 2012).

Additionally, network states during behavior are associated with hippocampal information processing with other cerebral regions, including the PFC. Moreover, it has been established that network patterns represent different communication mechanisms between the hippocampus and the PFC during exploration, sleep, and quiet wakefulness (Euston et al., 2012). Their role is still being investigated in different cognitive processes. In this section, the neural and behavioral aspects of the PFC and hippocampus during navigation and decision-making, are presented below.

1.2.1. Hippocampus, memory, and navigation

The hippocampus or hippocampal formation is a component of the limbic system (Anderson et al., 2006), a cortical structure found in the medial temporal lobe in all mammalian species that plays a fundamental role in spatial navigation and in several forms of learning and memory (Buzsáki, 2002; Eichenbaum, 1999). The hippocampal formation is an elongated structure with its long axis extending rostro dorsally in a C-

shaped fashion from the septal nuclei of the basal forebrain, over and behind the diencephalon, into the incipient temporal lobe caudoventrally (Watson et al., 2012). The role of the hippocampus in cognitive and behavioral processes can be separated topographically. It has been reported that the rostral or ventral hippocampus area (vHIP) is implicated in emotional and motivational behaviors, while the temporal or dorsal hippocampus area (dHIP) is related with spatial and memory processes (Anderson et al., 2006). Cytoarchitectonically, the hippocampal formation comprises three distinct regions (**Fig. S2**): the dentate gyrus; the hippocampus (or hippocampus proper), which is subdivided into three fields or cornu ammonis areas (CA3, CA2, and CA1); and the subiculum, a complex transitional output of the hippocampal zone (Ramon y Cajal, 1893; Lorente de No, 1933).

Recently, it has been documented that the hippocampus has a role in the coding and consolidation of declarative memory, especially episodic memory. Studies of loss of function in humans have contributed to significant findings in the brain area related to memory. One of the most notorious cases in neuroscience was the case study of patient H.M., who suffered from severe anterograde amnesia (declarative memory) after complete bilateral remotion of the medial temporal lobe, including the hippocampus, where procedural skills were not affected (Scoville and Milner, 1957). Other cases have been reported, such as that of patient R.B. who, after a brain injury in the hippocampal CA1 area, also suffered anterograde amnesia (Zola-Morgan et al., 1986). Declarative memory has also been investigated in animals. Compared to human studies, animal models offer significant advantages, since they allow a clear understanding of the cognitive processes that underlie behavior. A disadvantage is that animals cannot tell us what events they remember; instead, we infer their knowledge of past events from their behavior (Binder et al., 2015). Rodent studies show that the hippocampus circuits have a high capacity to process sensory information flows and then encode it in long-term memory. Thus, this processing would be crucial in the recognition of environmental changes, in order to adapt our behavior accordingly (Zemla et al., 2017).

In rodents, the discharge of principal hippocampal neurons is correlated with the process of encoding memory in the hippocampus as a way of encrypting and sending the information to other regions of the brain. A neural mechanism has been described in which representations of experience are expressed by the sequential firing of sets of pyramidal neurons when the animal explores an environment. Hippocampal pyramidal neurons are often active only in specific places in the environment, and they are called “place cells” (O'Keefe and Dostrovsky, 1971). In animal studies, place cells have been suggested to underlie spatial navigation in rodents (O’Keefe, 1976). Besides, the spatial knowledge acquired is consolidated via spontaneous recurrence of hippocampal place-cell activity during slow-wave sleep (SWS) in animals and humans (Wilson and McNaughton, 1994; Peigneux et al., 2004). However, place cells represent much more than a location. A variety of studies have shown that these neurons can respond to a composition of spatial and non-spatial information, such as external sensory stimuli and behavioral aspects relevant to the task that allows the animals to evaluate choices and options (Frank et al., 2000; Pastalkova et al., 2008).

Thus, in what concerns the connections between these two regions, the research focus is on memory and their respective processes. Nevertheless, the neural mechanism underlying the coordinated action of the hippocampus and the PFC is still unclear. Below, I will describe the physiological interactions in the hippocampus-PFC axis and the role of hippocampal rhythms that depend on cognitive and behavioral states, especially during navigation and decision-making.

1.2.2. Hippocampus and PFC interaction during navigation and decision-making

Several direct and indirect anatomical pathways connect the hippocampus and the PFC. In both rodents and primates, the PFC receives monosynaptic projections from the hippocampus (Hoover and Vertes, 2007). In the PFC, hippocampal projections differ in the septal or the temporal area: projections to the mPFC cortex are notably more robust from the temporal hippocampus and subiculum, compared with the

projections of the septal hippocampus area, which are less dense (Jay et al., 1992; Vertes et al., 2004). CA1 Hippocampal pyramidal cells synapse onto both pyramidal and local inhibitory interneurons in the PFC (Gabbott et al., 2002; Klausberger & Somogyi, 2008). There are no projections from CA2/CA3 or the dentate gyrus to the PFC (Jay et al., 1991).

In contrast to the hippocampus, the PFC does slightly project directly onto the hippocampus. More precisely, it was described by a monosynaptic projection in a transgenic mouse model. This modest projection originates in the anterior cingulate (a subdivision of the PFC) and terminates in the CA1 and CA3 subfields of the dorsal hippocampus (Rajasethupathy et al., 2015). Furthermore, the PFC mainly provides sets of selective afferents that densely innervate midline regions of the thalamus and, to a lesser extent, the caudal cortex which, in turn, has dense projections to the hippocampus (Vertes, 2002). Additionally, the PFC sends projections to the lateral entorhinal cortex with extensive reciprocal connections with all hippocampal and subiculum areas (Vertes, 2004; Cenquizca and Swanson, 2007). Hence, while the pathway between the hippocampus CA1-PFC axis is largely unidirectional, it may be reciprocal via three routes, a monosynaptic path across the anterior cingulate, and the bisynaptic way either through the thalamic nucleus reuniens or through the lateral entorhinal cortex.

The anatomical routes previously described between both regions can provide for directional and bi-directional physiological interactions. For instance, experiments performed under anaesthesia have shown PFC network responses to hippocampal stimulation (Jay et al., 1992; Takita et al., 2013). Besides, during exploration, PFC neurons responses are task selective, and the activity responses can be derived from hippocampal inputs, or PFC neurons to the hippocampus; the direction of interaction can even be dependent on the task level (Wierzynski et al., 2009; Place et al., 2016). Thus, it should be considered as part of an interacting network that subserves joint functions necessary for memory-guided behavior (Euston et al., 2012). The coordination in both structures is supported by many works that describe evidence of

network patterns in the local field potential (LFP), permitting a dynamical state of synchronization to allow cognitive function. In simple terms, LFP is the electric potential in the extracellular medium around neurons. This signal is available in many recording configurations, ranging from single-electrode recordings to multi-electrode arrays (Bédard and Destexhe, 2014). The LFP is produced by the synaptic currents (local and long-range inputs) from neurons in the proximity of the recording electrode, and the volume-conducted potential from regions that are distant to the electrode (Buzsáki et al., 2012). In the LFP, rhythmic oscillations at different frequencies are observed, and their rhythm reflects the neuronal activity in many regions of the brain. These network patterns manifest an organized activity of neuronal populations and are believed to support both local information processing and coordination between distant brain regions during different modes of cognitive processes (Buzsaki, 2002; Fries, 2015). The network patterns have been attributed certain roles, such as the processing of the local hippocampal network during animal behavior, such as theta, gamma, and fast oscillations, especially sharp-wave ripples (SWRs) (**Fig. S3**) (Buzsaki, 2002; Buzsáki, 2015). Similarly, rhythms in the PFC (theta and gamma oscillations) are involved in information processing (Buschman et al., 2012; Benchenane et al., 2011; Cho et al., 2015).

For the development of this thesis, some pattern network activities are important. Hence, it is necessary to understand the functional organization of the hippocampus-PFC axis and its participation in animal cognition, such as in memory and decision-making.

1.2.3. Theta oscillations and SWRs.

Theta oscillation is a synchronous oscillation in the range of 4-8 Hz (Buzsaki, 2002). In animals, its disruption or elimination due to lesions resulted in impairment on a spatial task, suggesting that theta oscillations are essential for the acquisition of spatial memory (Winson, 1972). In rodents, theta oscillations represent the “online”

state of the hippocampus and tend to be more prominent during active locomotion of the animal and rapid eye movement (REM) sleep than during quiescent states (Buzsaki, 2002). Hippocampal theta synchronizes PFC neurons during locomotion. For instance, PFC neurons fire phase-locked to hippocampal theta oscillations (Jones and Wilson, 2005; Benchenane et al., 2010). Besides, hippocampal and PFC areas exhibit an oscillatory coherence (a measure of neuronal synchronization) in theta rhythms (by LFP signals), during periods of memory-guided decision-making as compared to simple exploration (Jones and Wilson, 2005; Siapas et al., 2005; Benchenane et al., 2010).

SWRs are high-frequency (100-250 Hz) transient oscillations (~100 ms), whose characteristic oscillatory pattern is present during slow-wave sleep and states of quiet wakefulness states (Buzsaki, 2002). More precisely, this pattern of activity is most prominent in the apical dendritic layer of the CA1 region as a result of a strong depolarization by the CA3 collaterals, due to the synchronous bursting of CA3 pyramidal cells, providing short temporal windows for facilitating somatodendritic spike propagation and synaptic plasticity (Csicsvari et al., 1999). Hippocampal SWRs have numerous remarkable features that make them ideal for the consolidation of synaptic plasticity and the transfer of neuronal patterns (Buzsáki et al., 2003). For instance, many works demonstrate hippocampal reactivation during sleep and suggest that SWRs participate in memory consolidation. In simple terms, this refers to the stabilization of labile memory traces, and the transfer of information, which is initially encoded in the hippocampal circuit, to the neocortex for long-term storage (Wilson et al., 1994). By contrast, in the case of awake animals, SWRs still trying to elucidate its function, but the evidence suggesting a diverse role in reinforcement learning, planning, and prospective decision-making (Carr et al., 2011; Singer et al., 2013).

Since SWR and theta oscillations are different hallmark network states observed during behavior and are also associated with hippocampal information processing, it can be established that these two network patterns represent different

communication mechanisms between the hippocampus and the PFC. Their role in different cognitive processes is still being investigated. As reviewed in the previous section, the two structures interact in neuronal activity and influence each other over time during a navigation and decision-making task that will be detailed below.

1.2.4. Activity patterns in the hippocampus-PFC axis in decision-making during navigation

Hippocampus and PFC units interact in the theta frequency during exploration. For instance, in the PFC, some units show phase-locking to hippocampal theta oscillations, and the PFC units fire after the hippocampus units (Siapas and Wilson, 1998; Hyman et al., 2005). This suggests a potential mechanism where information can be exchanged through the oscillatory synchronization between the hippocampus and the PFC during behavior (Jones & Wilson, 2005). On the other hand, the modulation of PFC cells can be supported through LFP analysis between both regions. For example, theta coherence in the hippocampus-PFC axis increases at a specific place in the maze, specifically at the decision point, where the animal has to choose between arms (Jones and Wilson, 2005; Benchenane et al., 2010). This implies that there is a relationship in the hippocampus-PFC axis with the animal's performance. Furthermore, as behavioral performance stabilizes, coherence becomes much higher when the animal approaches a decision point for a correct choice (Jones and Wilson, 2005). Therefore, it is possible that coherence in theta is a reflection of the transmission of information about the current location and the possible trajectory to be made between the hippocampus and the PFC, possibly to ensure that a learned rule is executed correctly in a specific behavioral state (Yu and Frank, 2015).

On the other hand, the coupling between the hippocampus and the PFC during SWRs can have a distinct role in the animal's behavioral state. In PFC, specific neuronal representations are observed during hippocampal SWRs (Peyrache et al., 2011), and

hippocampal-PFC ensembles reactivate in a coordinated manner during SWRs (Jadhav et al., 2012). These observations suggest that SWRs could drive PFC activity during sleep and wakefulness. This possibility is consistent with an fMRI study in primates that reported increased BOLD signal activity on the entire cortical mantle (including PFC region) following SWRs (Logothetis et al., 2012). Accordingly, it has been proposed that SWRs could provide a convenient mechanism to consolidate memories during offline periods and recall memories during the wakeful state (Carr et al., 2011; Yu and Frank, 2015). On the other hand, hippocampal reactivation during awake SWRs is known to contribute to learning with a proposed role in memory consolidation and retrieval (Carr et al., 2011; Jadhav et al., 2012). Hence, the activation of the PFC after SWRs during sleep or quiescent states, as well as data from the primate fMRI study suggests that the interaction between the two regions during SWRs could be a mechanism where, during waking behavior, the reactivated representations of the hippocampus are used for deliberation (Yu and Frank, 2015).

1.3. OVERVIEW AND FORMULATION OF THE SCIENTIFIC QUESTION

Recently, convergent research in animal models has shown that the PFC participates in a wide variety of social behaviors (Bicks et al., 2015). The limitation is that these studies are based on subjects individually tested and in the presence of usually one peer. However, social behavior is more complicated than a dyadic interaction since different types of social interactions arise in groups of animals (Shemesh et al., 2013; de Chaumont et al., 2013). Social interactions can be contingent, as is when individuals meet randomly during the exploration of the environment or court a mating partner (Condrat et al., 2003). In contrast, social interactions also have inherent characteristics such as the establishment of hierarchies (Lindzey et al., 1961), which is very important given that it regulates the individual behavior of a subject in a given social group (Wang et al., 2011). However, most of the studies that describe the social hierarchy are under individual conditions.

On the other hand, decision-making is determined by intrinsic and extrinsic characteristics, such as information stored in the memory and external influences, such as social interaction (Insel and Fernald., 2004). It has been established that the behavior of an animal that is heading towards a target recruits brain regions such as the hippocampus and the PFC, which, in turn, are dynamically associated according to the needs of the ongoing behavior (Euston et al., 2012; Benchenane et al., 2011). Besides, functional connectivity between the dorsal hippocampus and the PFC is essential in regulating spatial navigation and decision-making (Euston et al., 2012; Matsumoto et al., 2007). However, it is still not clear whether or not the intrinsic connectivity of the PFC-hippocampus axis correlates with collective spatial navigation.

In particular, two questions of interest arise to be undertaken in this thesis. The first refers to social behavior and explores whether or not the decision-making process and task performance depends on contingent social interactions arising during

collective movement. The second question follows from the physiological description of the PFC-hippocampus axis and examines whether or not the intrinsic neuronal activity of the cortical network correlates with social behavior, such as dominance hierarchy and collective spatial navigation.

To answer the aforementioned questions, this thesis was carried out in three stages. First, in a novel task of collective spatial navigation, two parameters of behavior (performance and latency) were observed in animals, together with the establishment of the social dynamics they showed during the experiment days. In the second stage, the contingent social interaction that arises during collective behavior was evaluated. Lastly, the animals that performed social navigation tasks were selected in order to record their spontaneous rhythmic cortical activity with stereotaxically implanted multi-electrodes in both the hippocampus and the PFC, both of which are required for goal-directed spatial behavior. To do so, a simple social navigation task was developed, based on a T-shaped maze. Subsequently, I carried out cortical recordings under anaesthesia with multichannel electrodes, of animals that had performed social navigations task.

CHAPTER 2

HYPOTHESIS

The thesis committee approved the following general and specific hypotheses.

2.1. General Hypothesis

The process of individual decision-making during collective navigation tasks depends on the social context, and this phenomenon is correlated with the intrinsic connectivity of the hippocampus-PFC system.

2.2. Specific Hypothesis

The general hypothesis presented is divided into two specific hypotheses, one behavioral and one neurophysiological, respectively.

• Behavioural:

Specific Hypothesis 1: The individual's decision-making process during a collective spatial navigation task is affected by the social context.

• Neurophysiological:

Specific Hypothesis 2: The intrinsic connectivity of the hippocampus-PFC system is correlated with behavioral performance in a collective spatial navigation task.

CHAPTER 3

OBJECTIVES

The thesis committee approved the following general and specific objectives.

3.1. General objective

Describe and correlate the intrinsic connectivity of the hippocampus-PFC system with behavioral performance in social mice groups during collective spatial navigation tasks.

3.2. Specific objectives

The general objective presented is divided into three specific objectives.

Specific objective 1*:* Establish the behavioral effect of the social context on an individual performing a collective spatial navigation task.

Specific objective 2: Characterize the intrinsic cortical oscillatory activity of the hippocampus-PFC system and their spike timing concerning the social ranking system.

Specific objective 3*:* Correlate the intrinsic connectivity of the hippocampus-PFC system with behavioral performance in individuals performing a collective spatial navigation task.

CHAPTER 4

METHODS

4.1. EXPERIMENTAL DESIGN

4.1.1. Behavioral protocols

Efforts were performed to minimize the number of animals used and their suffering. All tests were conducted between 10.00 a.m. and 4.00 p.m. As in any behavioral work; animals should be in an optimal state of arousal for testing; leave them for 15–30 min after taking them into the testing room. All experimental procedures related to animal experimentation are approved by the Institutional Animal Ethics Committee of the Pontificia Universidad Católica de Chile (protocol code: CEBA 150914003 and CEBA 151223006).

4.1.2. Animals

The social group consists of four male sibling mice (C57BL/6J strain, n = 60, 20–30 g, 15–25 weeks). Each litter mice were separate group-housed and always lived in the same cage since weaning until the end of the experimental protocol. Animals were supplied by CIM (Centro de Investigaciones Médicas) and were housed in a temperature and humidity-controlled room (22 ± 1°C) with food and water ad libitum. The mice were kept under a 12 h:12 h light-dark cycle, from 8.00 a.m. to 8.00 p.m.

4.1.3. Tube test

I measure the hierarchical relation of animals within the same social group by the applied tube test to litter mice cages (Lyndsey et al., 1967). The tests consist of each mouse is placed to the ends of a narrow tube, and one mouse forces the other to back out of the tube with score 1 for the winner and 0 for the loser per session (wang et al., 2011). All mice were tested pair-wise for dominance for ten days using a round-robin design, and the social rank was assessed based on winning against the other cage mates (**Fig. 2B**).

4.1.4. T-maze apparatus

For this propose, I use a transparent Plexiglas material in the T-maze and Arena. The sizes are more than enough to permit one or various adult mouse to pass through the apparatus (**Fig. 2A**).

4.1.5. T-maze habituation

Animals (15 cages of 4 littermates) were individually placed in the maze and allowed to explore freely for 3-5 min for two days. Crumbs of sugared cereal were randomly distributed throughout the maze to stimulate exploration. Animals were then food-restricted to enhance exploration and learning of the arm baited with food, with 1.5 gr of pellet per animal per day. This treatment produced a general weight loss of about 20% in most animals.

4.1.6. T-maze test

We used transparent Plexiglas to manufacture the T-maze. During the individual phase, we trained animals individually to look for food in a fixed location, at the end of the maze

arms. Each animal had 10 trials per day, with a maximum duration of 90 second per trial (**Fig. 1**). During the first trials, if the mouse did not explore, it was gently pushed towards the baited arm. At the end of every trial, the mouse was placed back in the homecage with its siblings and the maze was quickly wiped with 10% EtOH to remove odour cues. In this way, the inter-trial interval for every mouse was around 10 minutes. For every trial we computed the latency or the time interval that every animal took to get from the start box to reach the food reward in the baited arm. In addition, we calculated the performance as the proportion of correctly performed trials based on the first decision to turn to the baited arm. Training finalized when animals reached the learning criterion, meaning that at least three out of four littermates in the box performed correctly six out of eight trials (75%) on two consecutive days. After reaching the learning criterion, we started the collective phase. Every animal performed four individual trials and the next trial was collective, with all four littermates placed in the start box. This was repeated twice, so to complete 10 total trials, 8 individual and 2 collective per day, during 5 consecutive days. During collective trials, reward was randomly assigned according to four options: right arm, left arm, both arms, or none. Videos of individual and collective tests were scored manually on a frame-by-frame basis. The experimenter was blind to the animal identity during scoring.

4.1.7. Manual Annotation of Behaviours

Individual and collective test videos were scored manually on a frame-by-frame basis using a Computer with a software VLC player. The investigator observer performing annotation was blind to experimental conditions. In manual scoring, each video was annotated as corresponding to individual accuracy, individual total latencies, individual correct latencies (only correct trials), collective accuracy, collective total latencies (all trials), and collective correct trials for each animal in a social group. In this way, the accuracy (proportion of correct trials) was annotated, and latencies were calculated along with a stopwatch and tabulated in MATLAB (MathWorks, Natick, MA).

4.2. RECORDING PROTOCOLS

I record simultaneous neuronal activity in the PFC and hippocampus once the behavioral T-maze testing experiments are finished.

4.2.1. Acute recordings

Animals were anesthetized with urethane (0.8 g/kg dissolved in saline, i.p.) and a mix of ketamine/xylazine (40 mg/kg ketamine; 4 mg/kg xylazine dissolved in saline, i.p.). Anesthesia was maintained with urethane administered every 20 minutes with a bomb when required. During the entire experiment, glucosamine solution (0.5-1 ml) was injected subcutaneously every 2 hours to maintain the animal hydrated, and body temperature was maintained at 36 ± 1°C using a heating pad (Harvard Apparatus, MA, USA) and monitored with a rectal probe connected to a temperature controller (Harvard Apparatus, MA, USA). The animals were placed in a stereotaxic device (Stoelting Co.). To simultaneously record the neuronal activity of the mPFC (cingulate and prelimbic cortex) and the CA1 area of the dorsal hippocampus, small craniotomies (1 mm) were drilled on the skull (right hemisphere) over the recording sites. The stereotaxic coordinates, indicated by the stereotaxic atlas (Franklin and Paxinos 2007), were (relative to bregma): mPFC, anteroposterior, +2 mm; mediolateral, +0.5 mm; and CA1 hippocampus, anteroposterior, −3 mm; mediolateral, +1.7 mm. The electrodes were slowly lowered via a motorized microdrive (Siskiyou, Grants Pass, OR, USA) to the recording positions. The electrodes were positioned at ∼1.0–2.0 mm dorsoventrally to record activity in the PFC, and ‘to record in the CA1 the electrodes were placed at ∼1.1 mm dorsoventrally using the firing of CA1 pyramidal cells and the appearance of SWR as the hallmark for functional localization of the hippocampus. Neuronal activity in the PFC was recorded extracellularly by using a 32 channel-silicon probe stained with DiI (A1x32-poly2-5mm, Neuronexus). Neuronal activity in the hippocampus was recorded

extracellularly by using a 16 channel-silicon probe (Neuronexus) stained with DiI (A1x16-5mm, Neuronexus) and inserted into the brain with a 30° angle towards the midline. Electrical activity was acquired with a 32-channel Intan RHD 2132 amplifier board connected to an RHD2000 evaluation system (Intan Technologies). Single-unit activity and local field potential (LFP; sampling rate 20 kHz) were digitally filtered between 300 Hz –5 kHz and 0.3 Hz – 2 kHz, respectively. Once a spiking multiunit was detected, the simultaneous mPFC and hippocampal recording started, and lasted for 10 min.

4.2.2. Histology

At the end of the electrophysiological recording, the mice were immediately perfused with 20 mL of the saline solution followed by 50 mL of 4% paraformaldehyde in phosphate-buffered saline (PBS, pH = 7.4). The brain was removed, incubated overnight in 4% paraformaldehyde in PBS buffer, and then stored in PBS buffer containing 0.2% sodium azide. Coronal mPFC brain slices (60 -80 µm) were prepared from paraformaldehyde-fixed brains with a vibratome (World Precision Instruments, Sarasota, USA) in ice-cold PBS buffer. For visualization, slices were washed three times in PBS buffer at room temperature and then placed on slides using a mounting medium (Dako) and then were stained with Nissl-staining. Images were acquired with an epifluorescence microscope for DiI labeling and Nissl-staining (Nikon eclipse Ci).

4.3. DATA ANALYSIS

4.3.1. Spike sorting

Neuronal spikes were extracted from mPFC recordings using Semiautomatic clustering KlustaKwik (https://github.com/kwikteam/klustakwik2/). This method was applied over the 32 channels of the silicon probe, grouped in eight pseudo-tetrodes of four nearby channels. Spike clusters were considered single units if their auto-correlograms had a 2-ms refractory period, and their cross-correlograms with all other clusters did not have sharp peaks within 2 Ms of 0 lag.

4.3.2. Brain-state and time-frequency analysis

Brain-states were defined based on the hippocampal LFP. The decomposition of LFP in the PFC and hippocampus was performed using a multi-taper Fourier analysis (Mitra and Pesaran 1999) implemented in the Chronux toolbox (http://www.chronux.org). LFP was downsampled to 500 Hz, and theta oscillations, non-theta epochs, and ripple episodes were recognized. Unless stated, the LFP from the dorsal CA1 stratum pyramidal was considered as the time-frame reference for the spike-timing of recorded cells. For spectral coherence, signals were divided into 2000 ms segments with 100 ms overlap and a time-bandwidth product (TW) of 5 and 9 tapers. Mean spectral power and coherence measures were calculated for theta (4–8 Hz) band for the entire record.

4.3.3 Theta oscillations detection

Theta oscillation was detected by calculating the continuous ratio between the envelopes of theta (4–8 Hz) and delta (2–3 Hz) frequency bands filtered from the hippocampus LFP and calculated by the Hilbert transform. A ratio of 1.4 SD or higher,

during at least 2 s defined epochs of theta oscillations. Recording episodes outside theta oscillations were defined as non-theta epochs.

4.3.4. Spike-LFP pairwise phase consistency (PPC)

I use a metric of oscillatory phase-locking between multiunit PFC discharge and hippocampal LFP activity. Briefly, the hippocampal LFP (filtered in the range of 1-200 Hz) and multiunit PFC activity (mean firing rate > 1 Hz) were used to calculate the PPC (Vinck et al., 2010) by using the FieldTrip MATLAB package (Oostenveld et al., 2011, http://www.fieldtriptoolbox.org/).

4.3.5. Sharp wave-ripples detection

Sharp wave-ripples were recorded in dorsal CA1, as close as possible to stratum pyramidale and considered as the time-frame reference for the spike-timing of the recorded neurons and population activity (LFP) in PFC. I used a recently described method for ripples detection (Logothetis et al. 2012) with some variation. Briefly, the hippocampus LFP was first down-sampled to 1 kHz, then band-pass filtered (100-200 Hz) using a zero-phase shift non-causal finite impulse filter with 0.5 Hz roll-off. Next, the signal was rectified, and low-pass filtered at 20 Hz with a 4th order Butterworth filter. This procedure yields a smooth envelope of the filtered signal, which was then z-score normalized using the mean and SD of the whole signal in the time domain. Epochs during which the normalized signal exceed a 3.5 SD threshold were considered as ripple events. The first point before threshold that reached 1 SD was considered the onset and the first one after threshold to achieve 1 SD as the end of events. The difference between onset and end of events was used to estimate the ripple duration. I introduced a 50 ms-refractory window to prevent double detections. To precisely determine the mean frequency, amplitude, and duration of each event, I performed a spectral analysis using Morlet complex wavelets of seven cycles. The Matlab toolbox

used is available online as the LAN toolbox (https://bitbucket.org/marcelostockle/lan-toolbox/wiki/Home.

4.3.6. Cross-correlation analysis

The activity of PFC neurons and hippocampal ripples was cross-correlated by applying the "sliding-sweeps" algorithm (Abeles, M. et al.; 1988). A time window of ± 1 s was defined with the 0-point assigned to the start time of a ripple. The timestamps of the PFC spikes within the time window were considered as a template and were represented by a vector of spikes relative to t = 0 s, with a time bin of 50 ms and normalized to the total number of spikes. Thus, the central bin of the vector contained the ratio between the number of PFC spikes elicited between ± 25 ms and the total number of spikes within the template. Next, the window was shifted to successive ripples throughout the recording session, and an array of recurrences of templates was obtained. Both PFC timestamps and start times of ripples were shuffled by a randomized exchange of the original inter-event intervals, and the cross-correlation procedure was performed on the pseudo-random sequence. The statistical significance of the observed repetition of spike sequences was assessed by comparing, bin to bin, the original sequence with the shuffled sequence. An original correlation sequence that presented a statistical distribution different from 1000 permutations was considered as statistically significant, with $p < 0.01$ probability, instead of a chance occurrence.

4.3.7. Statistic

I performed inter-subject comparisons to establish if behaviour and simultaneous cortico-hippocampal activity were different across social rank. We pooled neuronal data from all animal of a specific social rank in the same experimental group for all other statistical analysis. Data were tested for normality using the Kolmogorov–Smirnov test and then compared with the appropriate test with parametric analysis (one-way ANOVA

followed by Bonferroni post-hoc test). Comparison between behavioural parameters and other non-normally distributed parameters were analysed with non-parametric tests (Wilcoxon signed rank; Kruskal-Wallis test followed by Dunn's multiple comparisons post-hoc test). The statistical significance of the observed repetition of spike sequences was assessed by comparing, bin to bin, the original sequence with the shuffled sequence. An original correlation sequence that presented a statistical distribution different from 1000 permutations was considered as statistically significant, with $P < 0.01$ probability, instead of a chance occurrence. Linear correlations between parameters were analysed by Spearman correlation test. To calculate the P-value we used the circ_corrcl.m in the CircStat toolbox of MATLAB (The Mathworks, Inc.) and STATISTICA 7.0 software (StatSoft, Inc). Summary results of statistical tests are presented in **Table S3**.

CHAPTER 5

RESULTS

5.1. SPECIFIC OBJECTIVE 1: ESTABLISH THE BEHAVIORAL EFFECT OF THE SOCIAL CONTEXT ON AN INDIVIDUAL PERFORMING A COLLECTIVE SPATIAL NAVIGATION TASK

5.1.1. The contingent social interactions modulate decision-making during a collective spatial navigation task.

In the present doctoral thesis, I have studied the influence of the social context on individual decision-making during collective spatial navigation. For this, first, I reared together groups of four littermate male mice after weanling. Then, I developed a simple spatial navigation task based on a modified version of the T-maze (Olton, 1979), such that it could simultaneously accommodate all four littermates **(Fig. 1A)**. As a result, our T-maze was larger and wider than standard versions **(Fig. 2A)**. Moreover, the cognitive task was simplified so that animals performed one single test run per trial to find food in a baited arm. During the training phase of the test, mice were sequentially trained individually in the navigation task **(Fig. 1A)**. Each mouse performed ten individual trials per day. All animals had complete information about the task as they learned the fixed location of reward. Nevertheless, animals differed in individual preference as two randomly chosen mice per litter were trained to look for reward exclusively in the left arm, while the right arm was baited for the remaining two littermates. There was a large variance in performance between animals during the training phase **(Fig. 3A, 3B, 3C, 3D, 3E, and 3F)**, but overall, mice improved their performance linearly over time, defined as the proportion of correct choices during individual trials **(Fig. 4A)**. Besides,

animals progressively decreased their latency, defined as the time interval taken to reach the rewarded pocket in the baited arm **(Fig. 5A)**.

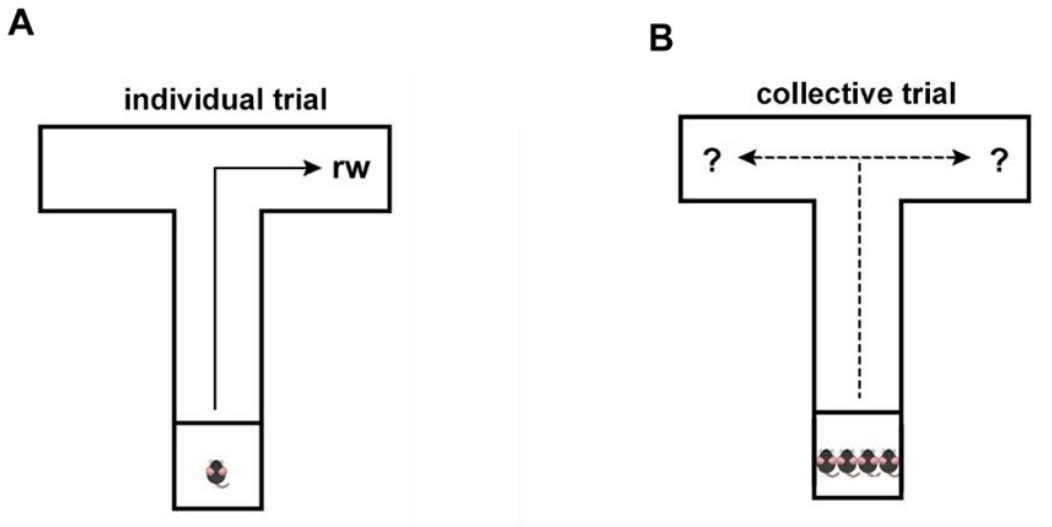

Figure 1. Collective spatial navigation task. *(**A**) In the training phase, littermate mice were individually trained (8 trials per day) to navigate the maze foraging for food located at the end of an arm. (**B**) In the testing phase, littermate mice, performed two blocks of four individual trials followed by one collective trial (i.e., all four littermates together). From every litter, two random mice were consistently trained to look for food in one arm and the remaining two mice in the opposite arm.*

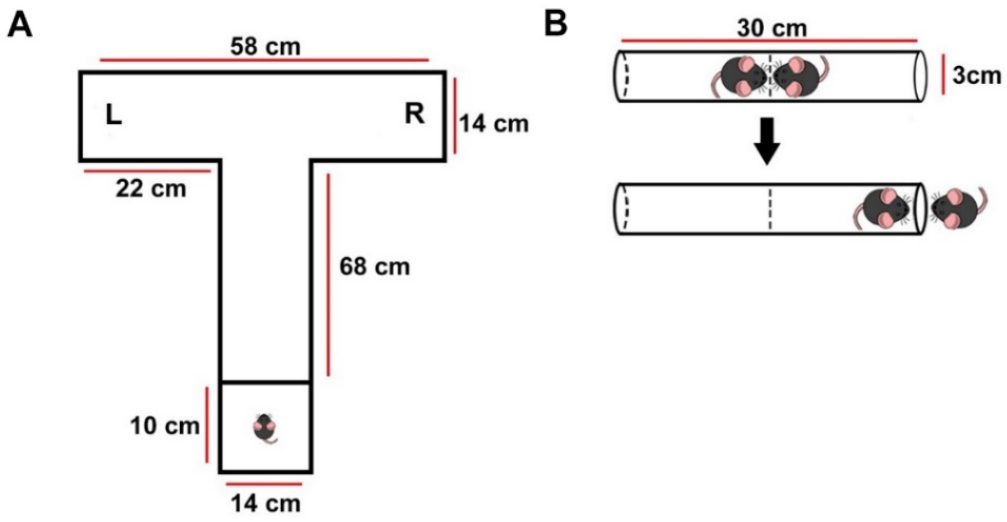

Figure 2. Dimensions of behavioral apparatuses. *T-maze (**A**) and tube test (**B**). Dimensions are in cm.*

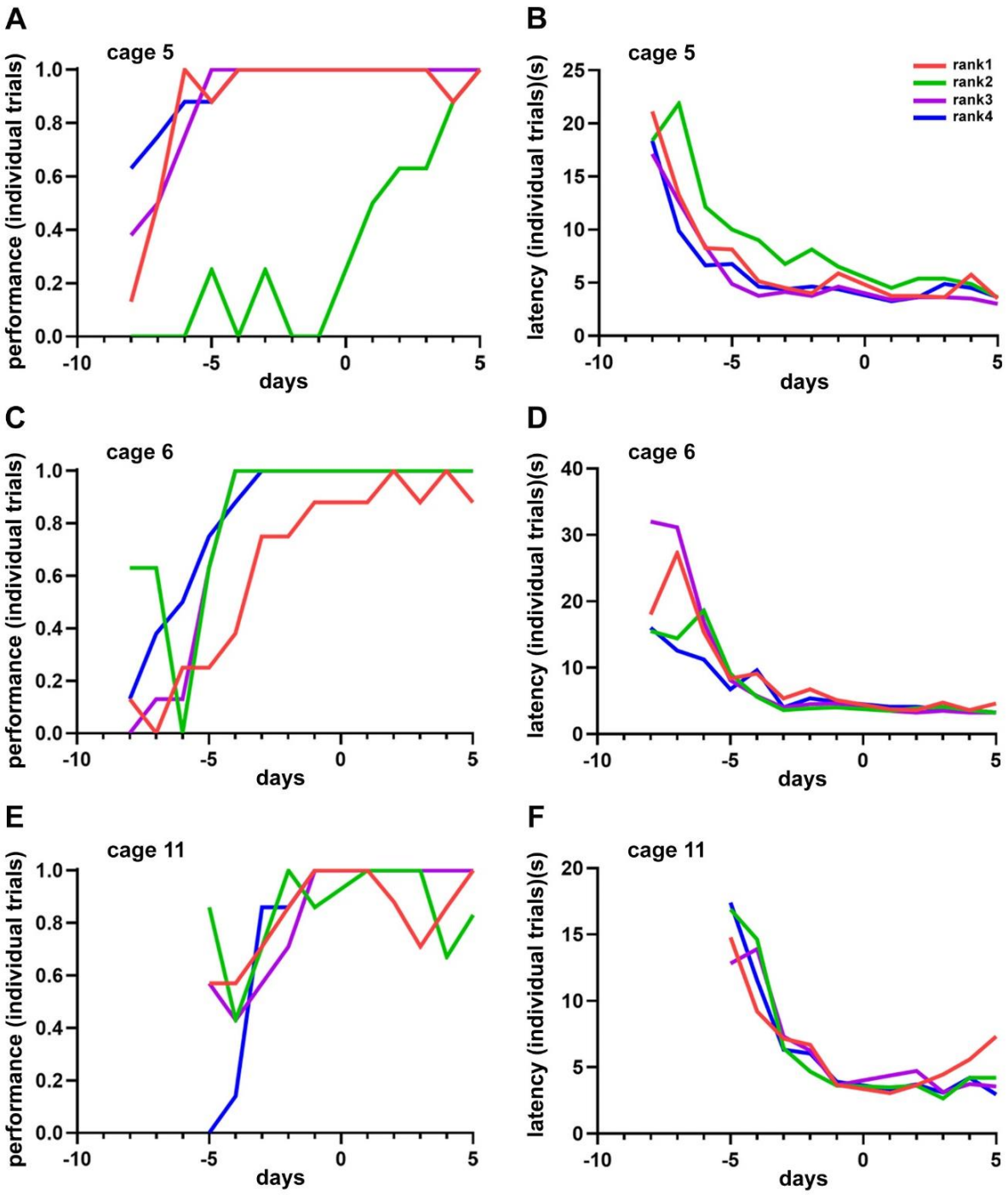

Figure 3. Example of learning curves according to social rank*. Curves are showing the performance (**A, C, E**) and latency (**B, D, F**) for individual cages of littermates. Colored lines represent averages.*

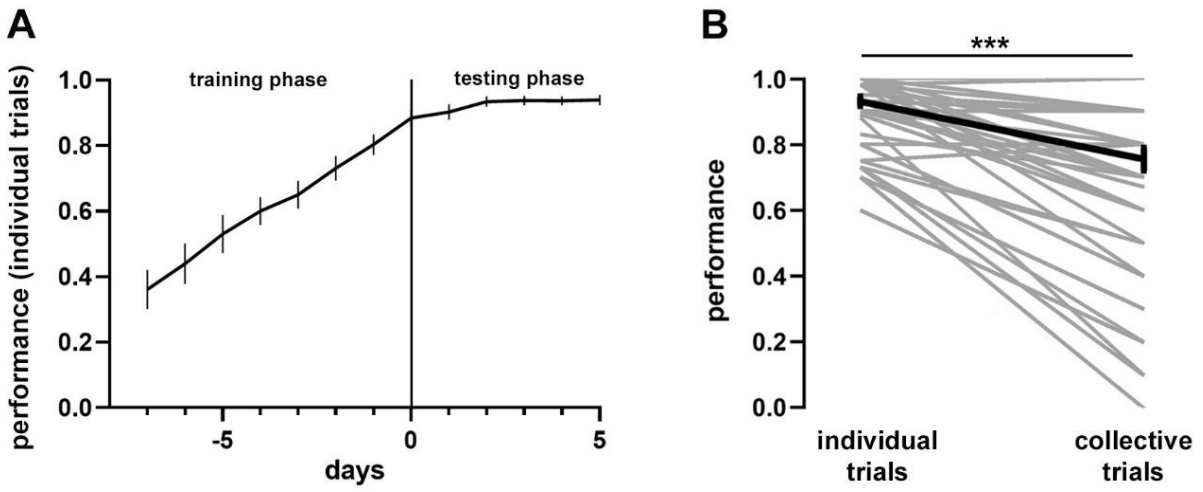

Figure 4. Behavioral performance in individual and collective trials. *(**A**) Average task performance (the proportion of correct arm choices) for all mice (n = 60 animals) tested individually during both training (days -7 to 0) and testing (days 1 to 5) task phases. (**B**) Average task performance for mice analyzed during the testing phase of the task (collective and individual trials). Gray lines are individual mice, and black lines represent population averages ± SEM, n = 60 animals. Wilcoxon signed-rank test, *** P < 0.001.*

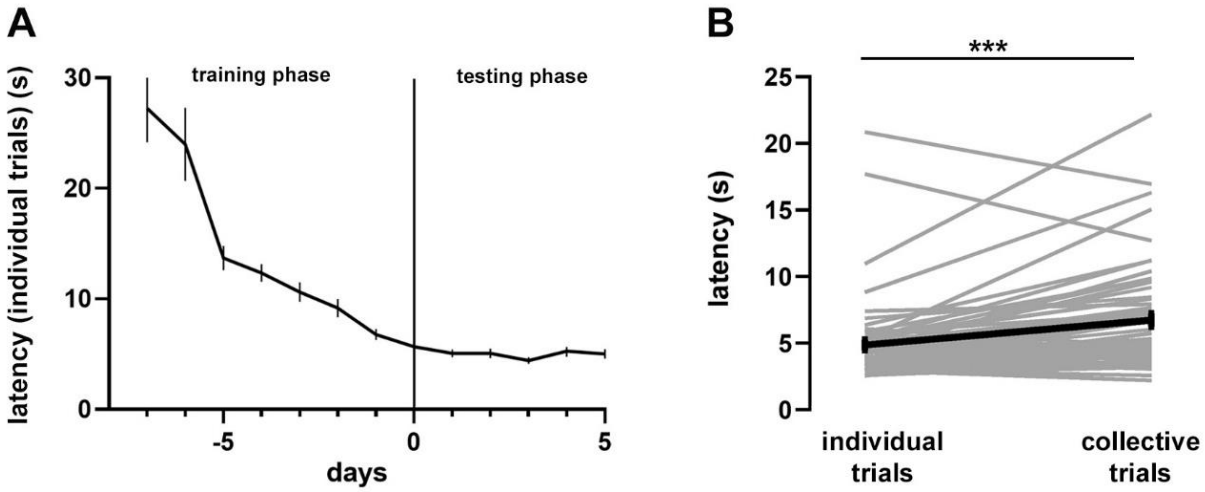

Figure 5. Behavioral time in individual and collective trials. *(**A**) Average task latency (time interval to reach the correct arm) for all mice (n = 60 animals) tested individually during both training (days -7 to 0) and testing (days 1 to 5) task phases. Average task latency (**B**) for individual mice during collective and individual trials of the testing phase of the task. Gray lines are individual mice, and black lines represent population averages ± SEM, n = 60 animals. Wilcoxon signed-rank test, *** P < 0.001.*

Throughout sessions, performance, and latency co-varied linearly **(R^2 = 0.642, P < 0.0001, Fig. 6A)**, suggesting their interdependence **(Table S1)**. Littermates were sequentially trained in the same session, and since learning rates varied among mice, the learning criterion was defined based on litter performance (3 of 4 littermates reaching 0.75 performance during two consecutive days). Once the learning criterion was reached, mice started the testing phase of the protocol, in which four consecutive individual trials were alternated with a collective trial so that all four littermates simultaneously performed the navigation **(Fig. 1B)**. To prevent learning of the reward location during collective trials, the arms were randomly baited in every collective trial, so there was no rule to be acquired, and therefore, to be able to focus on social interactions during collective navigation.

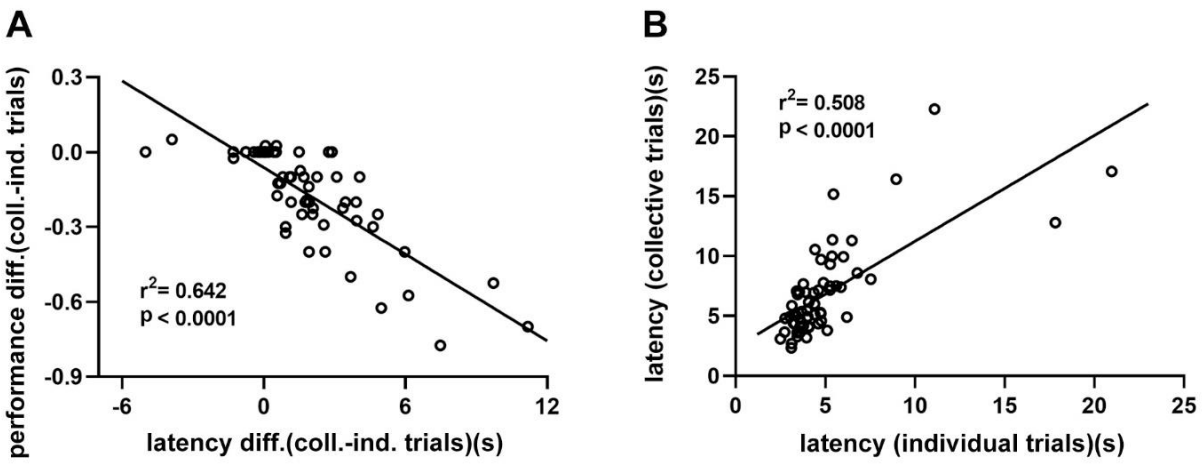

Figure 6. Linear regressions of behavioral parameters on mice performing the T-maze navigation test*. (**A**) Average of delta performance (collective – individual) vs delta latency (collective – individual) of all mice (r^2 = 0.642, P < 0.0001 and n= 60 animals). (**B**) Average of collective latency vs average individual latency of all animals (r^2 = 0.508, P < 0.0001, n = 60 animals). Circles denote the average of individual mice and the black line the best linear fitting.*

During the testing phase of the task, both performance and latency of individual trials reached a plateau and were stable over the remaining testing period, suggesting that the task had been acquired and consolidated **(Fig. 4A, Fig. 5A)**. When comparing the individual (0.93 ± 0.01) and collective (0.75 ± 0.03) trials, I found a significant drop in task performance **(P < 0.0001, Fig. 4B)**, suggesting a social effect in the process of decision-making of individual mice during collective navigation. The drop in performance was determined mainly by task acquisition in the previous training phase, as animals performing well during individual trials showed little effect on their performance during collective trials **(R^2 = 0.582, P < 0.0001, Fig. 7)**. Conversely, task latency during the testing phase increased for mice when comparing individual (4.99 ± 0.40 s) and collective (6.86 ± 0.49 s) trials **(P < 0.0001, Fig. 5B)**. Increased latency was proportional to the previous task acquisition since mice exhibiting short-latency during

individual trials increased less their latency during collective trials **(R^2 = 0.508, P < 0.0001, Fig. 6B)**. Hence, the social context produced a shift in decision-making, which was reflected in the decay of performance and a proportional increase in latency during goal-directed, collective spatial navigation.

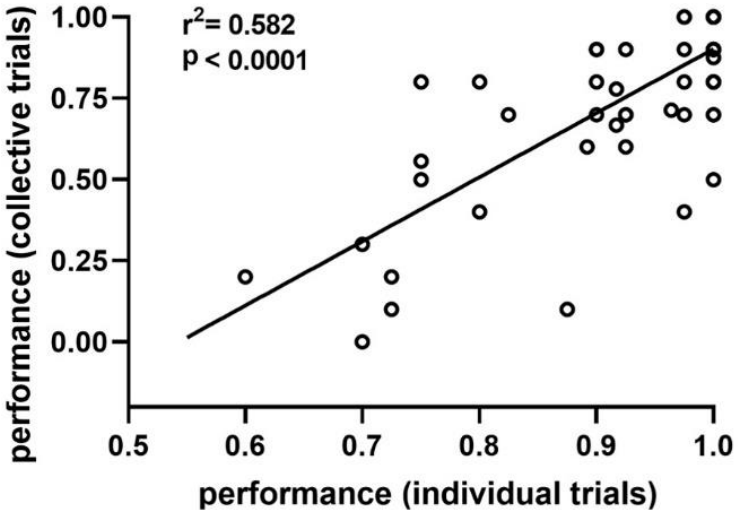

Figure 7. Linear regression of behavioral performance in mice performing the T-maze navigation test*. Linear regression (r^2 = 0.582, P < 0.0001, n = 60 animals) between average navigation performance of individual mice during individual trials against average navigation performance of individual mice during collective trials. Circles denote the average of individual mice and the black line the best linear fitting.*

Movement decisions in animal groups often depend on contingent social interactions among individuals (Conradt et al., 2003; Couzin et al., 2002). Indeed, during collective movement, animals tend to be attracted to other individuals to avoid being isolated and to align themselves with neighbors (Partridge et al., 1980; Partridge, 1982). Thus, it is possible reasoned that during collective movement, mice might modify their previously

learned trajectory depending on the distribution of animals in the maze arms. To test this idea, I calculated for every mouse the relative average density of animals in the selected arm and projected it against its average performance during collective trials **(R^2 = 0.2523, P < 0.0001, Fig. 8A)**. Importantly, the performance during collective trials was inversely proportional to the relative density of animals in the selected arm.

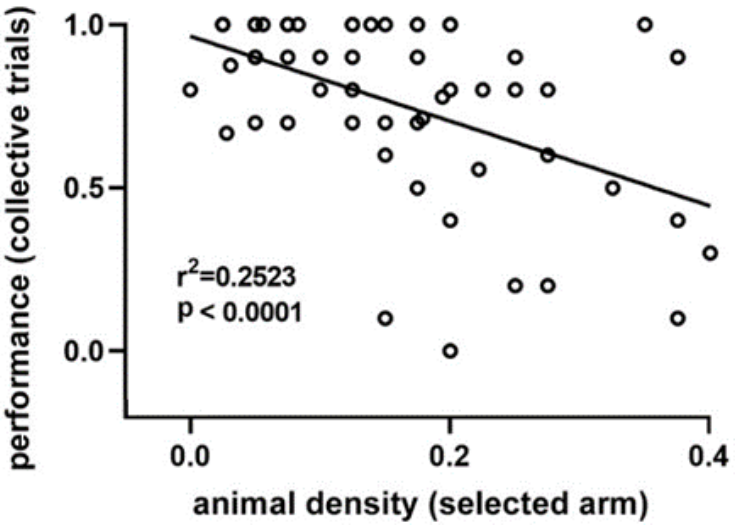

Figure 8. Linear regression of animal density and behavioral performance of mice performing the T-maze navigation test*. Linear regression (r^2 = 0.2523, P < 0.0001, n = 60 animals) between the proportion of mice located in the selected arm against average navigation performance of individual mice during collective trials. Circles denote the average of individual mice and the black line the best linear fitting.*

Conversely, there was no relation between the proportion of animals located in the opposite arm and performance during collective trials **(R^2 = 0.019, P = 0.2930, Fig. 9)**. That is the density of animals in the selected arm correlated with decreased task performance in the social context. To further explore this observation, I used a mixed

logistic model to assess the influence of the spatial distribution of animals on task performance during collective navigation **(Table 1 and Table 2)**. Thus, was confirmed the significant influence of animal density in the arms in shifting the decision-making strategy of individuals during collective navigation, with particular relevance to the proportion of mice located in the selected arm **(P = 6.41e-11)**. That is, the more animals accumulated in a lateral arm, the more likely it was a mouse to move to that arm, regardless of the previously learned reward location. Thus, sensory evidence arising during contingent social interactions can modulate memory-based learned reward values and bias decision-making during collective spatial navigation.

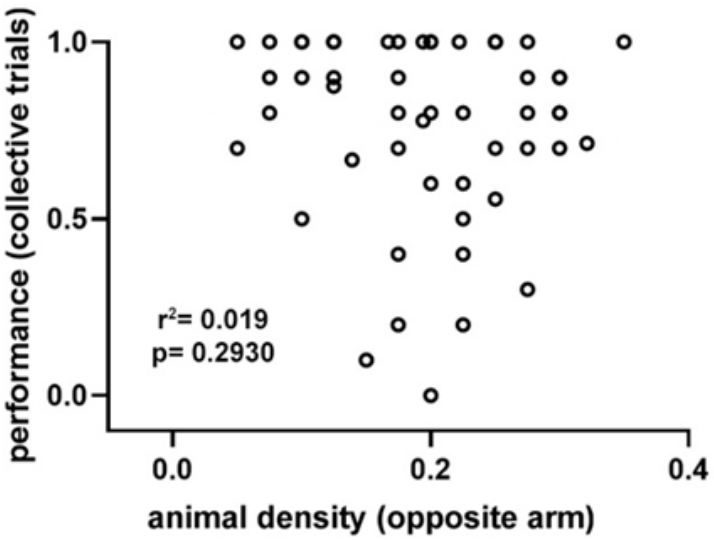

Figure 9. Linear regression of animal density and behavioral performance of mice performing the T-maze navigation test*. Linear regression between average animal density in the opposite arm navigation and performance of individual mice during collective trials (r^2 = 0.019, P = 0.2930, n = 60 animals). Circles denote the average of individual mice and the black line the best linear fitting.*

Parameter	estimate	SE	P
intercept	0.2721	0.8258	0.741770
individual performance	2.8035	0.8182	*0.000612*
animal density - selected arm	-3.1858	0.4876	*6.41e-11*
animal density - opposite arm	-1.5323	0.4978	*0.002085*
total animal density	1.0492	0.3206	*0.001066*

Table 1. *The mixed logistic model with fixed effects for collective task performance (n = 60 animals used for behavioral tests).*

Parameter	estimate	SE	P
intercept	-0.1794	1.3608	0.89513
individual performance	3.1845	1.3582	*0.01905*
animal density - selected arm	-2.4680	-3.075	*0.00211*
animal density - opposite arm	-1.1839	0.7862	0.13
total animal density	0.78	0.52	0.13

Table 2. *The mixed logistic model with fixed effects for collective task performance (n = 21 animals used for electrophysiological experiments).*

5.1.2. The social context influences the dominance hierarchy during a collective spatial navigation task

I found that contingent social interactions arising during collective navigation can modulate individual behavior. Next, I explored the role of inherent social interactions, such as the dominance hierarchy (Lindzey et al., 1969), on collective performance. For this, I first assessed the hierarchical social relations of mice with the tube test (Wang et al., 2011) in parallel to the spatial navigation task. This test measures the dominance tendency by placing pairs of mice in a narrow tube facing each other, where one mouse forces the other out backward to obtain a victory **(Fig. 2B)**. A social ranking was recognized based on the success rate of mice in pair-wise testing using a round-robin design **(Fig. 10A)**. As previously described, time in the tube was shorter as the ranking difference increased **(P = 6.92e-11, Fig. 10B)**.

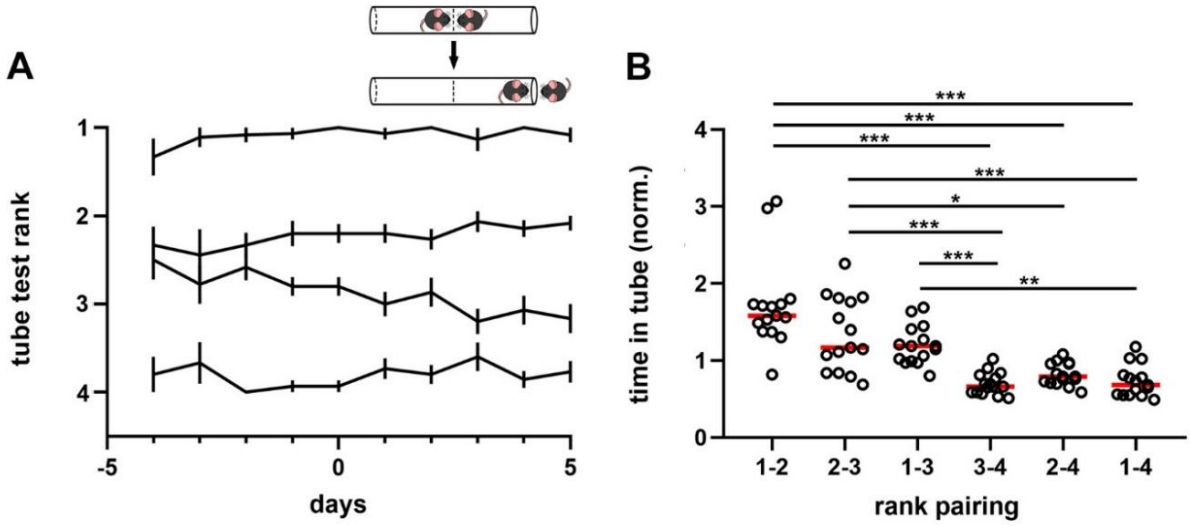

Figure 10. The dominance hierarchy of animals performing the collective spatial navigation task. *(**A**) Summary plot for all measured animals (n = 60 animals). Lines show average rank position based on the proportion of victories in the tube test (inset) correlative to the spatial navigation test (days -4 to 0, training phase; days 1 to 5, testing phase). Ranking 1 is dominant; ranking 2, first active subordinate; ranking 3, second active subordinate; ranking 4, submissive. Note ranking stability over time, particularly for dominant mice. Inset, schematic of the tube test used to identify the mice ranking system. (**B**) Normalized time spent in the tube for the six pairing conditions for all measured animals (n = 60 animals). One-way ANOVA, P = 6.92e-11. Black lines represent population average ± SEM, circles denote the average of individual mice, and the red lines are the population average. * P < 0.05; ** P < 0.01; *** P < 0.001.*

The dominance hierarchy was stable over time, particularly for the dominant mouse, whose position was rarely challenged during the whole experimental protocol **(Fig. 11)**.

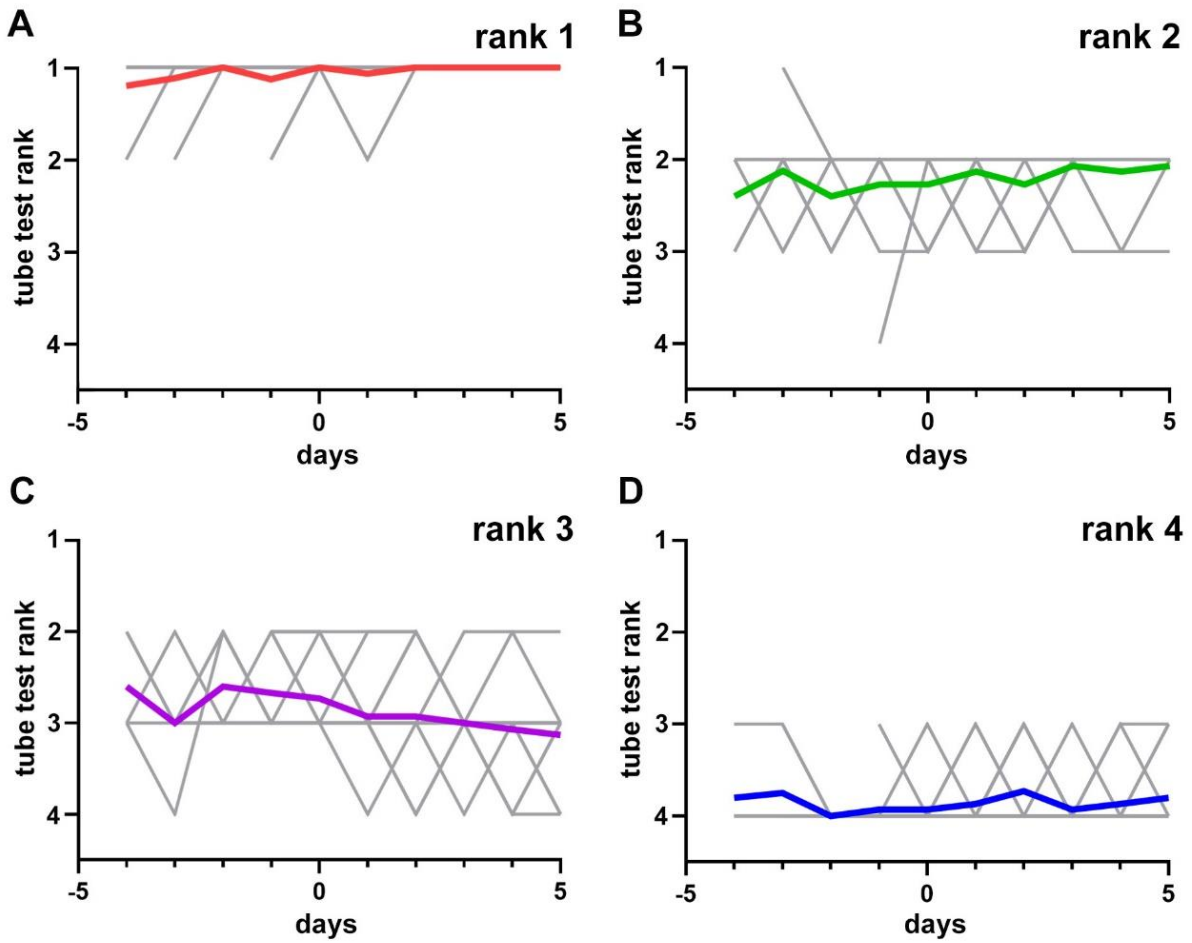

Figure 11. Summary of dominance hierarchy of animals performing the collective spatial navigation task*. Summary plots for all measured animals (n = 60 animals) according to social ranking. Days -5 to 0, training phase; days 1 to 5, testing phase. (**A**) Ranking 1 is dominant; (**B**) ranking 2, first active subordinate; (**C**) ranking 3, second active subordinate; (**D**) ranking 4, submissive. Colored lines represent averages, and gray lines are average of individual mice. Note ranking stability over time, particularly for dominant mice.*

Interestingly, the dominant mouse was not the largest animal in the group, as body masses were not different between rankings, neither under ad libitum access to food

(P = 0.822, Fig. 12A and Fig. 13) nor under food restriction during the navigation test **(P = 0.655 Fig. 12B and Fig. 13)**.

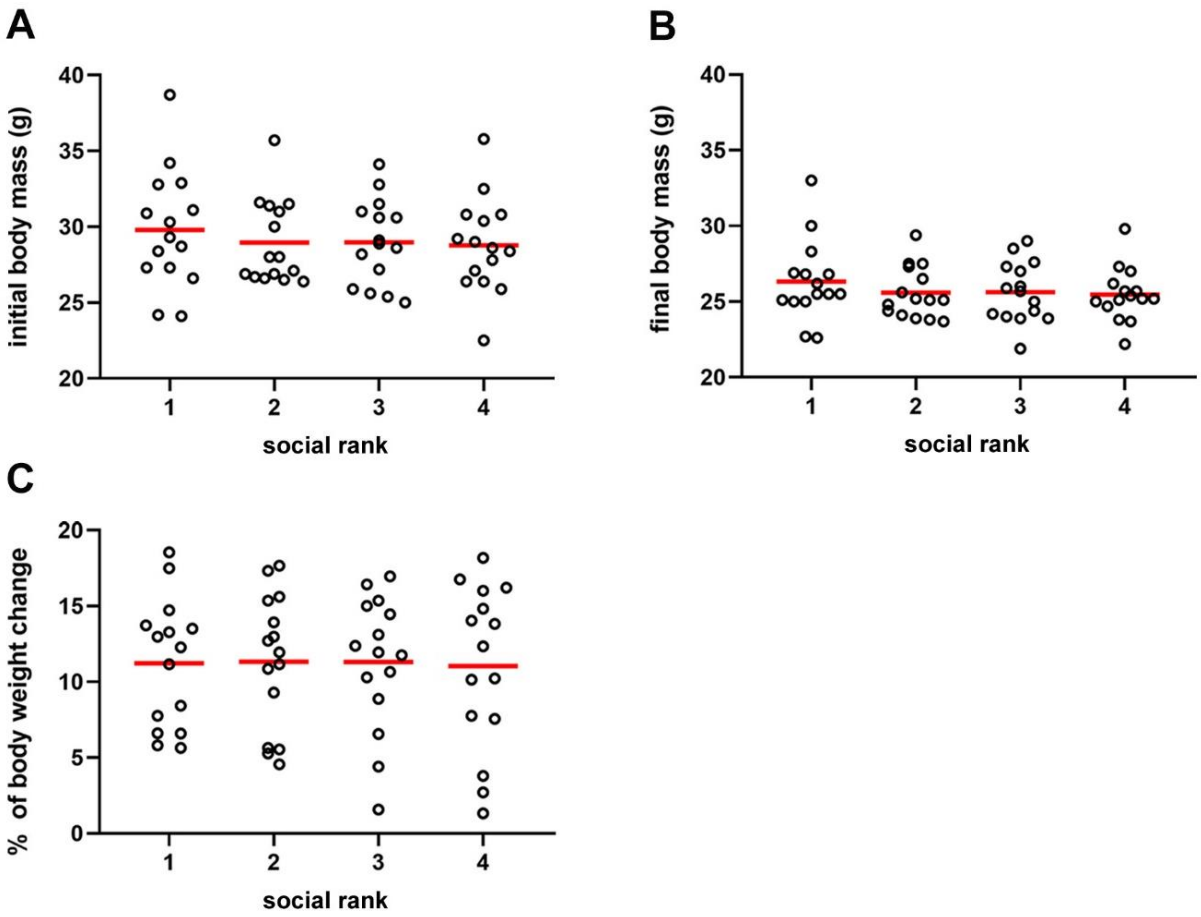

Figure 12. Summary body weight of animals performing the collective spatial navigation task. *Summary plots for all measured animals (n = 60 animals) according to social ranking with free access to food (**A**) and during food restriction (**B**). Note that dominant animals do not exhibit different body mass. (**C**) Maximal weight loss during food restriction protocol. Circles denote the average of individual mice, and the red lines are the population average. One-way ANOVA; A, P = 0.8216; B, P = 0.6554; C, P = 0.9983.*

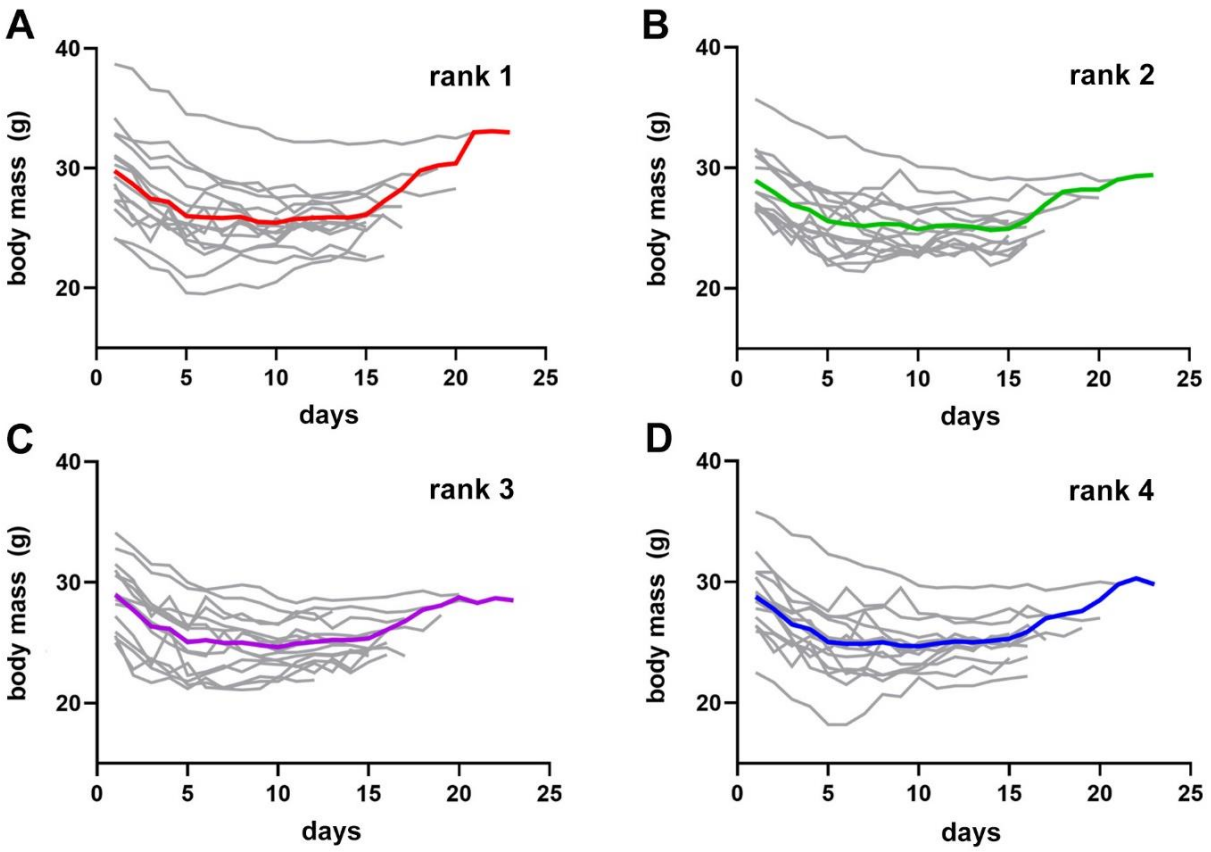

Figure 13. Bodyweight curves of animals performing the collective spatial navigation task. *Summary plots for all measured animals (n = 60 animals) according to social ranking. Day 0 represents the initial weight. (**A**) Ranking 1 is dominant; (**B**), ranking 2, first active subordinate; (**C**) ranking 3, second active subordinate; (**D**) ranking 4, submissive. Food was restricted from day 1 for every mouse until it reached roughly 85% of its original weight. Colored lines represent averages, and gray lines are average of individual mice.*

Also, the social rank was not relevant for task acquisition as neither performance nor latency **(P > 0.05, Fig. 14A; P > 0.05, fig. 14B)** were different between animals according to their dominance hierarchy during the training phase of the navigation task **(Fig 15)**. Similarly, the time required to reach the learning criterion was not different between social rankings and performance according to social ranking was stable during the testing phase of the test **(P = 0.459, Fig. 14C; P = 0.961, Fig. 14D)**.

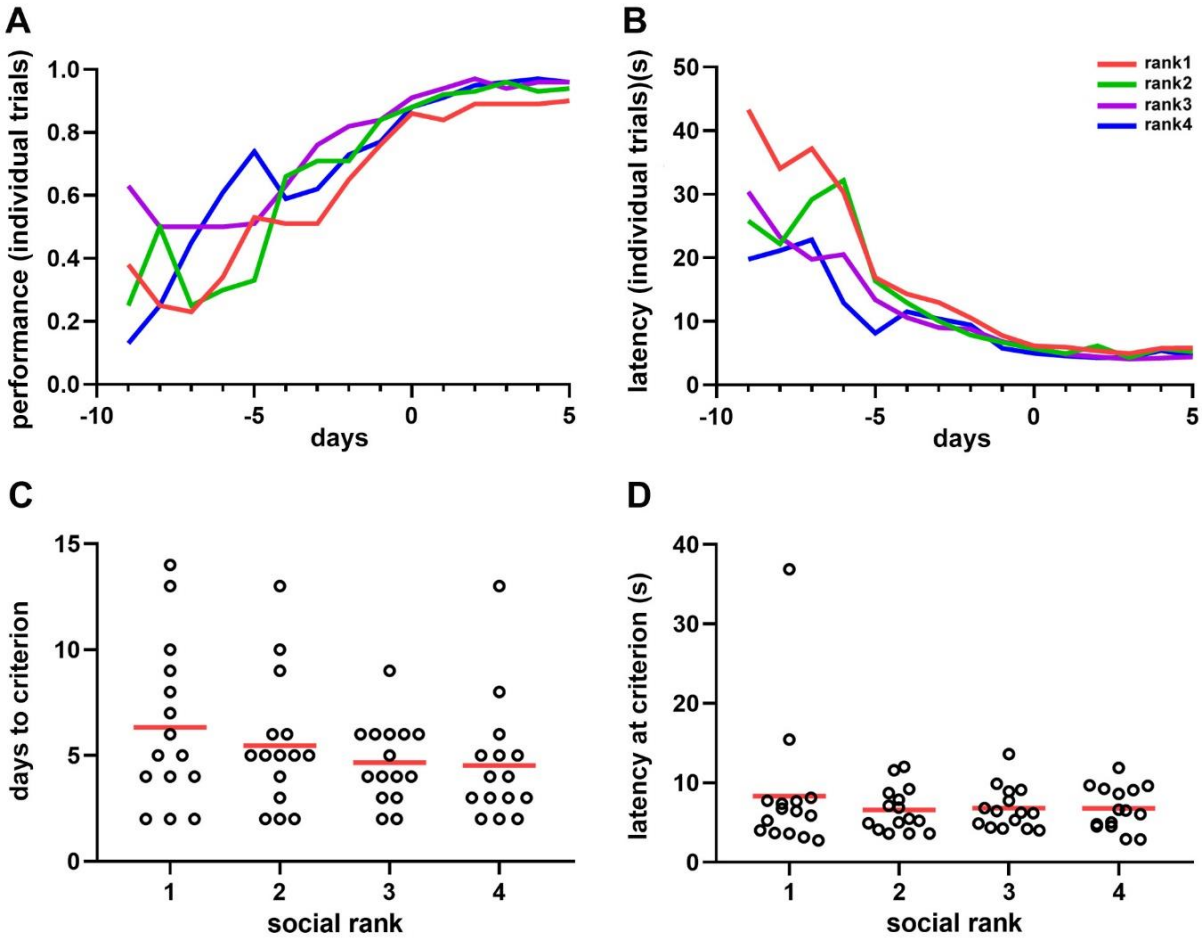

Figure 14. Average task performance of animals performing the collective spatial navigation task. *Summary plot for all measured animals (n = 60 animals) according to social rank in the proportion of correct arm decisions (**A**) and task latency. (**B**) Time interval to reach the correct arm for all mice (tested individually during both training (days -10 to 0) and testing (days 1 to 5) task phases (Kruskal-Wallis test, P corrected with FDR in A and B, P > 0.05. Differences between rankings were not significant. (**C**) Time to reach the learning criterion according to social ranking during the training phase. (**D**) Average task latency on the day animals reaches the learning criterion. Differences between rankings were not significant, Kruskal-Wallis test, P = 0.4585 in C; P = 0.9609 in D. Circles denote the average of individual mice, the red lines are the population average, and colored lines represent averages.*

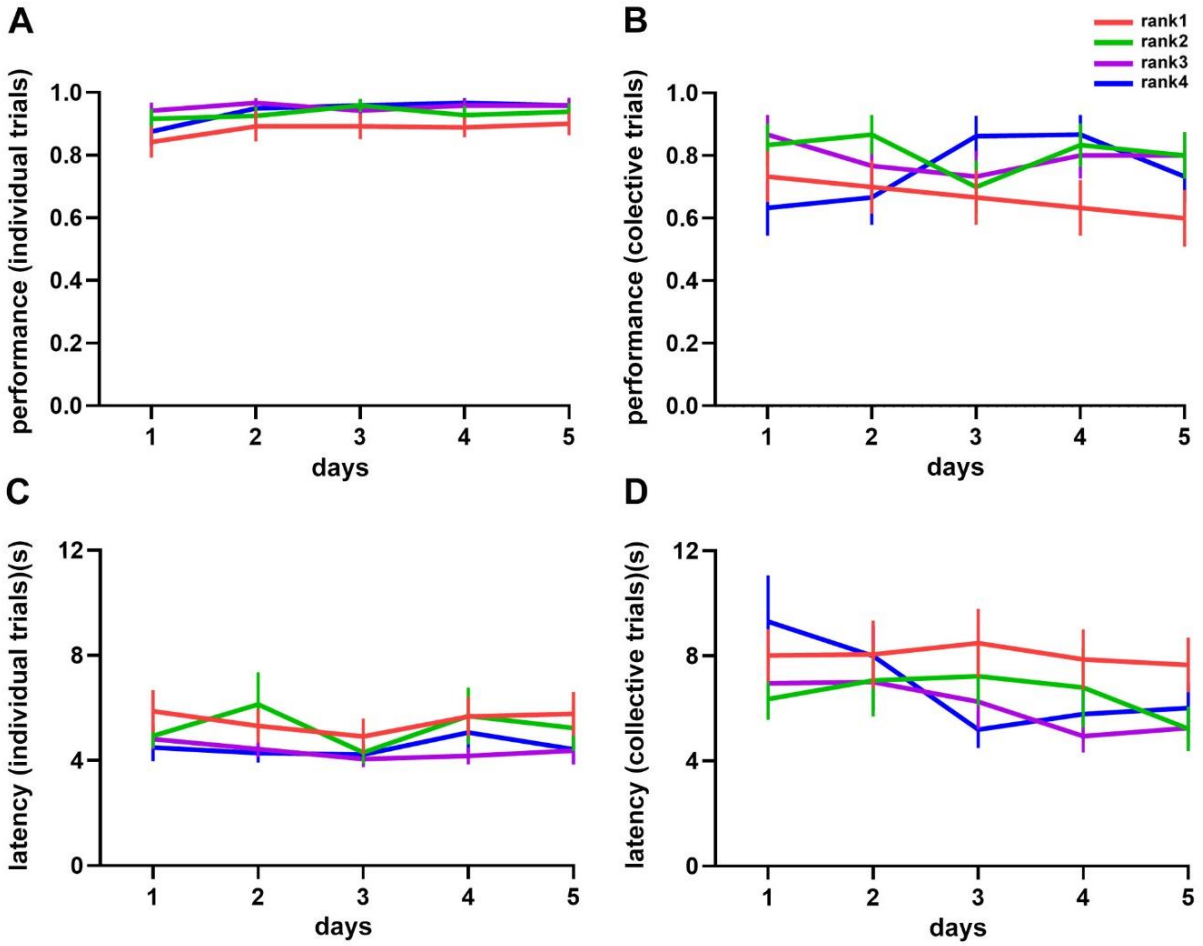

Figure 15. Average T-maze task performance during the testing phase of the task according to social rank*. Summary plot for all measured animals (n = 60 animals) according to social rank in behavioral performance (**A**, **B**) and latency (**C**, **D**) during the testing phase for the individual (**A**, **C**) and collective (**B**, **D**) trials for all animals (n = 60 animals). Colored lines represent population averages ± SEM.*

During the testing phase of the task, neither the drop in performance nor the increase in latency during collective trials was modulated by the dominance hierarchy, as it was not different between social groups **(P = 0.655, Fig. 16A; P = 0.565, Fig. 16B)**.

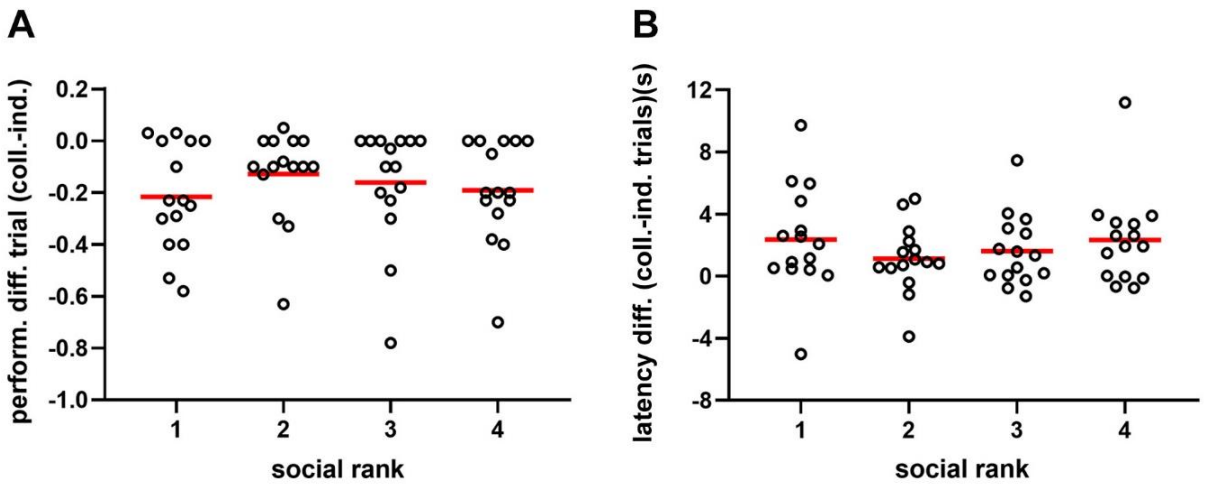

Figure 16. Summary of behavioral parameters of the T-maze task during the testing phase. *Summary plot for all measured animals (n = 60 animals) according to social rank in performance (**A**) and latency (**B**) difference between collective and individual trials during the testing phase of the task. One-way ANOVA, A, P = 0.655; B, P = 0.565. Circles denote the average of individual mice, and the red lines are the population average.*

I showed that contingent social interactions affect individual decision-making during spatial navigation, with the spatial distribution of animals in the maze being correlated with task performance. Hence, I compared between social groups the animal density in the selected arm during collective navigation. I found that when compared to the subordinate groups, dominant animals moved to the maze arm that was more densely populated, regardless of the location of reward **(P = 0.007, Fig. 17A)**. No such difference was detected in the opposite arm **(P = 0.228, Fig. 17B)**. Besides, the animals do not present differences in latencies from start box to the decision point in the T-maze according to social rank **(P = 0.275 Fig 18)**, evidencing that the animals present similar times of navigation towards the decision point. This result suggested that dominant mice may be more influenced by the social context than the other groups. I reasoned

that the predisposition of individual mice to change their decision according to the distribution of littermates in the maze could be assimilated to the influence of the social context on individual behavior. To obtain an estimate of such social influence, I computed for every individual mouse the regression coefficient of the spatial distribution of mice on the maze against its task performance in the social context and called it the 'peer susceptibility index' **(PSI, median = 0, IQR= 35.13)**. Since the PSI was proportional to the social influence on individual behavior, the larger its value, then the stronger the effect of the social context on task performance. Thus, negative values reflect a detrimental effect of the social context, whereas positive values indicate a beneficial effect on task performance. Importantly, the PSI was significantly different between dominant mice and the subordinate groups **(P = 0.008, Fig. 19)**, thus suggesting that dominant mice were more likely to shift their decision in the social context. Moreover, differences in the PSI did not result from different overall distributions of littermates in the maze during collective navigation according to the dominance hierarchy **(P = 0.178, Fig. 17C)**. Altogether, these results suggest that mice exhibit differential susceptibility to contingent social interactions, outlined by dominance hierarchy, an inherently social interaction.

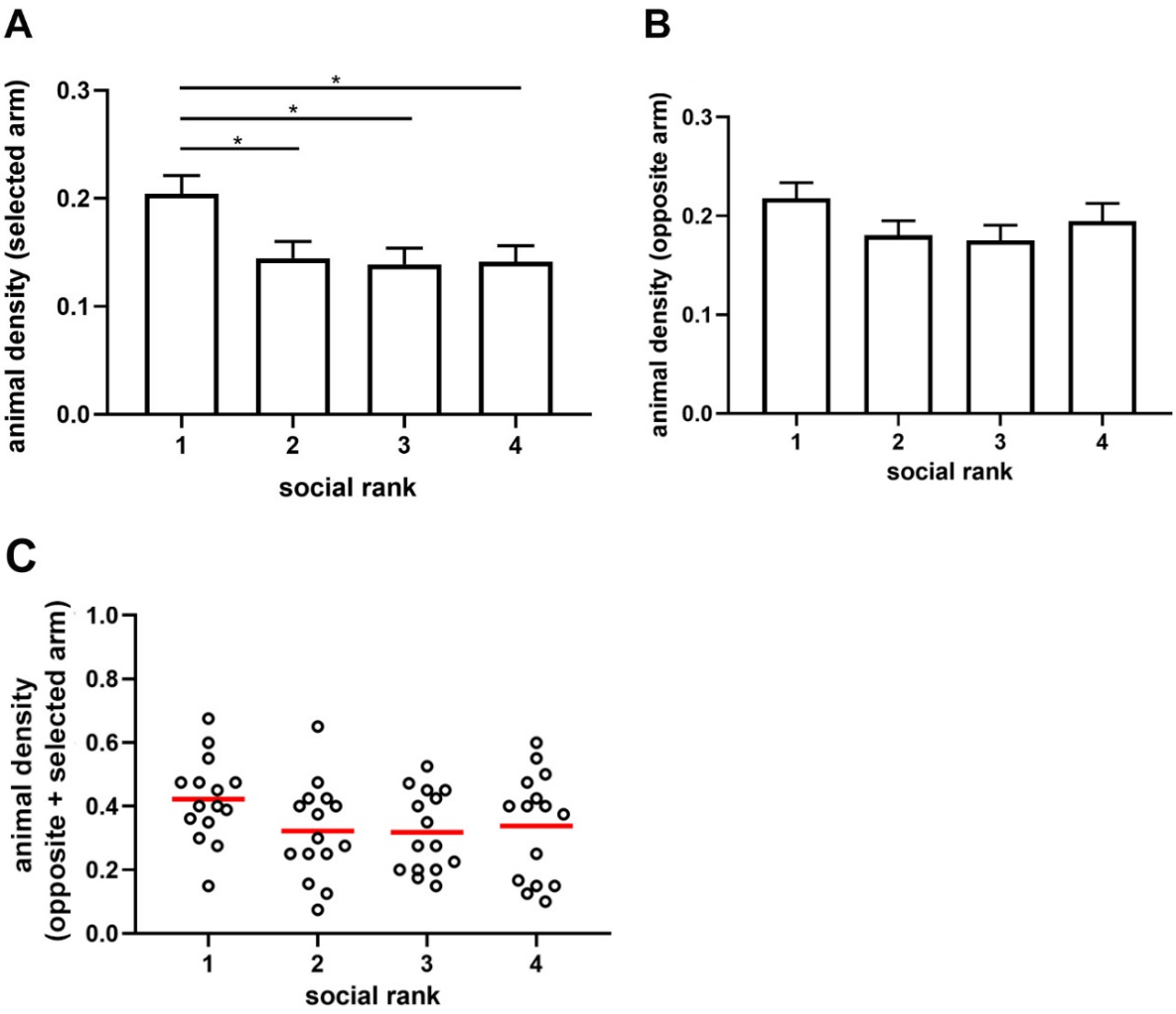

Figure 17. Animal density in the selected arm and social influence during collective navigation. *Summary plot for all measured animals (n = 60 animals) according to social rank in Animal density (**A**) in the selected arm, one-way ANOVA, P = 0.007, n = 60 animals. (**B**) Animal density in the opposite arm, one-way ANOVA, P= 0.228, n = 60 animals. (**C**) The average density of animals located in both lateral arms at the moment of the decision according to social ranking. One-way ANOVA, P = 0.178, n = 60 animals. Circles denote the average of individual mice; the red line is the population average, and bars represent average ± SEM. * P < 0.05.*

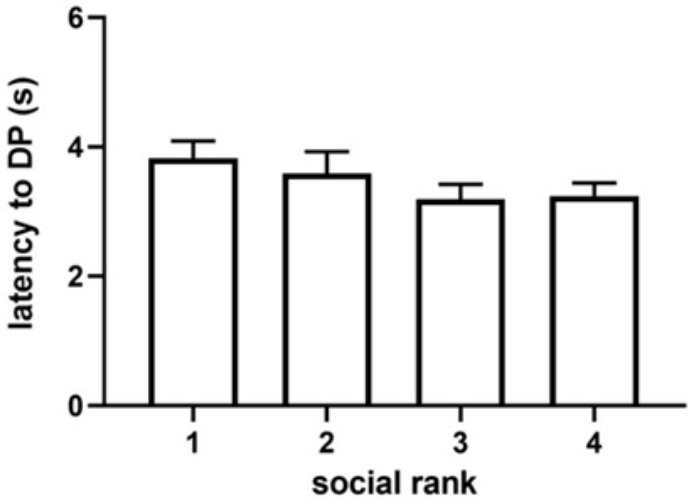

Figure 18. Latencies to decision point during collective navigation. *Latencies from start box to the decision point in the T-maze according to social rank. One-way ANOVA, P = 0.275, n = 60 animals. Bars represent average ± SEM.*

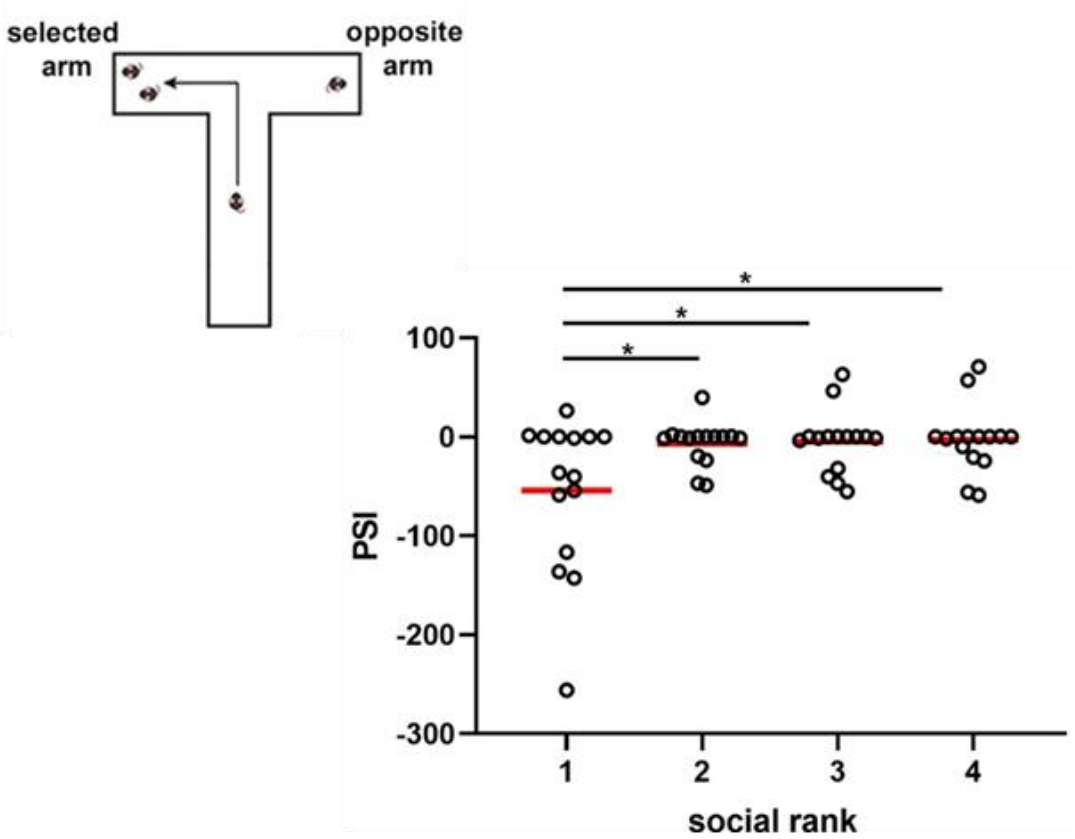

Figure 19. Social influence during collective navigation. *Peer sensitivity index (PSI) by social rank, one-way ANOVA, P = 0.0084, n = 60 animals. Circles denote the average of individual mice; the red line is the population average. * P < 0.05.*

5.2. SPECIFIC OBJECTIVE 2: CHARACTERIZE THE INTRINSIC CORTICAL OSCILLATORY ACTIVITY OF THE HIPPOCAMPUS-PFC SYSTEM AND THEIR SPIKE TIMING CONCERNING TO THE SOCIAL RANKING SYSTEM

5.2.1. The Intrinsic spiking activity in the PFC correlates with social ranking and dominance behavior

So far, I have shown that contingent social interactions can bias decision-making in the social context. Nevertheless, the influence of contingent social interactions in shifting decisions is delineated by a dominance hierarchy, an intrinsic social interaction. Previous studies have established the neural basis of a dominance hierarchy in the synaptic connectivity of the mPFC (Wang et al., 2011; Wang et al., 2014). Hence, I studied the relationship between intrinsic cortical dynamics and social ranking system. For that, I recorded spontaneous rhythmic cortical activity in animals with stereotaxically implanted multi electrodes in both the hippocampus and mPFC **(Fig. 20 and Fig. S4)**, which are both required for goal-directed spatial behavior (Negrón-Oyarzo et al., 2018). To focus on intrinsic activity and connectivity patterns during spontaneous cortical dynamics and minimize behavioral confounds resulting from different social rankings, I performed experiments under deep anesthesia. In order to compare relatively similar conditions, I first assessed the depth of anesthesia between groups. The power concentrated in the delta frequency band (0.5-4 Hz) of the PFC was not different between social groups **(P = 0.081, Fig. 21B)**, suggesting that the global cortical state was roughly similar **(Fig. 21A)**.

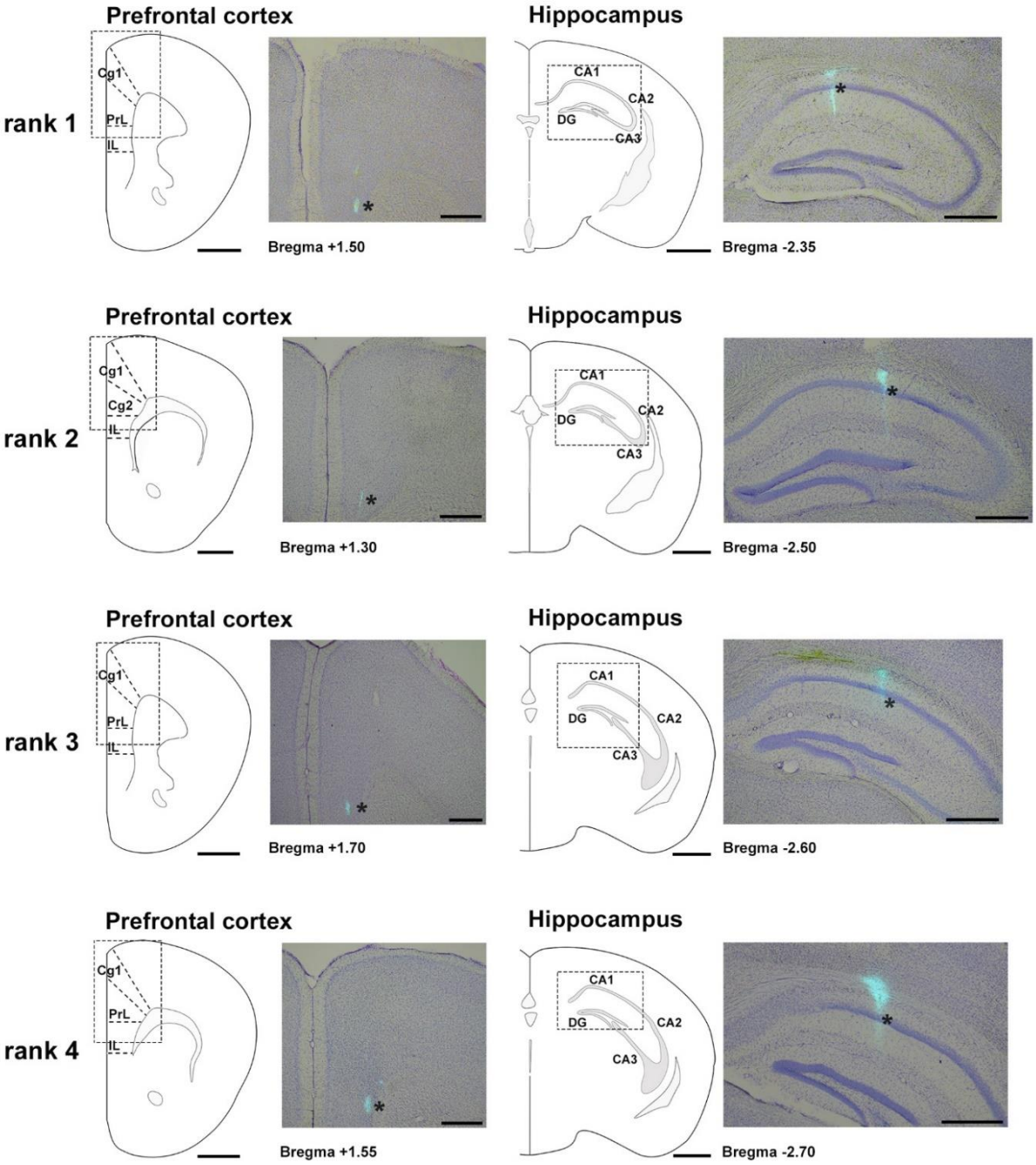

Figure 20. Anatomical location of recording electrodes*. Examples sorted by social ranking. Ranking 1 (mouse ID: CM99), ranking 2 (mouse ID: CM65), ranking 3 (mouse ID: CM64), ranking 4 (mouse ID: CM47). Brain sections were Nissl stained and superimposed to fluorescent micrographs showing electrode tracks (blue, asterisks) in both cortex and*

hippocampus. Cg1, cingulate cortex; PrL, prelimbic cortex; IL, infralimbic cortex. CA1, CA2, CA3, cornu ammonis fields; DG, dentate gyrus. Scale bar: 500 µm.

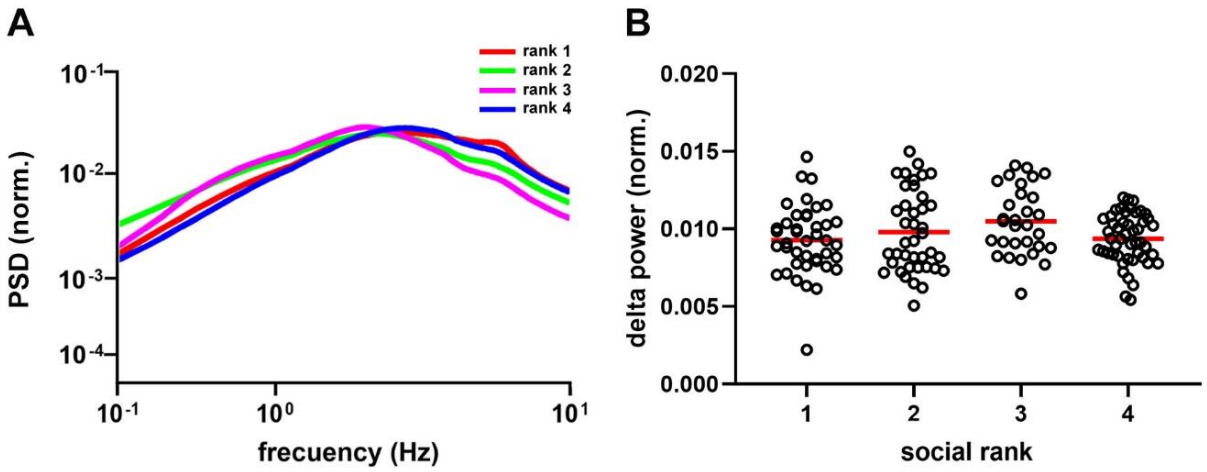

Figure 21. Delta waves oscillations in anesthetized mice*. Average (**A**) and peak (**B**) power spectral density of the PFC of anesthetized mice according to social ranking. Note that delta activity (0.5 - 4 Hz) is not different between social rankings. One-way ANOVA, P = 0.081, 159 sessions, n = 21 animals. Circles denote the average of individual mice, the red lines are the population average, and colored lines represent averages.*

It has been reported that dominant animals exhibit more substantial synaptic strength in the PFC than submissive mice (Wang et al., 2011). Hence, I tested whether such in vitro relation was translated into in vivo spiking patterns. For that, I first detected and extracted single-unit activity from the PFC recordings **(Fig. 22A and 22B)**. Indeed, I found that the overall firing rate in the PFC of dominant mice was larger than the subordinate groups **(P = 5.57e -11, Fig. 23A, Table S2)**. Moreover, the difference was specific to regular spiking cells **(P = 6.07e-12, Fig. 22D)**, putative principal neurons, as

it was not detected in fast-spiking units **(P = 0.624, Fig. 22C)**, putative interneurons. Hence, dominant mice exhibited larger levels of spontaneous spiking activity in the PFC.

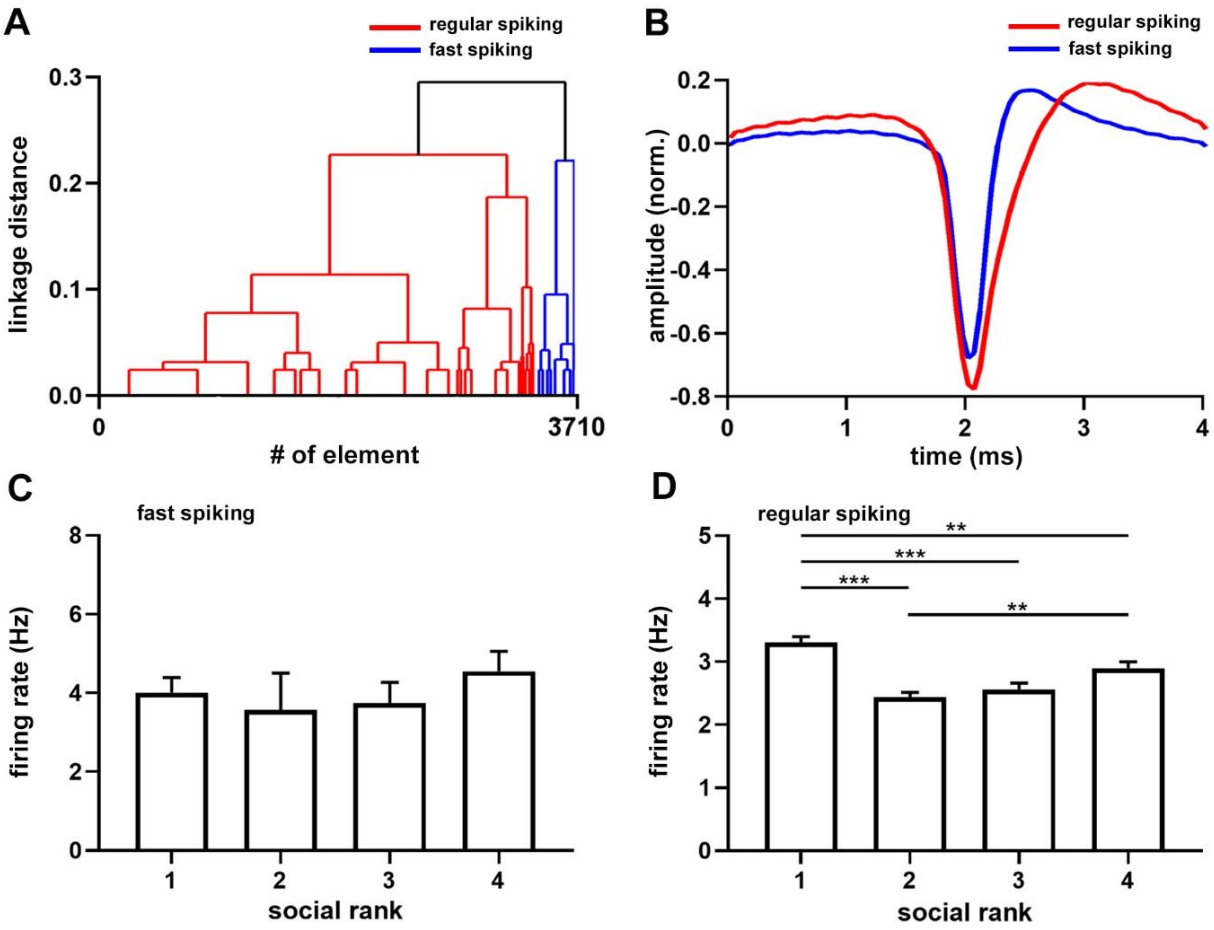

Figure 22. Cortical units recorded under anesthesia. *(**A**) Dendrogram of all recorded units (n = 3702, 22 animals). Red shows the largest cluster, regular spiking cells; blue shows the smallest cluster, fast-spiking cells. (**B**) Grand average of regular spiking (red, n = 320) and fast-spiking (blue, n = 3382) units. Neuronal firing rate sorted by social ranking for fast-spiking (**C**) and regular spiking (**D**) units. Note that regular spiking cells in dominant animal's discharge more than subordinate groups. One-way ANOVA, P = 0.6243 in C; P = 6.06e-12 in D. Bars represent average ± SEM. ** P < 0.01; *** P < 0.001.*

Recently, it has been reported that the firing rate in the PFC correlates with effortful activity and dominance behavior in the tube test (Zhou et al., 2017). Therefore, I compared intrinsic neural parameters and latency in the tube test **(Table 3)**. Interestingly, I found a significant positive correlation between the spontaneous prefrontal spiking activity (firing rate difference, winner-loser) and interaction time (latency difference, winner-loser) in the tube test **(R^2 = 0.226, P = 0.014, Fig. 23B)**. This result was further confirmed by multiple linear regression **(P = 0.009, Table 3)**. Furthermore, correlation was specific for regular spiking cells **(R^2 = 0.178, P = 0.032, Fig. 24B)**, putative pyramidal neurons, as it was not present in fast-spiking units **(R^2 = 0.106, P = 0.13, Fig. 24A)**, putative interneurons. Thus, the spontaneous firing rate in the PFC correlates with social ranking and dominance interaction time.

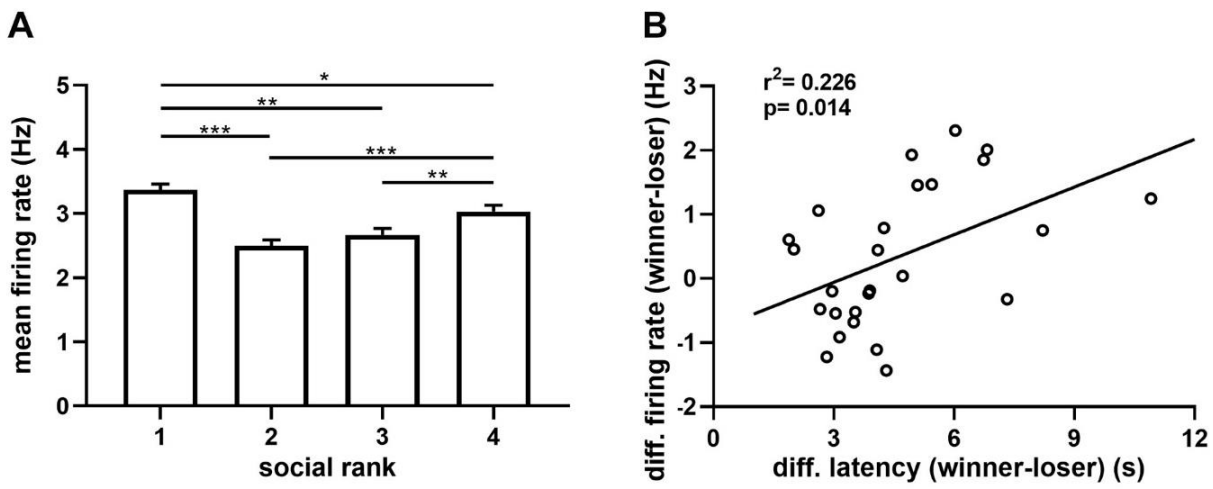

Figure 23. Intrinsic activity of PFC units and tube test task according to social rank. *(**A**) Average PFC single-unit firing rate by social ranking (n = 3702 units, 22 animals). (**B**) Linear regression between PFC firing rate difference (winner – loser) and tube test latency difference (winner – loser) (r^2 = 0.226, P = 0.014, n = 22 animals). Circles denote average of individual mice, black line the best linear fitting and bars represent average ± SEM. * P < 0.05; ** P < 0.01; *** P < 0.001.*

Parameter	estimate	SE	P
intercept	-0.14242	9.83315	0.98863
collective latency	0.47684	0.15791	*0.00862*
ripple frequency	0.01737	0.07250	0.81386
ripple amplitude	-0.48678	1.20544	0.69204
crosscorrelogram ripple-peak	-0.04911	0.90651	0.95751
crosscorrelogram post-ripple	1.79839	0.69635	*0.02081*

Table 3. *Multiple linear models for individual task latency (n = 21 animals used for electrophysiological experiments).*

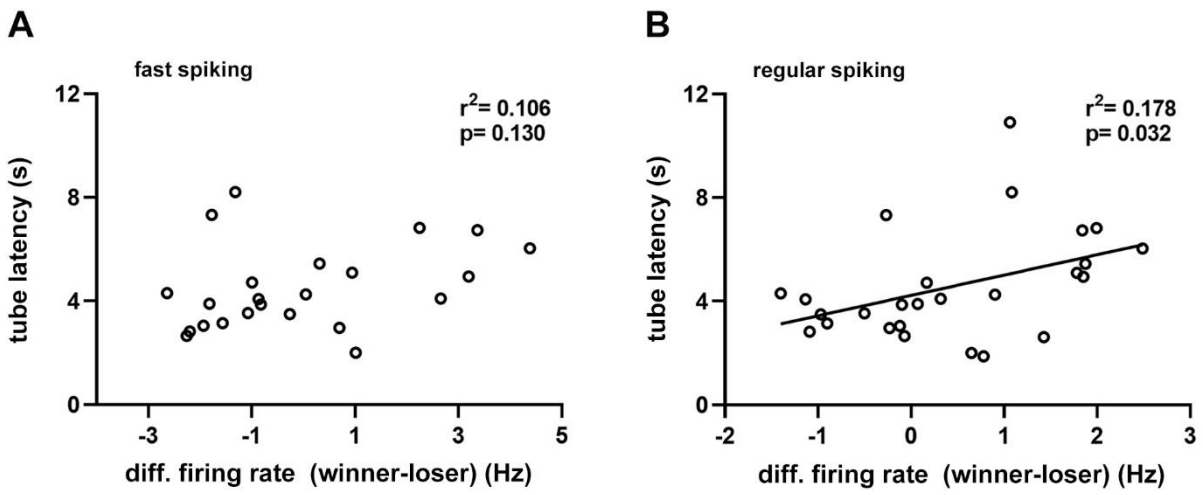

Figure 24. Linear regressions of Intrinsic neural parameters in PFC and behavioral latency in the tube test. *(**A**) Linear regression between the tube test latency difference (winner-loser) and the difference (winner-loser) of firing rate of fast-spiking cells (r^2 = 0.106, P = 0.130, n = 22 animals). (**B**) Linear regression between the tube test latency difference (winner-loser) and the difference (winner-loser) of firing rate of regular spiking cells (r^2 = 0.178, P = 0.032, n = 22 animals). Circles denote the average of individual mice and black lines the best linear fitting. Note that only regular spiking cells show a significant correlation.*

5.3. SPECIFIC OBJECTIVE 3: CORRELATE THE INTRINSIC CONNECTIVITY OF THE HIPPOCAMPUS-PFC SYSTEM WITH BEHAVIORAL PERFORMANCE IN INDIVIDUALS PERFORMING A COLLECTIVE SPATIAL NAVIGATION TASK

5.3.1. PFC intrinsic activity during hippocampal theta oscillations does not correlate with the process of decision-making during collective spatial navigation.

I investigated cortical oscillations across social groups. All animals exhibited epochs of prominent spontaneous theta oscillations **(4-8 Hz, Fig. 25A)** alternated with sharp-wave ripple episodes (100-250 Hz**, Fig. 27A**), characteristic of hippocampal exploratory and quiescent (Buzsáki, 2015) states; respectively. Theta oscillations, a marker of activated cortical states **(Fig. 25A)**, were prominent in the spectral distribution of field potentials **(Fig. 25B)** and consistently similar between social groups, showing comparable amplitude **(P = 0.388, Fig. 25C)**, frequency **(P = 0.052, Fig. 26A)**, and cumulative duration **(P = 0.099, Fig. 26B)**. Theta oscillations were also detected in the PFC, commonly associated with hippocampal theta waves **(Fig. 25A)**. Since oscillatory synchrony is a neural mechanism for the functional coupling of distributed neural circuits (Jones et al., 2005), I assessed the spontaneous spectral coherence in the local field potential activity of the hippocampo-PFC circuit. I identified elevated intercortical coherence in theta oscillations under anesthesia in all animals **(Fig. 25D)**, with no difference between social rankings **(P = 0.350, Fig. 25E)**. Cortical oscillations synchronize neuronal spiking, thus contributing to the temporal integration of neural activity. Therefore, I computed the oscillatory phase-locking of prefrontal neurons to hippocampal oscillations utilizing the pairwise phase consistency (PPC) (Hagan et al., 2012). As a population, prefrontal neurons were strongly modulated by hippocampal theta oscillations **(Fig. 25F)**, but there were no significant differences between social rankings **(P = 0.139, Fig. 25G)**. Then, I explored whether intrinsic cortical activity patterns of activated states correlated with animal behavior during spatial navigation.

For this, I performed multiple regression analyses, including several neural (theta oscillations) and behavioral (task performance) parameters. I did not detect significant regressors in this analysis **(Table 4 and Table 5)**.

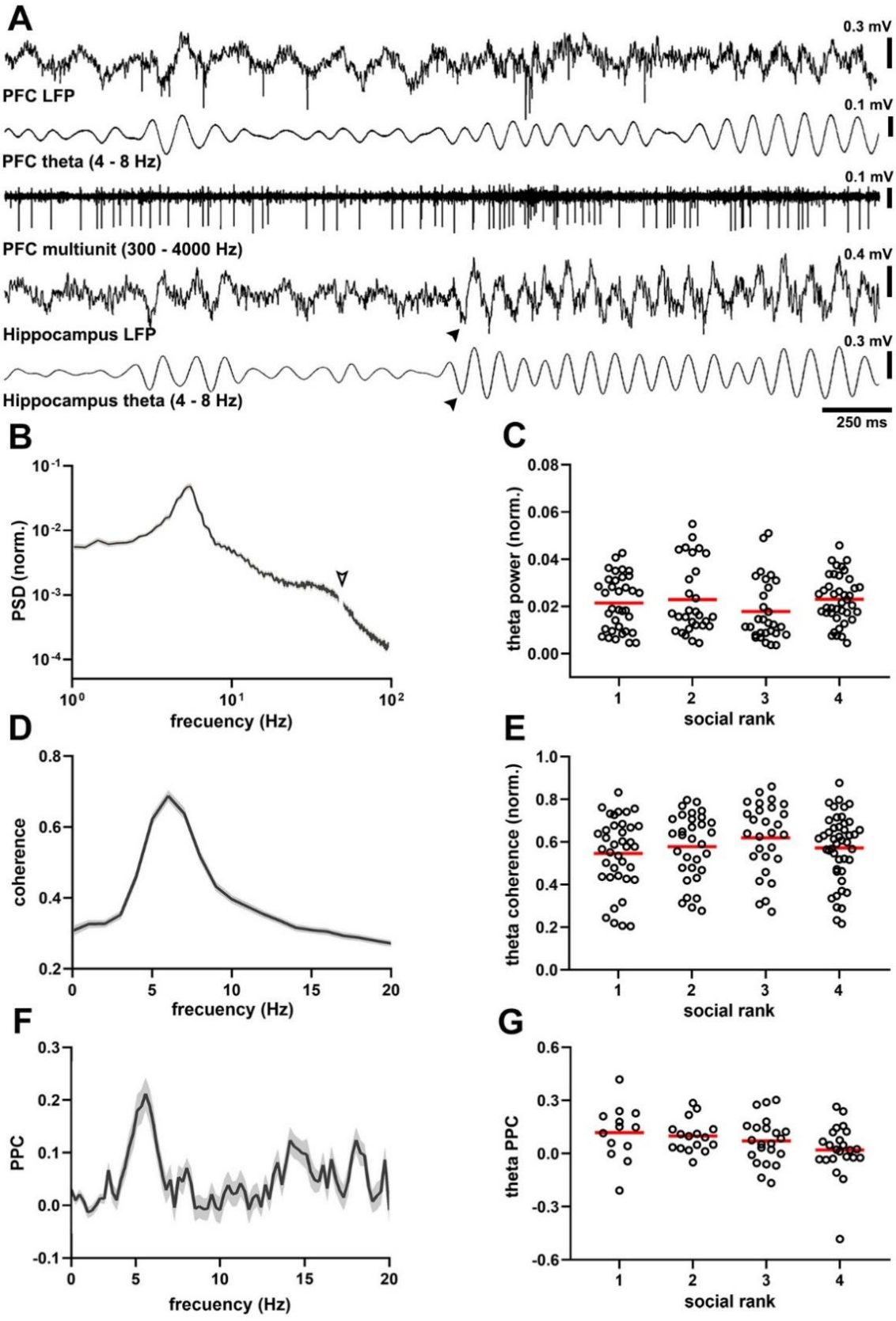
A
0.3 mV
PFC LFP
0.1 mV
PFC theta (4 - 8 Hz)
0.1 mV
PFC multiunit (300 - 4000 Hz)
0.4 mV
Hippocampus LFP
0.3 mV
Hippocampus theta (4 - 8 Hz)
250 ms
B
PSD (norm.)
frecuency (Hz)
C
theta power (norm.)
social rank
D
coherence
frecuency (Hz)
E
theta coherence (norm.)
social rank
F
PPC
frecuency (Hz)
G
theta PPC
social rank

Figure 25. Theta oscillatory activity in cortical networks. *(**A**) Example simultaneous recording of hippocampal (LFP HP) and prefrontal cortical (LFP PFC) activity showing theta oscillations (filtered 4-8 Hz) and cortical spiking activity (units PFC, filtered 300-4000 Hz) recorded in an urethane-anesthetized mouse (CM24reg05). Note prominent transitions into theta activity in the hippocampus precede the neocortex. (**B**) Power spectral density (PSD, n = 159 sessions, n = 21 animals). (**C**) Peak hippocampal theta amplitude by social ranking. One-way ANOVA, P = 0.3877 (n = 159 sessions, 21 animals). (**D**) Average hippocampo-cortical spectral coherence (n = 21 animals). (**E**) Peak hippocampo-cortical spectral coherence by social ranking One- way ANOVA, P = 0.350 (21 animals, 143 sessions. (**F**) Average pairwise phase consistency (PPC) between hippocampal units and PFC LFP from all recordings (n = 1958 units, 18 animals). (**G**) PPC by social ranking. P = 0.1387 (74 sessions, 18 animals). Black lines represent population average ± SEM, circles denote recordings sessions, and the red lines are the population average.*

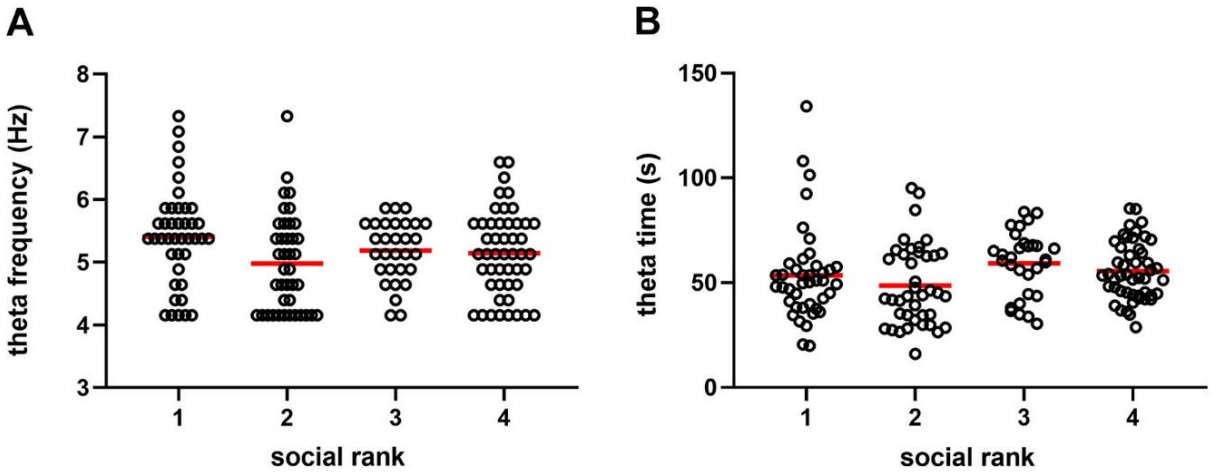

Figure 26. Parameters of theta oscillatory activity according to social rank. *Peak frequency (**A**) and cumulative duration (**B**) of hippocampal theta oscillations (4 – 8 Hz) in anesthetized mice according to social ranking. There were no significant differences between social rankings. One-way ANOVA, P = 0.0524, A; P = 0.0987, B; n = 159 sessions, 21 animals. Circles denote recordings sessions, and the red lines are the population average.*

Parameter	estimate	SE	P
intercept	1.05821	0.24175	*0.000469*
collective performance	0.31042	0.05827	*6.8e-05*
theta power	-1.62367	1.76202	0.370484
theta frequency	-0.06966	0.04583	0.148007
theta coherence	0.04803	0.12314	0.701632

Table 4. *Multiple linear models for individual task performance (n = 21 animals used for electrophysiological experiments).*

Parameter	estimate	SE	P
intercept	-11.6517	9.2605	0.22637
collective latency	0.4623	0.1547	*0.00871*
theta power	29.9151	70.4885	0.67693
theta frequency	2.2370	1.8760	0.25048
theta coherence	2.6051	4.5705	0.57660

Table 5. *Multiple linear models for individual task latency (n = 21 animals used for electrophysiological experiments).*

5.3.2. PFC intrinsic cortical activity and hippocampal sharp-wave ripples correlate with the process of decision-making during collective spatial navigation.

I investigated the quiescent states of the cortical network when sharp-wave ripples dominate cortical activity (Ylinen et al., 1995). All animals exhibited prominent sharp-wave ripples **(Fig. 27A)**, evident as short-lived, waxing, and waning oscillations **(Fig. 27B)**. Nevertheless, the amplitude of ripple oscillations was dependent on social ranking as dominant mice exhibited the largest sharp-wave ripples when compared to the subordinate groups **(P = 8.55e-18, Fig. 27C)**. The duration of ripples was not different between social groups **(P = 0.066, Fig 27D)**, yet their frequency was slower in the submissive group **(P = 5.46e-38, Fig. 27E)**.

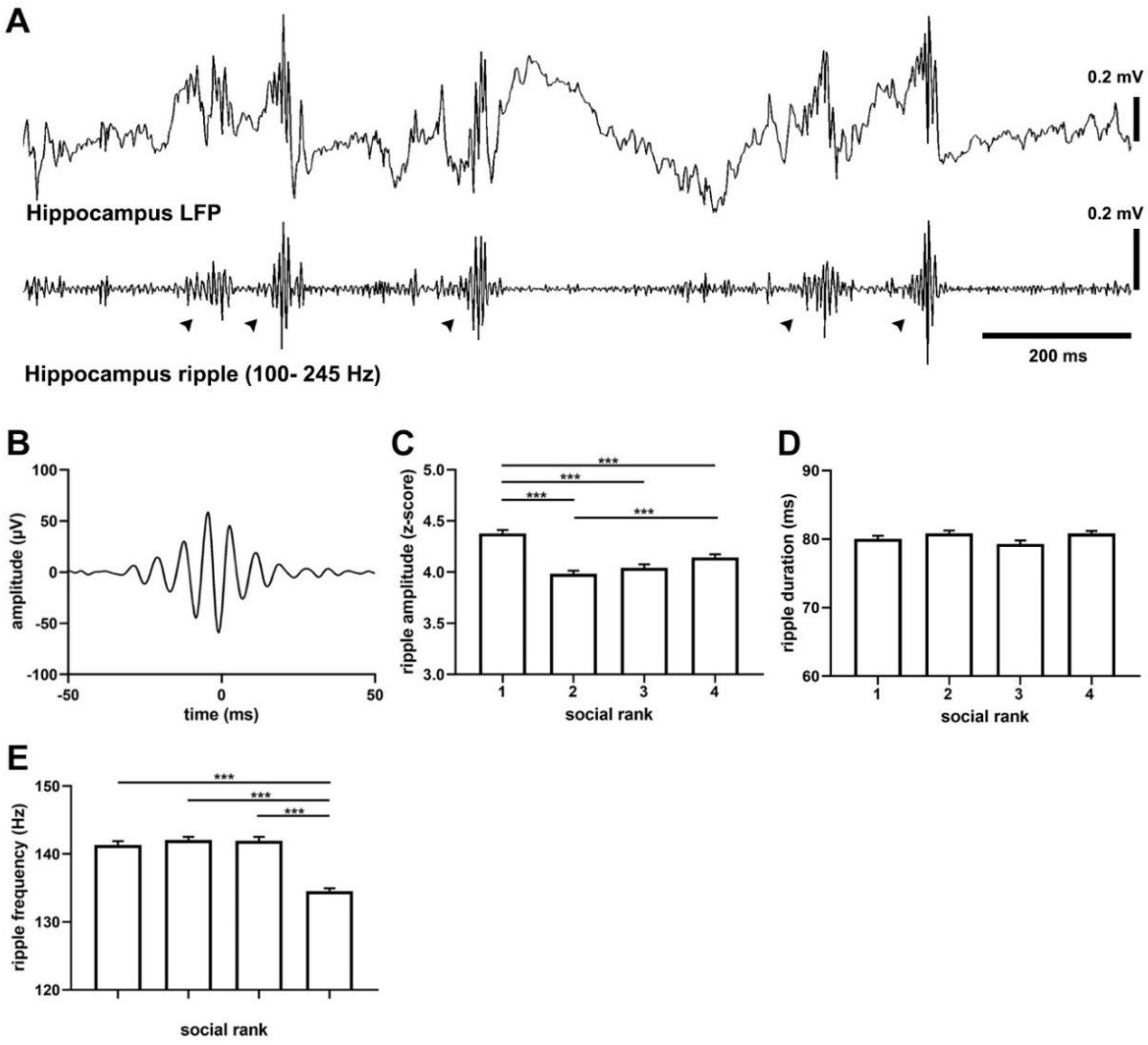

Figure 27. Hippocampal sharp-wave ripples. *(**A**) Example recording of hippocampal LFP activity with hippocampal sharp-wave ripples (SWRs, filtered 100-245 Hz) recorded in an urethane-anesthetized mouse (CM75reg06). (**B**) Grand average ripple episode (n = 18,571 events, 21 animals). Peak SWRs amplitude (**C**), cumulative duration (**D**), and frequency (**E**) according to social rank. One-way ANOVA, P = 8.55e-18 in C; P = 0.066 in D, P = 5.46e -38 in E. Bars represent average ± SEM. *** P < 0.001.*

Sharp wave ripples powerfully synchronize neuronal spike-timing across the neocortex (Remondes et al., 2015; Logothetis et al., 2012), including the PFC (Siapas et al., 1998). Thus, I computed the crosscorrelation function between hippocampal sharp-wave ripples and the neuronal spike-timing in the PFC. As previously described, prefrontal neuronal spiking was synchronized with hippocampal ripples (Negrón-Oyarzo et al., 2015). Cortical spiking activity increased preceding the onset of hippocampal ripples, which was apparent in the cross correlogram **(Fig. 28B)**, yet maximal cross-activation exhibited little difference between social groups **(P = 0.002, Fig. 28C)**. After the ripple episode, neocortical activation rapidly decreased but did not return immediately to baseline. Instead, it reached a plateau of sustained neuronal discharge **(P = 2.81e-07, Fig. 28D)**. Such post-ripple activation was manifest in paired hippocampo-cortical recordings as a prolonged afterdischarge of prefrontal neurons well beyond the end of ripple oscillations **(Fig. 29)**. The post-ripple afterdischarge was stronger in dominant mice than subordinate groups, suggesting enhanced functional connectivity following sharp-wave ripple episodes. These observations were robust and confirmed by shuffling procedures but were also apparent when assessing the entire neuronal population **(P = 7.71e-47, Fig. 30C)**. Moreover, differences in the post-ripple afterdischarge were not the result of different temporal distributions of sharp-wave ripples, as inter-ripple intervals were similar across social groups **(P > 0.05, Fig. 30D)**.

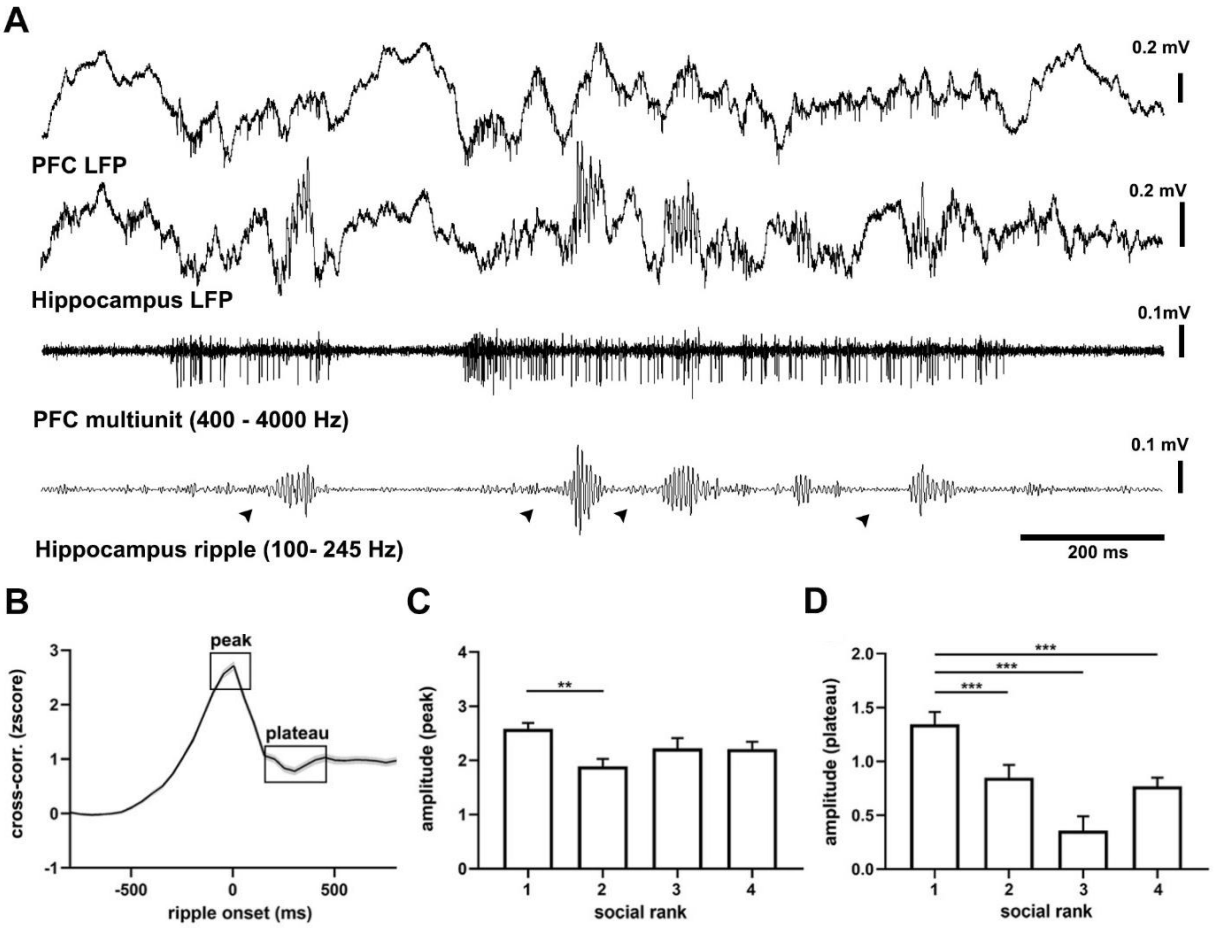

Figure 28. Functional connectivity in cortical networks according to social rank. *(**A**) Example simultaneous recording of hippocampal (LFP HP) and prefrontal cortical (LFP PFC) activity showing hippocampal sharp-wave ripples (SWRs, filtered 100-250 Hz) and cortical spiking activity (units PFC, filtered 300-4000 Hz) recorded in an urethane-anesthetized mouse (CM99reg05). (**B**) Average cross correlogram between the onset of SWRs and PFC units (n = 21 animals). Note sustained component after the peak. (**C**) Cross correlogram ripple-peak amplitude by social ranking. One-way ANOVA, P = 0.002, n = 658 units. (**D**) Cross correlogram post-ripple amplitude by social ranking. One-way ANOVA, P = 2.81e-07, n = 658 units. The black line represents the population average ± SEM, and bars represent average ± SEM.*

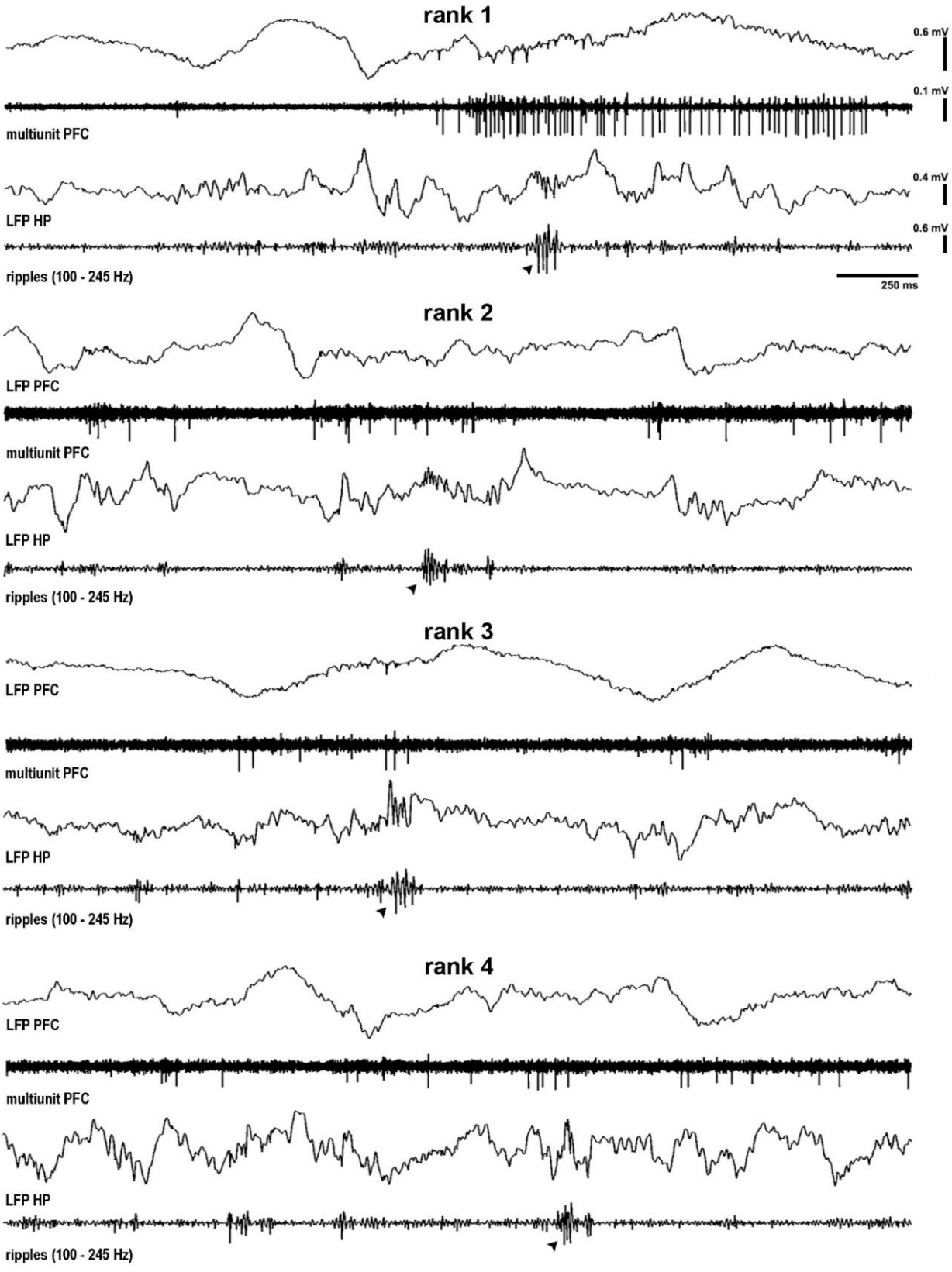
rank 1
0.6 mV
0.1 mV
multiunit PFC
0.4 mV
LFP HP
0.6 mV
ripples (100 - 245 Hz)
250 ms
rank 2
LFP PFC
multiunit PFC
LFP HP
ripples (100 - 245 Hz)
rank 3
LFP PFC
multiunit PFC
LFP HP
ripples (100 - 245 Hz)
rank 4
LFP PFC
multiunit PFC
LFP HP
ripples (100 - 245 Hz)

Figure 29. Examples of hippocampus sharp-wave ripples and cortical spiking records according to social rank*. Example of simultaneous recordings of hippocampal (LFP HP) and prefrontal cortical (LFP PFC) activity showing hippocampal sharp-wave ripples (SWRs, filtered 100-250 Hz) and cortical spiking activity (units PFC, filtered 300-4000 Hz) recorded in urethane-anesthetized mice sorted by social ranking. Ranking 1 (mouse ID:CM24_reg05), ranking 2 (mouse ID: CM73_reg02), ranking 3 (mouse ID: CM28_reg02), ranking 4 (mouse ID: CM98_reg01).*

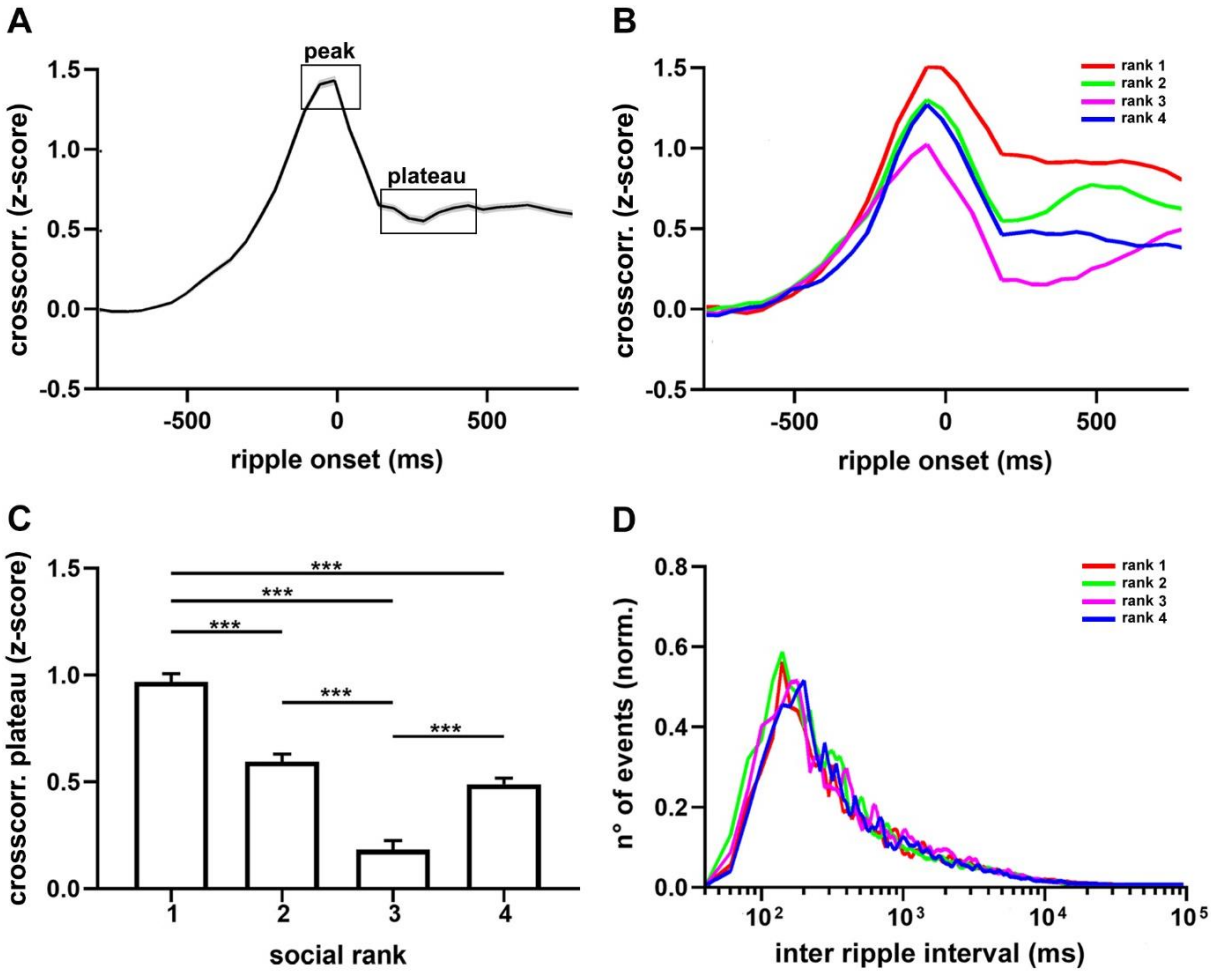

Figure 30. Functional connectivity between the hippocampus and PFC according to social rank. (***A***) *Average cross correlogram between the onset of sharp-wave ripples and prefrontal units (n = 3702 events, 21 animals). Note a sustained component after the peak. (**B**) Average cross correlogram sorted by social ranking. (**C**) Cross correlogram post-ripple amplitude by social ranking. One-way ANOVA, P = 7.71e-47 n = 3702 units. (**D**) Interevent interval histogram for sharp-wave ripples separated by social ranking. Distributions were not significantly different (One-way ANOVA, p > 0.05, corrected with FDR). The black line represents population average ± SEM; colored lines represent averages respect to social rank, and bars represent average ± SEM.*

I tested whether intrinsic hippocampo-PFC connectivity by means sharp-wave ripples was related to task performance during spatial navigation. For that, I performed multiple linear regressions between behavior (task performance) and neural activity (sharp-wave ripples). I found that the amplitude of the post-ripple cross correlogram correlated with both the performance **(R^2 = 0.235, P = 0.026, Fig. 31A)** and latency **(R^2 = 0.404, P = 0.002, Fig. 31B)** of individual trials, but not during collective navigation **(Table 6 and Table 7)**. Interestingly, the strength of post-ripple hippocampo-cortical connectivity also correlated with the PSI **(R^2 = 0.328, P = 0.007; Fig. 32)**, but not during the ripples cross correlogram peak **(Table 8 and Table 9)**. Since the PSI reflects the influence of the social context on task performance **(P = 0.008, Fig. 19B)**, these results suggest that intrinsic cortical connectivity may be relevant for the process of decision-making during collective spatial navigation.

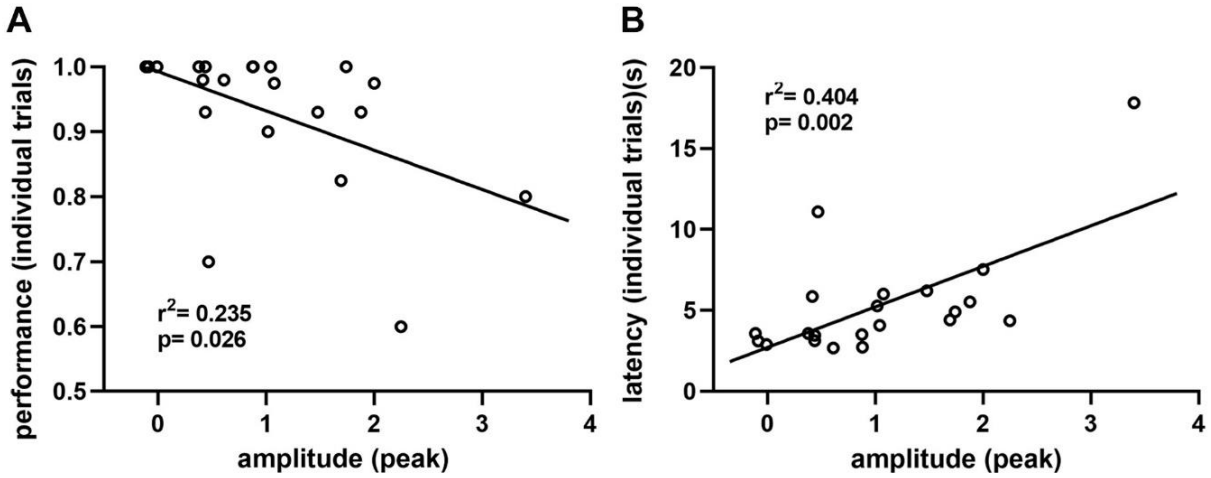

Figure 31. Linear regressions of functional connectivity and behavioral parameters in the hippocampo-PFC axis on mice performing the T-maze navigation test*. (**A**) Average cross correlogram peak amplitude against average individual performance (r^2 = 0.235, P = 0.026, n = 21 animals). (**B**) Average cross correlogram post-ripple amplitude against average individual latency (r^2 = 0.404, P = 0.002, n = 21 animals). Circles denote the average of individual mice and black lines the best linear fitting. The regressions in A and B are statistically significant.*

Parameter	estimate	SE	P
intercept	0.843824	0.185007	*0.000375*
collective performance	0.346942	0.046636	*2.08e-06*
ripple frequency	-0.002180	0.001444	0.151925
ripple amplitude	0.039210	0.025525	0.145326
crosscorrelogram ripple-peak	0.005932	0.016553	0.725076
crosscorrelogram post-ripple	-0.050519	0.012887	*0.001364*

Table 6. *Multiple linear models for individual task performance (n = 21 animals used for electrophysiological experiments).*

Parameter	estimate	SE	P
intercept	4.1093	0.5823	*2.11e-05*
neuronal firing rate difference	1.1343	0.3552	*0.00855*
PPC difference	2.7736	9.3354	0.77192
crosscorrelogram ripple-peak difference	-0.6268	0.5366	0.26739
crosscorrelogram post-ripple difference	0.3177	0.4178	0.46298

Table 7. *Multiple linear models for latency difference (winner-loser) in the tube test (n = 21 animals used for electrophysiological experiments).*

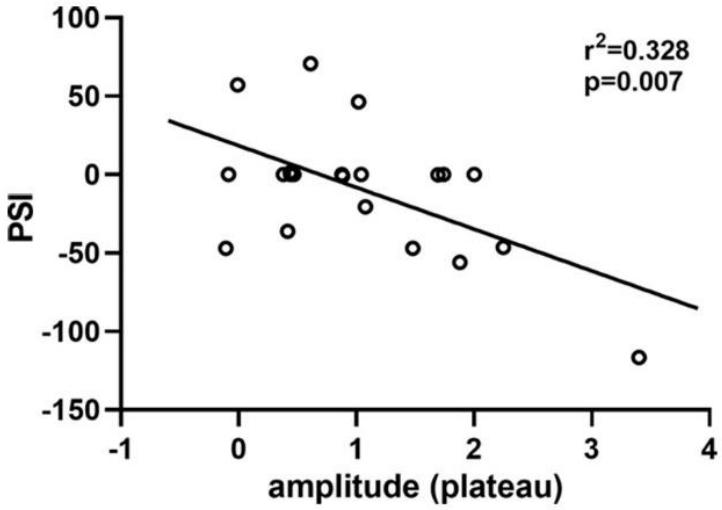

Figure 32. Linear regression of functional connectivity in the hippocampo-PFC axis and peer sensitivity index on mice performing the T-maze navigation test*. Linear regression between cross correlogram post-ripple amplitude against PSI of individual mice during collective trials (r^2 = 0.328, P = 0.007, n=21 animals). Circles denote the average of individual mice and the black line the best linear fitting. The regression is statistically significant.*

Parameter	estimate	SE	P
intercept	58.76	35.37	0.1206
neuronal firing rate	-23.24	12.23	0.0798
PPC	40.08	142.05	0.7823
crosscorrelogram ripple-peak	11.86	10.72	0.2888
crosscorrelogram post-ripple	-26.43	10.37	*0.0242*

Table 8. *Multiple linear models for the PSI (n = 21 animals used for electrophysiological experiments).*

Parameter	estimate	SE	P
intercept	-9.7985	151.0599	0.949
ripple frequency	0.1181	1.0649	0.913
ripple amplitude	0.4150	18.5729	0.982
crosscorrelogram ripple-peak	5.9279	11.9300	0.626
crosscorrelogram post-ripple	28.1367	10.0703	*0.013*

Table 9. *Multiple linear models for the PSI (n = 21 animals used for electrophysiological experiments).*

5.3.3. SPIKING ACTIVITY IN THE PREFRONTAL CORTEX CORRELATES WITH THE TIMING OF GOAL-DIRECTED SPATIAL NAVIGATION

So far, our results suggested that the connectivity during sharp-wave ripples and not the activity during theta oscillations may be relevant for task performance. Nonetheless, I explored another neural process that accounts explicitly for the effect of social interaction during the collective movement. To further investigate this idea, I explored whether intrinsic cortical activity patterns correlated with task performance. Thus, I found that intrinsic cortical spiking activity of the PFC correlated directly with the timing of collective navigation (*the latency difference between collective and individual trials)* (**R^2 = 0.246, P = 0.019, Fig. 33B**), but not with task performance (**R^2 = 0.116, P = 0.121, Fig. 33A**). Multiple regression analysis, including several neural parameters, confirmed that the firing rate of prefrontal neurons was a significant regressor (**R^2 = 0.28, P = 0.0283, Table 10**). Moreover, the effect was specific only for principal cells (**R^2 = 0.269, P = 0.013, Fig. 34B**), as interneurons did not show significant regression (**R^2 = 0.087, P = 0.195, Fig. 34A)**. Given that cortical neuronal spiking was specifically correlated with the social effect on task latency, this result suggests that intrinsic levels of neuronal

activity in the PFC during activated states account, at least partially, for the social effect on the temporal organization of decision-making during spatial navigation.

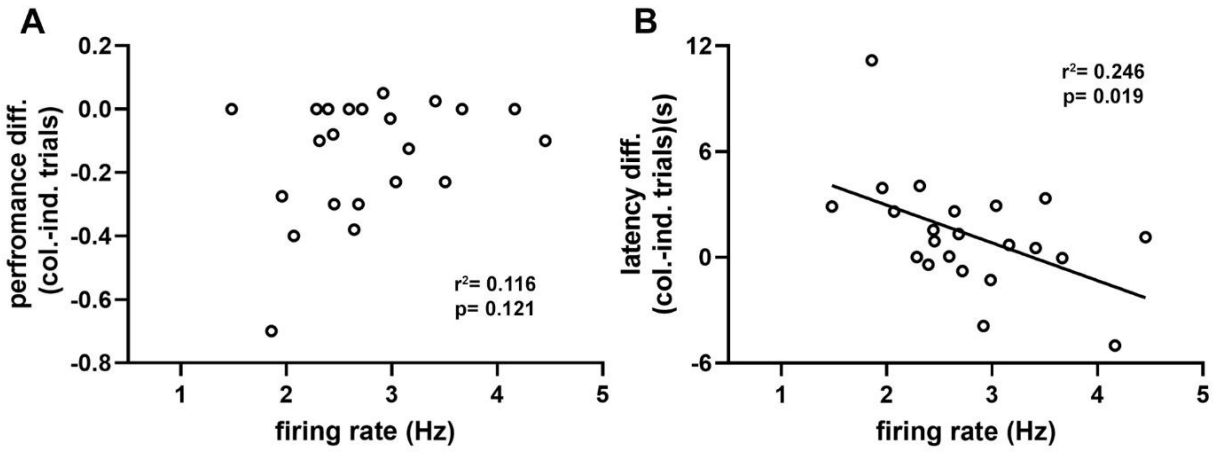

Figure 33. Linear regression of intrinsic PFC spiking activity and behavioral parameters in the PFC on mice performing the T-maze navigation test*. **(A)** Linear regression between PFC firing rate against behavioral performance (the performance difference between collective and individual trials) (r^2 = 0.116 P = 0.121 n=21 animals). **(B)** Linear regression between PFC firing rate against the timing of collective navigation (the latency difference between collective and individual trials) (R^2 = 0.246, P = 0.019, n = 21 animals). Circles denote the average of individual mice and the black line the best linear fitting. The regressions in B is statistically significant.*

Parameter	estimate	SE	P
intercept	4.6228	9.9841	0.6492
firing rate PFC	-2.0076	0.8378	*0.0283*
hippocampus theta frequency	0.7691	1.8931	0.6896
hippocampus-PFC theta coherence	-2.7663	5.2036	0.6019

Table 10. *Multiple linear models for social (collective – individual) task latency (n = 21animals used for electrophysiological experiments).*

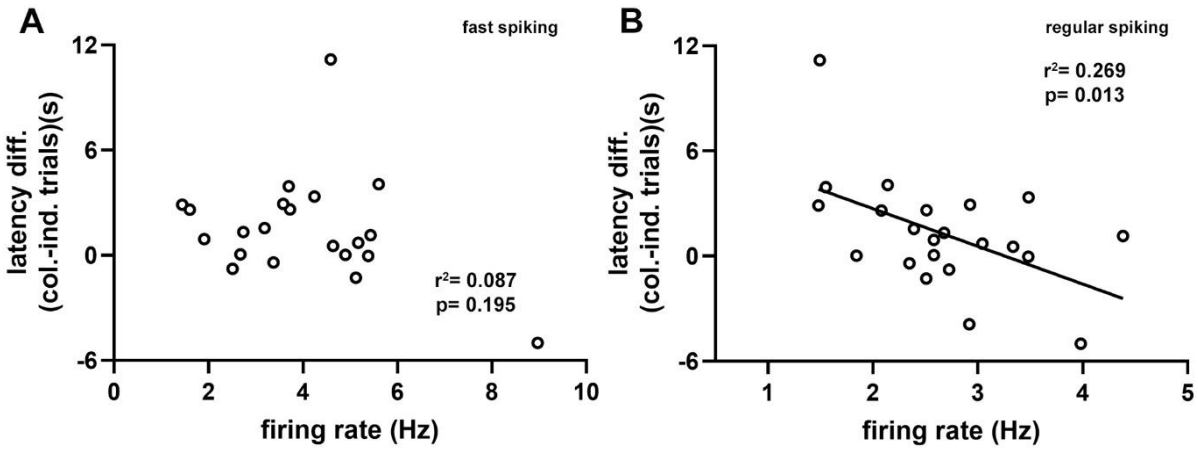

Figure 34. Linear regression of Intrinsic neural parameters in PFC and the timing of collective navigation on mice performing the T-maze navigation test. (A) *Linear regression between firing rate of fast spiking PFC cells against the timing of collective navigation (the latency difference between collective and individual trials) (R^2 = 0.087 P = 0.195 n = 21 animals).* ***(B)*** *Linear regression between firing rate of regular spiking PFC cells against the timing of collective navigation (the latency difference between collective and individual trials) (R^2 = 0.269, P = 0.013, n = 21 animals). Circles denote the average of individual mice and the black line the best linear fitting. The regressions in B is statistically significant.*

CHAPTER 6

DISCUSSION

My results show that social interactions modulated goal-directed spatial behavior acquired individually during collective performance. The social effect was reflected in modifications of two critical aspects of individual decision-making: latency and performance (according to the first specific hypothesis). The task timing, or the time interval taken to reach the rewarded arm, was correlated with intrinsic cortical activity (according to the second specific hypothesis). Also, the task outcome, or the proportion of correct choices, was dependent on contingent social information provided by the spatial distribution of animals collectively moving. Moreover, the influence of contingent social information was dependent on the social ranking and correlated with the intrinsic connectivity of the hippocampal-prefrontal circuit (according to the general hypothesis). In the following paragraphs, the results obtained from the experiments during the collective task and findings from acute records of animals that performed behavioral tasks will be discussed.

6.1. NAVIGATION AND FORAGING DURING THE COLLECTIVE PERFORMANCE OF THE TASK

In collective movements, group members have to choose between either moving or staying, and, in cases of concurrent alternatives (as in my experimental design), have to choose either one direction or another. On the other hand, random trajectories could not account for regular patterns and emergent properties assigned to collective movements on a large scale such as shape, density of individuals, and polarity of orientation (Couzin and Krause, 2003; Conradt, 2012; Sumpter, 2006). Therefore, this means that different behavioral processes could influence the decision.

Given that trained individuals had complete information about the navigation task, it may be expected that mice would maintain their stereotyped, efficient navigation strategy during the collective phase of the navigation task. Instead, animals flexibly switched strategies and privileged information from contingent social interactions, which resulted in the significant loss of performance and increased latency during collective movement. The shift in decision-making was not directly related to dominance hierarchy, but contingent social interactions taking place during collective navigation. Indeed, task performance was significantly correlated with the distribution of animals in the maze, regardless of the previously learned fixed location of food reward. Recent studies have shown that as experience increases, mice shift their sensory-based strategy to more efficient, stereotyped foraging based on spatial-memory that varies little in response to sensory cues (Gire et al., 2016). Possibly, social experience is different in the sense that it recruits all sensory modalities and activates circuits for the recognition and interaction with conspecifics provided by visual and olfactory cues from the social group that permits goes to the reward and join in feeding with others (Galef and Girardeau, 2001; Insel and Fernald, 2004).

Decision-making implies several different issues for the animals: whether moving at all or staying in the same place, when to go (time) and where to go (direction), moving cohesively or in another direction. Regarding cohesion, collective movement is an important part of the decision process and has received little attention in behavioral studies. A manner of evaluating the collective movement is by the quantification of animal latencies in the T-maze. My data show that animals do not present differences in latencies from start box to the decision point in the T-maze. This is important for two reasons. First, the animals are motivated to run across the T-maze towards a reward. Second, because is possible that occur a group cohesion during movement. This means, can be maintained if the group members decide either to follow each other or to stop at the same time (Insel and Fernald, 2004; Torquet, 2018).

Given the preceding, there is a strongly correlated group structure among mice, as more information about group behavior is contained in the joint position of mice than what can be extracted from summing all the information provided by the interactions between pairs of mice (Shemesh et al., 2013; de Chaumont et al., 2012). Besides, gregarious animals are known to be able to use information conveyed by their conspecifics, like group coordination during movement. Indeed, decision-making may be influenced by conspecifics' behavior when individuals consider both their own information and the behavior of others when deciding (Kerth et al., 2006; Couzin et al., 2005; Petit and Bon, 2010).

Different behavioral processes could influence the decision, depending on their time of occurrence. Indeed, individuals might differ in their characteristics (age, sex, dominance status), internal state (level of satiety, reproductive status) or sensitivity to external stimuli (Torquet, 2018).

Consequently, social behaviors require access to the observation of more than two individuals. Currently, highly standardized social interaction tests are available.

However, these tests are mainly based on simple (dyadic) social interactions that lack ethologically relevant behavioral markers such as contingent social interaction (de Chaumont et al., 2012; de Chaumont et al., 2019). This fundamental high-order structure in mice social behavior (Shemesh et al., 2013) is consistent with the effects that I describe and supports the idea of studying collective behavior of animal groups instead of focusing on individuals or dyads.

Thus, mice groups may be composed of animals that differ in their cognitive capabilities and communicative abilities, adding degrees of complexity in social task. This is particularly important, for example, for the formation and description of social dynamics in animals, without the need to observe extended periods for the formation of contingent social dynamics.

6.2. DOMINANCE HIERARCHY AND SOCIAL INTERACTIONS DURING COLLECTIVE BEHAVIOR

Ranking systems emerge in social groups to determine several aspects of individual's behavior, such as priority access to food, mating opportunities, territory, or other limited resources. Rodents establish dominance hierarchy when living in high-density conditions based on social interactions so that one subject acts as dominant over the other subordinate individuals. The ranking is ordered for all individuals, so the lowest ranking, the submissive, dominates none of the others. Dominance hierarchy can be assessed and quantified by several tests, including the agonistic behavior assay, the barber test, and the ultrasonic test, among others. Although, the reliability and validity of each assay in measuring the dominance behavior may be context-dependent (Drews, 1993), the high consistency of ranking results of multiple assays supports the notion that dominance is a standard variable underlying a variety of behaviors that use different sensorimotor skills (Wang et al., 2011, Wang et al., 2014).

Here, I used the tube test that provides a quantitative measure of aggressiveness minimizing physical contact between competing mice, thereby preventing injuries. In each trial, one mouse forces its opponent outside of a neutral area, permitting identification of dominant and subordinate mice. The test is consistent with other dominance tests previously validated based on transitivity, consistency, and stability (Wang et al., 2011; Zhou et al., 2017; Kingsbury et al., 2019). In agreement with previous reports, I found that a social hierarchy was organized and established in a litter of four mice, confirming that dominant and subordinate animals exhibited large differences in the tube test constituting a form of intrinsic social interaction.

Additionally, similar to previous reports, the time spent in the tube was significantly shorter when the submissive mouse was involved or as rank distance increased (Wang et al., 2011; Zhou et al., 2017). Moreover, it was noteworthy that rank did not correlate with the weight, given that the body size (in terms of body mass) correlates with dominance in gregarious birds and mammals (Chase et al., 2011; Bush et al., 2016). The result obtained could be explained because, in the natural environment, the dominance status fluctuates over time in association with changing competitive ability and health (Holekamp et al., 2016). In contrast, mice in a controlled environment (like a laboratory) form a despotic society over time (Sapolsky, 2005), with repeated interactions among members of a social group resulting in stable asymmetric relationships reducing the aggressivity and conflict between individuals.

Regarding collective behavior, I found that the dominance hierarchy had no direct relation with decision-making during collective behavior in the spatial navigation task. However, it distinctly affected the influenceability of individuals to contingent social information. Previous studies have shown that effective leadership and social decision-making during collective movement do not require inherent differences between individuals, such as dominance hierarchy or body size (Couzin et al., 2005). By studying decision-making during social interactions, I have established that dominant mice are

not leaders as they do not guide navigation during collective behavior. This pattern is completely at odds with the acquisition of the navigation task, in which dominant and subordinate groups showed comparable performance and latency.

Conversely, dominant mice seem to be more sensitive to contingent social interactions and shift their decisions accordingly to ongoing behavior. Due to technical reasons, it is difficult to evaluate signals or cues in social behavior in the video records during the collective test. Even so, this could be because dominant animals are paying more attention to the behavior of the rest mediated by behavioral cues or signals and social responses whose dynamics may be modulated by the ongoing collective movement itself (Kerth et al., 2006; Petit and Bon, 2010; King, 2010).

6.3. DOMINANCE HIERARCHY, INTRINSIC PFC ACTIVITY AND COMPETITIVE INTERACTIONS IN THE TUBE TEST

The formation of social hierarchies is associated with the activity of specific brain areas. To date, the circuits controlling dominance hierarchy behavior are not completely understood. Even so, different brain regions have been described that influence the expression of dominance behaviors, in particular, PFC and subcortical regions (DRN, PAG, BLA, and hypothalamic areas, Rosvold et al., 1954; Bard et al., 1958; Lukaszewska et al., 1984; Warden et la., 2012; Audero et al., 2013; Hoover and Vertes, 2007). Recent studies have shown that at the synaptic level, social dominance in mice involves specific synapses in the PFC region. Precisely, the focus is on excitatory synapses of layer V pyramidal neurons of the mPFC (the principal output of this structure) and show that the strength of synaptic transmission mediated by the neurotransmitter glutamate matches social ranking in mice (Wang et al., 2011). Also, an increased amplitude of spontaneous postsynaptic currents in the mPFC increased social dominance behaviors (Anacker et al., 2019). I have tested whether such in vitro relation was translated into in vivo spiking activity in the mPFC under anesthesia. My

results show that intrinsic cortical dynamics revealed significant differences according to social ranking, as dominant mice exhibited distinct intrinsic cortical activity that segregated them from the subordinate groups, with larger PFC firing rates. Hence, intrinsic cortical activity seemingly differentiates the dominance hierarchy.

On the other hand, the tube test is used to measure moment-to-moment competition of mice. Previous studies have identified a subpopulation of mPFC neurons that encode distinct social dominance behaviors during a competitive encounter. For example, during push and resistance behaviors, active putative pyramidal cells in the mPFC showed an increase in average firing rate and their firing rate did not increase during retreat behavior. In addition, optogenetic light stimulation of pyramidal mPFC neurons in a subordinate mouse just before and during a tube test increased both number and duration of dominance behaviours and resulted in a win match, indicating that pyramidal mPFC neuron activation was sufficient to elevate rank in this test. Importantly, mPFC activation does not seem to enhance basal aggression level or change social recognition (Zhou et al., 2017).

Thus, single-cell responses collectively form stable representations of push, retreat, and approach behavior, suggesting a role for mPFC neurons in regulating multiple, and sometimes opposing, behavioral strategies (Kingsbury et al., 2019). A limitation of my thesis is that I do not have simultaneous video analyses and chronic recordings of mice during encounters in the tube test. Even so, I evaluated the intrinsic neural parameters of different hierarchical positions in a competitive encounter. In particular, the intrinsic activity of PFC neurons with the interaction time in the tube test. I found a significant positive correlation between the spontaneous mPFC spiking activity (firing rate difference, winner-loser), and interaction time (latency difference, winner-loser) in the tube test. Also, the correlation was specific for putative pyramidal neurons and was not present in putative interneurons. Hence, intrinsic spiking activity in the PFC correlates with dominance behavior.

Another limitation of my study is that I have not measured the plasma concentration of sexual hormones such as testosterone during T-maze task and competitive interactions in the tube test. Testosterone hormone is important for increasing and maintaining social status (Dreher et al., 2016; Boksem et al., 2013) and preclinical findings, including neuroendocrinological manipulations in rodents, have demonstrated a causal link between post-victory testosterone pulses and the winner effect (Fuxjager et al., 2010). Winning a territorial fight, causes a surge in testosterone which could enhance an individual's ability to win future encounters by increasing aggression (Fuxjager et al., 2010; Fuxjager et al., 2017). The mechanisms by which testosterone pulses increase future ability to win include long-term plasticity in the neurobiological circuits that control aggression (Fuxjager et al., 2010).

Lastly, the other physiological limitation for my study is the possibility of occurring stress in litter mice. It has been suggested that chronic stress could alter social dominance behavior (D'Amato et al., 2001). In addition, stress is highly associated with a low rank in a social hierarchy (Beery et al., 2015; Williamson et al., 2017). Besides there are relationships between dominance and plasma corticosterone, a stress hormone. For example, subordinate males that living in social hierarchies had significantly higher levels of plasma corticosterone than alpha males and pair-housed subordinate males (Williamson et al., 2017). Also, in test social-dependent namely social avoidance test, dominant mice, but not subordinates, were the ones susceptible to developing social avoidance and depression-like behavior after social defeats. Thus, this finding reflecting that subordinate animals are used to being defeated during social hierarchy establishment, making them more resilient to subsequent social stress, while dominant mice may respond more strongly to unpredicted defeats (Larrieu et al., 2017).

Even so, in my data, the experimental protocols minimize agonistic behaviors among the animals that could infer in the interpretations of the physiological results discussed previously.

6.4. DOMINANCE HIERARCHY AND INTRINSIC HIPPOCAMPAL ACTIVITY

The hippocampus or hippocampal formation is a component of the limbic system (Anderson et al., 2006), a cortical structure found in the medial temporal lobe in all mammalian species that plays a fundamental role in spatial navigation as well as several forms of learning and memory (Buzsáki, 2002; Eichenbaum, 1999). Besides, the hippocampus constitutes a central hub of the medial temporal lobe, which synchronizes neuronal activity along the temporal cortical axis. Notably, it establishes coherent activity with the frontal lobe required for learning and memory (Battaglia et al., 2011; Siapas et al., 2005; Peyrache et al., 2009). Two characteristic oscillatory patterns of activity are present in the hippocampus, namely, theta oscillations and SWRs, which define certain brain states in behaving animals (Battaglia et al., 2011). Each of these activity patterns seems to be associated with a specific phase of memory formation.

The hippocampal theta rhythm is a prominent network activity of the 'on-line' hippocampus that can be separated into atropine-sensitive (type-2) and atropine-resistant (type-1) components (Masquelier et al., 2009). Since then, substantial evidence has accumulated, demonstrating that the theta rhythm serves an essential network-level role in hippocampal learning and memory. For example, theta oscillations facilitate plasticity and support mnemonic processes requiring inter-regional signal integration. (Siapas et al., 2005; Mizuseki et al., 2009; Masquelier et al., 2009). Conversely, suppression of the theta rhythm impairs learning and memory (Pan and McNaughton, 1997; Robbe et al., 2006; McNaughton,2006).

An important point to consider in my hippocampal records is the quality of anesthesia is similar in litter animals regardless of their social ranking. This allows all records to be comparable to each other. This is important because theta frequency has been reported to be dependent on the amount of anesthesia (Perouansky et al., 2010). Besides, my analyses of the theta parameter show that there are no differences in power and maximum frequency of intrinsic theta activity related to social rank.

Importantly, the duration of theta periods during the records was similar in all records, and do not present differences according to social ranking. During anesthesia, the septohippocampal theta associated with movement (type 2) is suppressed, and the primary input to the hippocampus would be through the entorhinal cortex through a higher theta rhythm (type 1) (Buzsaki et al., 1985). Therefore, septal theta would play a negligible role in the recordings. Even so, it cannot be ruled out the septal theta's effect during the exploration, and that could generate differences in spatial memory encoding according to the social ranking.

On the other hand, ripples frequency is lower in submissive animals, and it is presumable that the duration of ripples in submissive mice is longer to equalize (like a mechanism compensation) the number of cycles per ripple across litter mice. The analysis and comparison of ripple duration, however, revealed no difference in social hierarchy-associated. Thus, submissive mice expressed a reduction in the frequency of ripple events compared to active subordinates and dominant animals. This particular phenomenon could be due to CA3 connectivity. Studies suggest that the strength of CA3 input onto CA1 pyramidal cells is essential in regulating ripple frequency. For example, simultaneous CA3 and CA1 recordings determine the correlation between the power of CA3 population bursts and the frequency of the resulting high-frequency events in CA1 (Sullivan et al., 2011; Wiegand et al., 2016). Their results showed a positive correlation indicating that the more robust CA3 input results in increased CA1 ripple frequency (Sullivan et al., 2011). Besides, mice knockout of CA3 innervation to CA1 presents reduced ripple frequency in CA1 and deficits in the consolidation of contextual fear memory (Nakashiba et al., 2009). In my data, the observed decrease in CA1 ripple frequency in submissive mice may, therefore, result from the possible reduction in functional synaptic innervation of CA1 from CA3 (Barnes et al., 1992; Wiegand et al., 2016).

A possible effect of social hierarchy regarding ripple frequency is the impact on the intrinsic neuronal circuit during ripple events in the hippocampus. For example, it has

been described that hippocampal interneurons and pyramidal cells are most active near the trough of the ripple oscillation (Buzsáki et al., 1992). Given that, individual neurons express tuning to specific phases around the trough and could occur small changes in their spike timing affecting synaptic plasticity. The selective response of neurons to the phase of the ripple may facilitate the ordered segmentation of cell assemblies during a sharp-wave ripple event (Davidson et al., 2009; Wu and Foster, 2014; Wiegand et al., 2016). Thus, a possible social hierarchy-associated alteration in-phase coupling or phase coding could interfere with the segregation of cell assemblies during ripple oscillations and impact memory consolidation. Another plausible option could be the differential activity between dominant and submissive mice during quiescent states, for example, when dominant animals exploring the environment make a pause or stop. Despite not having a track of the animals during the T-maze task, those moments may be highly relevant for temporal prospection or planning compared with subordinate mice.

Hence, by recording LFP in anesthetized litter mice, I show here evidence for functionally distinct oscillation patterns in the dorsal CA1 hippocampus. Indeed, my physiological characterization leads to propose that ripple hippocampal oscillation patterns present specific activity according to social ranking.

6.5. INTRINSIC PFC ACTIVITY AND DECISION-MAKING DURING COLLECTIVE BEHAVIOR

Social relationships shape individual behavior and affect decision-making (Torquet et al., 2018). Even though dominance hierarchy arises by recurrent social interactions, it causally results from the synaptic efficacy of excitatory transmission in the mPFC (Wang et al., 2011). Hence, dominance hierarchy results from intrinsic neural activity and connectivity patterns. I found that intrinsic neuronal discharge in the mPFC was proportional to task latency, a proxy of temporal executive control,

and this observation partially accounted for the effect of social interactions during goal-directed spatial navigation.

The mPFC is essential for decision making and executive behavior (Euston et al., 2012). I report here that intrinsic cortical dynamics expressed in the spontaneous activity of the anesthetized brain partially accounts for the effect of social interactions during collective decision-making. Naturally, my observations cannot fully account for the shifting in decision-making strategies. At least two additional factors can be put forward. First, I did not record the mPFC ongoing activity during task performance, nor do I have detailed information about the instantaneous locomotion speed, movement patterns, or pauses and stops during collective movement, which is more informative about current cortical processing and computations during decision-making. Second, the intrinsic activity of other cortical regions contributes to goal-directed spatial navigation. For example, the orbitofrontal cortex (OFC) is thought to play an important role in adaptive and goal-directed behavior (Sul et al., 2010). Besides, OFC encodes variables that are relevant for behavior in decision-making, such as updating values of expected outcomes and shifting decisions (Rushworth et al., 2007; Gremel and Costa, 2013).

Previous studies have established that orbitofrontal circuits encode the shift between goal-directed and habitual actions (Gremel and Costa, 2013), thus allowing flexible and efficient decision-making. This is also consistent with recent findings showing that the orbitofrontal cortex integrates prior (i.e., memory) with current (i.e., sensory) information to guide adaptive behavior (Nogueira et al., 2017). Besides, the medial prefrontal cortex establishes robust anatomical connectivity with the orbitofrontal cortex (Euston et al., 2012), and these reverberant connections are undoubtedly crucial in shifting strategies of decision-making.

Sharp wave ripples powerfully synchronize neuronal spike-timing across the neocortex (Remondes et al., 2015; Logothetis et al., 2012), including the PFC

(Siapas et al., 1998). In my results, cortical spiking activity increased preceding the onset of hippocampal ripples, which was apparent in the cross correlogram. Besides, the post-ripple afterdischarge was stronger in dominant mice than subordinate groups, suggesting enhanced functional connectivity following sharp-wave ripple episodes. Moreover, differences in the post-ripple afterdischarge were not the result of different temporal distributions of sharp-wave ripples, as inter-ripple intervals were similar across social groups.

Additionally, my results show that the coordinated activity between hippocampal ripples and prefrontal neuronal spiking was significantly correlated with the PSI, reflecting the effect of contingent social information on task performance. Importantly, hippocampal-prefrontal coordination during sharp-wave ripples has been proposed as a neural substrate for decision-making (Yu and Frank, 2015). Indeed, hippocampal spiking during ripples can represent past or potential future experiences (Joo and Frank., 2018), and ripple disruptions can affect memory performance (Jadhav et al., 2012; Girardeau et al., 2009).

Therefore, sharp-wave ripples support both memory consolidation and memory retrieval, which could be at the service of associated cognitive processes such as decision-making. It has been shown that adverse environmental conditions, such as stress, can disrupt intrinsic hippocampal-cortical connectivity during sharp-wave ripples (Negrón-Oyarzo et al., 2015). Importantly, such disruptions are accompanied by alterations in long-term memory (Negrón-Oyarzo et al., 2015). Current results suggest that the levels of intrinsic hippocampal-cortical connectivity can sustain goal-directed behavior in social groups.

6.6. GENERAL CONCLUSIONS AND FUTURE PERSPECTIVES

My work mainly explored the collective navigation during the decision-making task and the intrinsic matrix activity in the hippocampal-PFC axis in litter mice. My results show that goal-directed spatial behavior - acquired individually - can be disrupted by contingent social interactions during collective navigation. Likewise, performance in the social context was critically dependent on both the previous individual learning process, during the training phase, and contingent social interactions arising during navigation in the testing phase.

On the other hand, social dominance was adopted as a manner to evaluate social dynamics during collective movement. In this thesis, I explored a competitive paradigm, namely the tube test, which was consistent with other paradigms based on transitivity, consistency, and stability. My results show that the dominance hierarchy was stable over time. Interestingly, the dominance hierarchy had no direct relation with task performance during collective behavior; yet, it distinctly modulated the susceptibility of individuals to contingent social interactions arising during spatial navigation. Moreover, intrinsic cortical dynamics revealed significant differences according to social ranking. For example, dominant mice exhibited distinct intrinsic cortical activity and connectivity patterns that segregated them from the subordinate groups, with larger mPFC firing rates, larger hippocampal SWR episodes, and stronger coupling between mPFC neurons and hippocampal SWR episodes. Besides, intrinsic cortical dynamics, specifically the post-ripple cortical connectivity, correlated with the PSI; that is, the factor of social influence on individual task performance. Overall, cortical connectivity directly correlates with task performance during individual trials and the social influence on individual behavior.

Finally, to further understand decision-making in the social context, future studies will have to assess not only the PFC's ongoing activity during decision-making but also the contribution of intrinsic network dynamics in other related cortical regions. Hence, intrinsic cortical activity and connectivity patterns seemingly outline the boundaries of social behavior.

REFERENCES

Abeles M & Gerstein GL (1988). Detecting spatiotemporal firing patterns among simultaneously recorded single neurons. Journal of Neurophysiology 60(3):909—924.

Adhikari A, Topiwala MA, & Gordon JA (2011). Single units in the medial prefrontal cortex with anxiety-related firing patterns are preferentially influenced by ventral hippocampal activity. Neuron 71(5):898--910.

Allison, T. (2000). Social perception from visual cues: role of the STS region. Trends Cogn. Sci. 4, 267–278

Amodio, D.M. and Frith, C.D. (2006). Meeting of minds: the medial frontal cortex and social cognition. Nat. Rev. Neurosci. 7, 268–277.

Anacker AMJ, Moran JT, Santarelli S (2019). Enhanced Social Dominance and Altered Neuronal Excitability in the Prefrontal Cortex of Male KCC2b Mutant Mice Autism Res. May; 12(5): 732–743.

Anderson PK (1961). Density, social structure, and nonsocial environment in house-mouse populations and the implications for regulation of numbers∗. Transact. N. Y. Acad. Sci. 23, 447–451.

Audero, E. (2013). Suppression of serotonin neuron firing increases aggression in mice. J. Neurosci. 33, 8678–8688

Avale, M.E. (2011). Prefrontal nicotinic receptors control novel social interaction between mice. FASEB J. 25, 2145–2155

Baddeley A. (1996). Exploring the central executive. Q J Exp Psychol; 49:5–28.

Ballerini M, Cabibbo N, Candelier A, Cavagna A, Cisbani E, Giardina I, et al. (2008). Interaction ruling animal collective behavior depends on topological rather than metric distance: evidence from a field study. Proc. Natl. Acad. Sci. U.S.A. 105, 1232–1237.

Barnes CA, Rao G, Foster TC, McNaughton BL (1992). Region-specific age effects on AMPA sensitivity: electrophysiological evidence for loss of synaptic contacts in hippocampal field CA1. Hippocampus 2:457–468.

Bartra, O. (2013). The valuation system: a coordinate-based meta-analysis of BOLD fMRI experiments examining neural correlates of subjective value, Neuroimage, 76, pp. 412-427

Battaglia F, Benchenane K, Sirota A, Pennartz C & Wiener, S (2011). The hippocampus: hub of brain network communication for memory. Trends in cognitive sciences 15, 310–318

Bault, N. et al. (2011). Medial prefrontal cortex and striatum mediate the influence of social comparison on the decision process. Proc. Natl. Acad. Sci. U.S.A. 108, 16044–160499

Bechara, A., Damasio, A. R., Damasio, H., & Anderson, S. W. (1994). Insensitivity to future consequences following damage to human prefrontal cortex. Cognition, 50, 15.

Bechara, A., Damasio, H., Tranel, D., & Anderson, S. W. (1998). Dissociation of working memory from decision making within the human prefrontal cortex. Journal of Neuroscience, 18, 428–437.

Bedard C and Destexhe A (2014). Local field potentials: Interaction with the extracellular medium. Encyclopedia of Computational Neuroscience. Springer. September 20.

Beery, A. K. & Kaufer, D. (2015). Stress, social behavior, and resilience: insights from rodents. Neurobiol Stress 1, 116–127,

Behrens, T.E.J. et al. (2009). The computation of social behavior. Science 324, 1160–1164.

Benchenane K, Tiesinga PH, Battaglia FP (2011). Oscillations in the prefrontal cortex: a gateway to memory and attention. CurrOpin Neurobiol, 21:475-485.

Benchenane K., Peyrache A., Khamassi M., Tierney P.L., Gioanni Y., Battaglia F.P. (2010). Coherent theta oscillations and reorganization of spike timing in the hippocampal–prefrontal network upon learning Neuron, 66, pp. 921–936.

Bicks L, Koike H, Akbarian S, Morishita H (2015). Prefrontal Cortex and Social Cognition in Mouse and Man. Front. Psychol., 26 November

Binder, S.; Dere, E.; Zlomuzica, A. (2015). A critical appraisal of the what-where-when episodic-like memory test in rodents: Achievements, caveats and future directions. Prog. Neurobiol., 130, 71–85.

Boksem, M.A.S., Mehta, P.H., Van den Bergh, B., van Son, V., Trautmann, S.T., Roelofs, K., Smidts, A., and Sanfey, A.G. (2013). Testosterone inhibits trust but promotes reciprocity. Psychol. Sci. 24, 2306–2314.

Brown VJ, Bowman EM. (2002). Rodent models of prefrontal cortical function. Trends Neurosci; 25:340–3.

Buckley, M. J., Mansouri, F. A., Hoda, H., Mahboubi, M., Browning, P. G., Kwok, S. C., Tanaka, K. (2009). Dissociable components of rule-guided behavior depend on distinct medial and prefrontal regions. Science, 325, 52–58.

Buschman TJ, Denovellis EL, Diogo C, Bullock D, Miller EK (2012). Synchronous oscillatory neural ensembles for rules in the prefrontal cortex. Neuron, 76:838-846.

Bush JM, Quinn MM, Balreira EC, Johnson MA (2016). How do lizards determine dominance? Applying ranking algorithms to animal social behaviour. Anim Behav, 118:65-74.

Buzsáki G, Buhl DL, Harris KD, Csicsvari J, Czeh B, Morozov A (2003). Hippocampal network patterns of activity in the mouse. Neuroscience 116:201–211.

Buzsáki G, Czopf j, Kondákor I, Kellényi L (1986). Laminar Distribution of Hippocampal Rhythmic Slow Activity (RSA) in the Behaving Rat: Current-Source Density Analysis, Effects of Urethane and Atropine. Brain Res. Feb 12;365(1):125-

Buzsáki G, Horváth Z, Urioste R, Hetke J, Wise K (1992). High-frequency network oscillation in the hippocampus. Science 256:1025–1027.

Buzsaki G (2015). Hippocampal sharp wave-ripple: a cognitive biomarker for episodic memory and planning. Hippocampus, 25:1073-1188.

Buzsaki, G. (2002). Theta oscillations in the hippocampus. Neuron 33, 325–340.

Cardinal RN, Pennicott DR, Sugathapala CL, Robbins TW, Everitt BJ. (2001). Impulsive choice in rats by lesions of the nucleus accumbens core. Science; 292:2499–501.

Carr, M. F., Jadhav, S. P., & Frank, L. M. (2011). Hippocampal replay in the awake state: A potential substrate for memory consolidation and retrieval. Nature Neuroscience, 14, 147–153.

Carter R, (2012). A distinct role of the temporal-parietal junction in predicting socially guided decisions Science, 337, pp. 109-111.

Cenquizca, L. A., and Swanson, L. W. (2007). Spatial organization of direct hippocampal field CA1 axonal projections to the rest of the cerebral cortex. Brain Res. Rev. 56, 1–26.

Chase ID (1982). Dynamics of hierarchy formation: The sequential development of dominance relationships. Behaviour.80(3/4):218–240.

Chase ID, Seitz K (2011). Self-structuring properties of dominance hierarchies: a new perspective. Adv Genet, 75:51-81.

Chiao, J.Y. et al. (2008). Knowing who's boss: fMRI and ERPo of social dominance perception. Group Process. Intergroup Relat. 11, 201–214.

Cho KK, Hoch R, Lee AT, Patel T, Rubenstein JL, Sohal VS (2015). Gamma rhythms link prefrontal interneuron dysfunction with cognitive inflexibility in Dlx5/6(+/S) mice. Neuron,85:1332-1343.

Conradt L (2012). Models in animal collective decision-making: information uncertainty and conflicting preferences. Interface Focus. Apr 6; 2(2):226-40.

Conradt L, Roper TJ (2003). Group decision-making in animals. Nature 421:155–158.

Coolen, I., Van Bergen, Y., Day, R. L., and Laland, K. N. (2003). Species difference in adaptive use of public information in sticklebacks. Proc. Biol. Sci. 270, 2413–2419.

Coolen, I., Ward, A. J. W., Hart, P. J. B., and Laland, K. N. (2005). Foraging nine-spined sticklebacks prefer to rely on public information over simpler social cues. Behav. Ecol. 16, 865–870.

Coricelli G, Nagel R (2009). Neural correlates of depth of strategic reasoning in medial prefrontal cortex Proceedings of the National Academy of Sciences, 106, pp. 9163-9168

Couzin D, and Franks N (2003). Self-organized lane formation and optimized traffic flow in army ants. Proc. Biol. Sci. 270, 139–146.

Couzin ID, Krause J, Franks NR, Levin SA (2005). Effective leadership and decision-making in animal groups on the move. Nature 433:513–516.

Couzin ID, Krause J, James R, et al (2002). Collective memory and spatial sorting in animal groups. J Theor Biol 218:1–11.

Couzin, I.D. and Krause, J. (2003). Self-organization and collective behavior in vertebrates. Adv. Stud. Behav. 32, 1 –75

Covington HE, Lobo MK, Maze I, Vialou V, Hyman JM, Zaman S, LaPlant Q, Mouzon E, Ghose S, Tamminga CA, Neve RL, Deisseroth K, Nestler EJ (2010). Antidepressant effect of optogenetic stimulation of the medial prefrontal cortex. J Neurosci.;30:16082–16090.

Crone, EA, and van der Molen, MW (2004). Developmental changes in real life decision making: performance on a gambling task previously shown to depend on the ventromedial prefrontal cortex. Dev. Neuropsychol. 25, 251–279

Csicsvari J, Hirase H, Czurkó A, Mamiya A and Buzsáki G (1999) Oscillatory Coupling of Hippocampal Pyramidal Cells and Interneurons in the Behaving Rat. Journal of Neuroscience 1 January 1999, 19 (1) 274-287.

Cummins, D. (2000). How the social environment shaped the evolution of mind. Synthese 122, 3–28.

D'Amato, F. R., Rizzi, R. & Moles, A. (2001). A model of social stress in dominant mice: effects on sociosexual behaviour. Physiol Behav 73, 421–426.

Davidson TJ, Kloosterman F, Wilson MA (2009) Hippocampal replay of extended experience. Neuron 63:497–507.

Daw ND, O'Doherty JP, Dayan P, Seymour B, Dolan RJ. (2006). Cortical substrates for exploratory decisions in humans. Nature.; 441:876–879.

Day RL, Macdonald T, Brown C, Laland K N, and Reader SM (2001). Interactions between shoal size and conformity in guppy social foraging. Anim. Behav. 62, 917–925.

De Chaumont F, Coura RD-S, Serreau P, et al (2012). Computerized video analysis of social interactions in mice. Nat Methods 9:410–417.

De Chaumont F, Ey E, Torquet N, Lagache T, Dallongeville S, Imbert A, Legou T , Le Sourd AM, Faure P , Bourgeron T, Olivo-Marin J (2019). Real-time Analysis of the Behaviour of Groups of Mice via a Depth-Sensing Camera and Machine Learning. Nat Biomed Eng. 2019 Nov;3(11):930-942.

Dreher, J.-C., Dunne, S., Pazderska, A., Frodl, T., Nolan, J.J., and O'Doherty, J.P. (2016). Testosterone causes both prosocial and antisocial status-enhancing behaviors in human males. Proc. Natl. Acad. Sci. USA 113, 11633–11638.

Drews C (1993). The concept and definition of dominance in animal behaviour. Behaviour 125, 283

Eichenbaum H. (1999). The hippocampus and mechanisms of declarative memory. Behav Brain Res.; 103:123–133.

Eslinger PJ, Flaherty-Craig C V, and Benton AL (2004). Developmental outcomes after early prefrontal cortex damage. Brain Cogn. 55, 84–103.

Euston DR, Gruber AJ, McNaughton BL (2012) The role of medial prefrontal cortex in memory and decision making. Neuron 76:1057–1070.

Fellows, L.K.; Farah, M.J. (2007). The role of ventromedial prefrontal cortex in decision making: Judgment underuncertainty or judgment per se? Cereb. Cortex, 17, 2669–2674.

Fiske ST (2010). Interpersonal stratification: Status, power, and subordination. Handbook of Social Psychology.941–982.

Frank L.M., Brown E.N., Wilson M. (2000). Trajectory encoding in the hippocampus and entorhinal cortex. Neuron, 27, pp. 169–178.

Fries P (2015). Rhythms for cognition: communication through coherence. Neuron, 88:220-235.

Fujii, N. (2009) Social state representation in prefrontal cortex. Soc. Neurosci. 4, 73–84

Fuster JM (1997) The Prefrontal Cortex. Anatomy, Physiology and Neuropsychology of the Frontal Lobe. Philadelphia-New York: LipincottRaven

Fuster, JM (2015). The Prefrontal Cortex, 5th Edn. New York, NY: Academic Press.

Fuxjager, M.J., Forbes-Lorman, R.M., Coss, D.J., Auger, C.J., Auger, A.P., and Marler, C.A. (2010). Winning territorial disputes selectively enhances androgen sensitivity in neural pathways related to motivation and social aggression. Proc. Natl. Acad. Sci. USA 107, 12393–12398.

Fuxjager, M.J., Trainor, B.C., and Marler, C.A. (2017). What can animal research tell us about the link between androgens and social competition in humans? Horm. Behav. 92, 182–189.

Gabbott, P., Headlam, A., & Busby, S. (2002). Morphological evidence that CA1 hippocampal afferents monosynaptically innervate PV-containing neurons and NADPH-diaphorase reactive cells in the medial prefrontal cortex (Areas 25/32) of the rat. Brain Research, 946, 314–322.

Galef, B. G. (2007). “Social learning in rodents,” in Rodent Societies. eds P. W. Sherman and J. Wolff (Chicago: University of Chicago Press), 207–215.

Galef, B. G. Jr., and Giraldeau, L.-A. (2001). Social influences on foraging in vertebrates: Causal mechanisms and adaptive functions. Anim. Behav. 61, 3–15

Ghazanfar, A.A. and Santos, L.R. (2004) Primate brains in the wild: the sensory bases for social interactions. Nat. Rev. Neurosci. 5, 603–616.

Girardeau G, Benchenane K, Wiener SI, et al (2009) Selective suppression of hippocampal ripples impairs spatial memory. Nat Neurosci 12:1222–1223.

Gire DH, Kapoor V, Arrighi-Allisan A, et al (2016) Mice Develop Efficient Strategies for Foraging and Navigation Using Complex Natural Stimuli. Curr Biol 26:1261–1273.

Gremel CM, Costa RM (2013) Orbitofrontal and striatal circuits dynamically encode the shift between goal-directed and habitual actions. Nat Commun 4:2264.

Groenewegen HJ, Uylings HB (2000) The prefrontal cortex and the integration of sensory, limbic and autonomic information. Prog. Brain Res. 126:3- 28:3-28.

Hagan MA, Dean HL, Pesaran B (2012) Spike-field activity in parietal area LIP during coordinated reach and saccade movements. J Neurophysiol 107:1275–1290.

Hausfater, G., Altmann, J., Altmann, S., (1982). Long-term consistency of dominance relations among female baboons (Papio cynocephalus). Science 217, 752–755.

Heidbreder, C.A., and Groenewegen, H.J. (2003). The medial prefrontal cortex in the rat: evidence for a dorso-ventral distinction based upon functional and anatomical characteristics. Neurosci. Biobehav. Rev. 27, 555–579.

Helbing D, and Molnar, P (1995). Social force model for pedestrian dynamics. Phys. Rev. E 51, 4282–4286.

Hillman KL, Bilkey DK. (2012) Neural encoding of competitive effort in the anterior cingulate cortex. Nat Neurosci. Sep;15(9):1290-7.

Holekamp K, Staruss E (2016) Aggression and dominance: an interdisciplinary overview. Current Opinion in Behavioral Sciences. December 2016.

Holson, R.R. (1986) Mesial prefrontal cortical lesions and timidity in rats. III. Behavior in a semi-natural environment. Physiol. Behav. 37, 239–247

Hoon, J., Kim, H., Huh, N., Lee, D., Whan, M. (2010) Distinct roles of rodent orbitofrontal and medial prefrontal cortex in decision making. Neuron.; 66(3): 449–460.

Hoover, W.B. and Vertes, R.P. (2007) Anatomical analysis of afferent projections to the medial prefrontal cortex in the rat. Brain Struct. Funct. 212, 149–179

Hosokawa, T. and Watanabe, M. (2012) Prefrontal neurons represent winning and losing during competitive video shooting games between monkeys. J. Neurosci. 32, 7662–7671

Hyman J.M., Zilli E.A., Paley A.M., Hasselmo M.E. (2005) Medial prefrontal cortex cells show dynamic modulation with the hippocampal theta rhythm dependent on behavior. Hippocampus, 15, pp. 739–749.

Insel TR, Fernald RD (2004) How the brain processes social information: searching for the social brain. Annu Rev Neurosci 27:697–722.

Jadhav SP, Kemere C, German PW, Frank LM (2012) Awake hippocampal sharp-wave ripples support spatial memory. Science 336:1454–1458.

Jay, T. M., Thierry, A. M., Wiklund, L., & Glowinski, J. (1992). Excitatory amino acid pathway from the hippocampus to the prefrontal cortex: Contribution of AMPA receptors in hippocampo-prefrontal cortex transmission. European Journal of Neuroscience, 4, 1285–1295.

Jay, T.M., and Witter, M.P. (1991). Distribution of hippocampal CA1 and subicular efferents in the prefrontal cortex of the rat studied by means of anterograde transport of Phaseolus vulgaris-leucoagglutinin. J. Comp. Neurol. 313,574–586.

Jones, M. W., & Wilson, M. A. (2005). Theta rhythms coordinate hippocampal– prefrontal interactions in a spatial memory task. PLoSBiol, 3, e402.

Joo HR, Frank LM (2018) The hippocampal sharp wave-ripple in memory retrieval for immediate use and consolidation. Nat Rev Neurosci 19:744–757.

Kaidanovich-Beilin O, Lipina T, Vukobradovic I, Roder J, and Woodgett JR (2011). Assessment of social interaction behaviors. J. Vis. Exp. 48:2473.

Kerth, G, Ebert, C, Schmidkte, C (2006). Group decision making in fission-fusion societies: evidence from two-field experiments in Bechstein's bats. Proc. R. Soc.B. 273, 2785–2790.

Kim Y, Venkataraju KU, Pradhan K, Mende C, Taranda J, Turaga SC, et al. (2015). Mapping social behavior-induced brain activation at cellular resolution in the mouse. Cell Rep. 10, 292–305.

King A (2010) Follow Me! I'm a Leader if You Do; I'm a Failed Initiator if You Don't? Behav Processes. Jul;84(3):671-4.

Kingsbury L, Huang S, Wang J, Gu K, Golshani P, Wu Y, Hong W (2019) Correlated Neural Activity and Encoding of Behavior Across Brains of Socially Interacting Animals. Cell Jul 11;178(2):429-446.e16.

Klausberger, T., & Somogyi, P. (2008). Neuronal diversity and temporal dynamics: The unity of hippocampal circuit operations. Science, 321, 53–57.

Kogan, J. H., Frankland, P. W., and Silva, A. J. (2000). Long-term memory underlying hippocampus-dependent social recognition in mice. Hippocampus 10, 47–56.

Lachlan RF, Crooks L, and Laland KN (1998). Who follows whom? Shoaling preferences and social learning of foraging information in guppies. Anim. Behav. 56, 181–190.

Laland, K. N., and Williams, K. (1997). Shoaling generates social learning of foraging information in guppies. Anim. Behav. 53, 1161–1169.

Larrieu, T., Cherix, A., Duque, A., Rodrigues, J., Lei, H., Gruetter, R., and Sandi, C. (2017). Hierarchical status predicts behavioral vulnerability and nucleus accumbens metabolic profile following chronic social defeat stress. Curr. Biol. 27, 2202–2210.

Lee D, Rushworth MF, Walton ME, Watanabe M, Sakagami M. (2007). Functional specialization of the primate frontal cortex during decision making. J. Neurosci.; 27:8170–8173.

Lindzey G, Winston H, Manosevitz M (1961) Social Dominance in Inbred Mouse Strains. Nature 191:474.

Logothetis N.K., Eschenko O., Murayama Y., Augath M., Steudel T., Evrard H.C. (2012) Hippocampal–cortical interaction during periods of subcortical silence Nature, 491, pp. 547–553.

Lorente de No R (1933) Studies on the structure of the cerebral cortex. I. The area entorhinalis. J Psychol Neurol 45:381-438.

Lukaszewska, I. et al. (1984) Food-motivated behavior in rats with cortico-basomedial amygdala damage. Behav. Neurosci. 98, 441–451

Masquelier T, Hugues E, Deco G, Thorpe SJ (2009) Oscillations, phase-of-firing coding, and spike timing-dependent plasticity: An efficient learning scheme. J Neurosci; 29:13484–93.

Matsumoto M, Matsumoto K, Abe H, Tanaka K (2007) Medial prefrontal cell activity signaling prediction errors of action values. Nat Neurosci 10:647–656.

Mazur A. (1985) A biosocial model of status in face-to-face primate groups. Social Forces. 64(2):377– 402.

McNaughton N, Ruan M, Woodnorth MA (2006) Restoring theta-like rhythmicity in rats restores initial learning in the Morris water maze. Hippocampus; 16:1102–10.

Miller, E. K., & Cohen, J. D. (2001). An integrative theory of prefrontal cortex function. Annual Review of Neuroscience, 24, 167–202.

Mitra, P. P. & Pesaran, B. (1999). Analysis of dynamic brain imaging data. Biophys J 76(2), 691–708.

Mizuseki K, Sirota A, Pastalkova E, Buzsaki G (2009) Theta oscillations provide temporal windows for local circuit computation in the entorhinal-hippocampal loop. Neuron; 64:267–80.

Morgan T., Laland, K (2012). The biological bases of conformity. Front. Neurosci 6:87.

Nakashiba T, Buhl DL, McHugh TJ, Tonegawa S (2009) Hippocampal CA3 output is crucial for ripple-associated reactivation and consolidation of memory. Neuron 62:781–787.

Negrón-Oyarzo I, Espinosa N, Aguilar-Rivera M, et al (2018) Coordinated prefrontal-hippocampal activity and navigation strategy-related prefrontal firing during spatial memory formation. Proc Natl Acad Sci USA 115:7123–7128.

Negrón-Oyarzo I, Neira D, Espinosa N, et al (2015) Prenatal Stress Produces Persistence of Remote Memory and Disrupts Functional Connectivity in the Hippocampal-Prefrontal Cortex Axis. Cereb Cortex 25:3132–3143.

Noack J, Murau R, and Engelmann M (2015). Consequences of temporary inhibition of the medial amygdala on social recognition memory performance in mice. Front. Neurosci. 9:152.

Nogueira R, Abolafia JM, Drugowitsch J, et al (2017) Lateral orbitofrontal cortex anticipates choices and integrates prior with current information. Nat Commun 8:14823.

O'Keefe J., Dostrovsky J. (1971), The hippocampus as a spatial map. Preliminary evidence from unit activity in the freely-moving rat. Brain Research, 34 pp. 171–175.

O'Keefe, J. (1976). Place units in the hippocampus of the freely moving rat. Exp. Neurol., 51, 78–109.

Olton, D. S. (1979). Mazes, maps, and memory. American Psychologist, 34(7), 583–596.

Ongur D, Price JL. (2000). The organization of networks within the orbital and medial prefrontal cortex of rats, monkeys and humans. Cereb Cortex; 10:206–19.

Pan WX, McNaughton N. (1997) The medial supramammillary nucleus, spatial learning and the frequency of hippocampal theta activity. Brain Res; 764:101–8.

Partridge BL (1982) The structure and function of fish schools. Scientific American 246:114–123.

Peigneux, P.; Laureys, S.; Fuchs, S.; Collette, F.; Perrin, F.; Reggers, J.; Phillips, C.; Degueldre, C.; Del Fiore, G.; Aerts, J. (2004). Are spatial memories strengthened in the human hippocampus during slow wave sleep? Neuron, 44, 535–545.

Partridge BL, Pitcher T, Cullen JM, Wilson J (1980) The three-dimensional structure of fish schools. Behav Ecol Sociobiol 6:277–288.

Passetti F, Humby T, Everitt BJ, Robbins TW. (2000). Mixed attentional and executive deficits in medial frontal cortex lesioned rats. Psychobiology; 28:261–71.

Pastalkova, E., Itskov, V., Amarasingham, A., & Buzsaki, G. (2008). Internally generated cell assembly sequences in the rat hippocampus. Science, 321, 1322–1327.

Perouansky M, Rau V, Ford T, Irene S, Perkins M, Eger E, Pearce R (2010) Slowing of the Hippocampal θ Rhythm Correlates with Anesthetic-Induced Amnesia. Anesthesiology Dec;113(6):1299-309.

Peters, J.; D'Esposito, M. (2016). Effects of medial orbitofrontal cortex lesions on self-control in intertemporal choice. Curr. Biol., 26, 2625–2628.

Petit O, Bon R (2010) Decision-making Processes: The Case of Collective Movements. Behav Processes. Jul;84(3):635-47.

Petrides, M., and Pandya, D. N. (1994). "Comparative architectonic analysis of the human and the macaque frontal cortex," in Handbook of Neuropsychology, Vol. 9, Sect. 12: The Frontal Lobes, eds F. Bolder and H. Spinnler (Amsterdam: Elsevier), 17–58.

Peyrache A, Khamassi M, Benchenane K, Wiener, S & Battaglia F (2009). Replay of rule-learning related neural patterns in the prefrontal cortex during sleep. Nat Neurosci 12, 919–926

Peyrache, A., Battaglia, F. P., & Destexhe, A. (2011). Inhibition recruitment in prefrontal cortex during sleep spindles and gating of hippocampal inputs. Proceedings of the National Academy of Sciences of the United States of America,108, 17207–17212.

Place R, Farovik A, Brockmann M, Eichenbaum H (2016). Bidirectional prefrontal–hippocampal interactions support context-guided memory. Nat Neurosci, 19:992-994.

Pratt, S.C. (2005). Quorum sensing by encounter rates in the ant Temnothorax albipennis. Behav. Ecol. 16, 488–496.

Rajasethupathy, P., Sankaran, S., Marshel, J. H., Kim, C. K., Ferenczi, E., Lee, S. Y., et al. (2015). Projections from neocortex mediate top-down control of memory retrieval. Nature 526, 653–659.

Ramon y Cajal S (1893) Estructura de la asta de ammon y fascia dentata. Anal Soc espan Historia natural 22:53-114.

Remondes M, Wilson MA (2015) Slow-γ Rhythms Coordinate Cingulate Cortical Responses to Hippocampal Sharp-Wave Ripples during Wakefulness. Cell Rep 13:1327–1335.

Robbe D, Montgomery SM, Thome A, Rueda-Orozco PE, McNaughton BL, Buzsaki G (2006) Cannabinoids reveal importance of spike timing coordination in hippocampal function. Nat Neurosci; 9:1526–33.

Rose JE, Woolsey CN. (1948) The orbitofrontal cortex and its connections with the mediodorsal nucleus in rabbit, sheep and cat. Res Publ Assoc Nerv Ment Dis; 27:210–32

Rudebeck, P. H., Walton, M. E., Millette, B. H., Shirley, E., Rushworth, M. F., and Bannerman, D. M. (2007). Distinct contributions of frontal areas to emotion and social behaviour in the rat. Eur. J. Neurosci. 26, 2315–2326.

Rudebeck, P.H. et al. (2006) A role for the macaque anterior cingulate gyrus in social valuation. Science 313, 1310–1312

Rushworth MF, Behrens TE. (2008). Choice, uncertainty and value in prefrontal and cingulate cortex. Nat. Neurosci.; 11:389–397.

Sapolsky R, (2005) The Influence of Social Hierarchy on Primate Health. Science 308, 648

Savin-Williams, R.C., (1980). Dominance hierarchies in groups of middle to late adolescent males. J. Youth Adolesc. 9, 75–85.

Schjelderup-Ebbe T (1922). Beitrage zur Sozialpsycholgie des Haushuhns. Zeitschrift Psychol. 88, 225–252.

Scoville, W.B.; Milner, B. (1957). Loss of recent memory after bilateral hippocampal lesions. J. Neurol. Neurosurg. Psychiatry, 20, 11–21.

Seeley T (2003). Consensus building during nest-site selection in honeybee swarms: the expiration of dissent. Behav. Ecol. Sociobiol. 53, 417–424.

Shemesh Y, Sztainberg Y, Forkosh O, et al (2013) High-order social interactions in groups of mice. Elife 2: e00759.

Siapas AG, Lubenov EV, Wilson MA (2005) Prefrontal phase locking to hippocampal theta oscillations. Neuron; 46:141–51.

Siapas AG, Wilson MA (1998) Coordinated interactions between hippocampal ripples and cortical spindles during slow-wave sleep. Neuron 21:1123–1128

Singer AC, Carr MF, Karlsson MP, Frank LM (2013). Hippocampal SWR activity predicts correct decisions during the initial learning of an alternation task. Neuron, 77:1163-1173.

Stumper, D (2006) The Principles of Collective Animal Behaviour. Philos Trans R Soc Lond B Biol Sci Jan 29;361(1465):5-22.

Sul J, Kim H, Huh N, Lee D, Jung M (2017) Distinct Roles of Rodent Orbitofrontal and Medial Prefrontal Cortex in Decision Making. Neuron May 13;66(3):449-60.

Sullivan D, Csicsvari J, Mizuseki K, Montgomery S, Diba K, Buzsáki G (2011) Relationships between hippocampal sharp waves, ripples, and fast gamma oscillation: influence of dentate and entorhinal cortical activity. J Neurosci 31:8605–8616.

Takita, M., Fujiwara, S. E., & Izaki, Y. (2013). Functional structure of the intermediate and ventral hippocampo-prefrontal pathway in the prefrontal convergent system. Journal of Physiology – Paris, 107, 441–447.

Tolman EC. (1948) Cognitive maps in rats and men Psychological Review, 55, pp. 189–208.

Torquet N, Marti F, Campart C, et al (2018) Social interactions impact on the dopaminergic system and drive individuality. Nat Commun 9:3081.

Tsao, D.M. (2006). A cortical region consisting entirely of face-selective cells Science, 311, pp. 670-674

Uylings HBM, van Eden CG. (1990) Qualitative and quantitative comparison of the prefrontal cortex in rat and in primates, including humans. Prog Brain Res; 85:31–62.

Vaidya, A.R.; Fellows, L.K. (2015). Ventromedial frontal cortex is critical for guiding attention to reward-predictive visual features in humans. J. Neurosci., 35, 12813–12823.

Van den Bos R, Jolles J, Homberg J (2013). Social Modulation of Decision-Making: A Cross-Species Review. Front Hum Neurosci. Jun 26; 7:301.

Vertes RP (2002). Analysis of projections from the medial prefrontal cortex to the thalamus in the rat, with emphasis on nucleus reuniens. J Comp Neurol. Jan 7;442(2):163-87.

Vertes RP (2004) Differential projections of the infralimbic and prelimbic cortex in the rat. Synapse 51:32-58.

Vertes, R.P., Hoover, W.B., Szigeti-Buck, K., and Leranth, C. (2007). Nucleus reuniens of the midline thalamus: link between the medial prefrontal cortex and the hippocampus. Brain Res. Bull. 71, 601–609.

Wallis JD. (2007). Orbitofrontal cortex and its contribution to decision-making. Annu. Rev. Neurosci.

Wang F, Kessels HW, Hu H (2014) The mouse that roared: neural mechanisms of social hierarchy. Trends Neurosci 37:674–682.

Wang F, Zhu J, Zhu H, et al. (2011) Bidirectional control of social hierarchy by synaptic efficacy in the medial prefrontal cortex. Science 334:693–697.

Warden, M.R. et al. (2012) A prefrontal cortex-brainstem neuronal projection that controls response to behavioural challenge. Nature 492, 428–432.

Watson C, Paxinos G, Puelles L. (2012) The mouse nervous system. Academic Press. San Diego, CA, USA. –1039.

Wiegand JP, Gray D, Schimanski L, Lipa P, Barnes CA, Cowen SL (2016) Age Is Associated with Reduced Sharp-Wave Ripple Frequency and Altered Patterns of Neuronal Variability. Journal of Neuroscience 18 May, 36 (20) 5650-5660.

Wierzynski, C. M., Lubenov, E. V., Gu, M., & Siapas, A. G. (2009). State-dependent spike-timing relationships between hippocampal and prefrontal circuits during sleep. Neuron, 61, 587–596.

Williamson, C. M., Lee, W., Romeo, R. D. & Curley, J. P. (2017). Social context-dependent relationships between mouse dominance rank and plasma hormone levels. Physiology & Behavior 171, 110–119.

Wilson MA, McNaughton BL (1994). Reactivation of hippocampal ensemble memories during sleep. Science, 265, pp. 676–679.

Winson, J (1972). Interspecies differences in the occurrence of theta. Behav. Biol. 7, 479–487.

Wu X, Foster DJ (2014). Hippocampal replay captures the unique topological structure of a novel environment. J Neurosci 34:6459–6469.

Yizhar O, Fenno LE, Prigge M, Schneider F, Davidson TJ, O'Shea DJ. (2011). Neocortical excitation/inhibition balance in information processing and social dysfunction. Nature; 477:171–8.

Ylinen A, Bragin A, Nádasdy Z, et al. (1995). Sharp wave-associated high-frequency oscillation (200 Hz) in the intact hippocampus: network and intracellular mechanisms. J Neurosci 15:30–46.

Yoshida, W. (2010). Neural mechanisms of belief inference during cooperative games J Neurosci, 30, pp. 10744-10751

Yu JY, Frank LM (2015) Hippocampal-cortical interaction in decision making. Neurobiol Learn Mem 117:34–41.

Zemla, R.; and Basu, J. (2017). Hippocampal function in rodents. Curr Opin Neurobiol. Apr; 43: 187–197.

Zhou T, Zhu H, Fan Z, et al (2017). History of winning remodels thalamo-PFC circuit to reinforce social dominance. Science 357:162–168.

Zink, C.F. et al. (2008). Know your place: neural processing of social hierarchy in humans. Neuron 58, 273–283.

Zola-Morgan, S.; Squire, L.R.; Amaral, D.G. (1986). Human amnesia and the medial temporal region: Enduring memory impairment following a bilateral lesion limited to field CA1 of the hippocampus. J. Neurosci.,6, 2950–2967.

SUPPLEMENTAL FIGURES

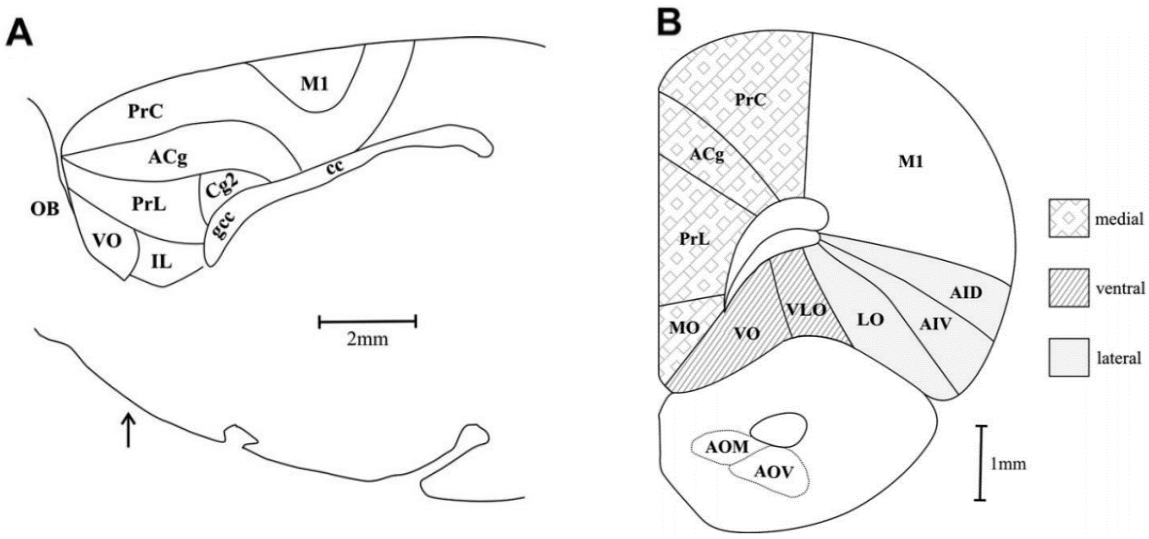

Figure S1. Map of the approximate boundaries of the regions of the frontal cortex of the rat. ***(A)*** *Lateral view, 0.9 mm from the midline.* ***(B)*** *Unilateral coronal section, approximately 3.5 mm forward of bregma (depicted by the arrow above). The different shadings represent the three major subdivisions of the prefrontal cortex (medial, ventral, and lateral). Abbreviations: ACg, anterior cingulate cortex; AID, dorsal agranular insular cortex; AIV, ventral agranular insular cortex; AOM, medial anterior olfactory nucleus; AOV, ventral anterior olfactory nucleus; cc, corpus callosum; Cg2, cingulate cortex area 2; gcc, genu of the corpus callosum; IL, infralimbic cortex; LO, lateral orbital cortex; M1, primary motor area; MO, medial orbital cortex; OB, olfactory bulb; PrL, prelimbic cortex; PrC, precentral cortex; VLO, ventrolateral orbital cortex; VO, ventral orbital cortex. Taken from Dalley JW et al., Neurosci Biobehav Rev. 2004 Nov;28(7):771-84.*

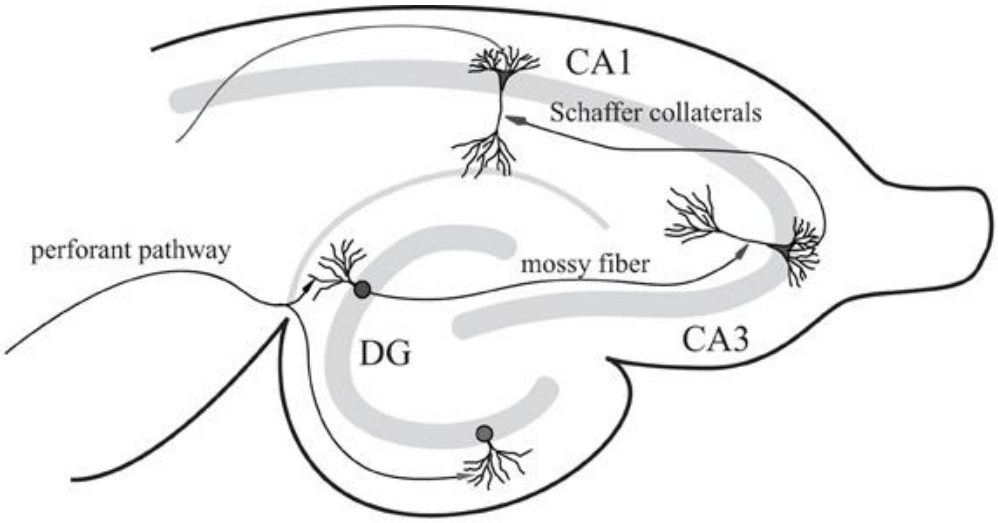

Figure S2. A rat hippocampal slice and its major intrinsic pathways. *The input signals from perforant path fibers excite dentate granule cells. Dentate output, in turn, excites CA3 pyramidal cells through mossy fibers. The output from CA3 is transmitted to CA1 pyramidal cells through Schaffer collaterals. This so-called "trisynaptic pathway" is the major network involved in hippocampal neuronal information processing. Taken from Hsiao et al., Front Neural Circuits. 2013 Feb 20;7:20.*

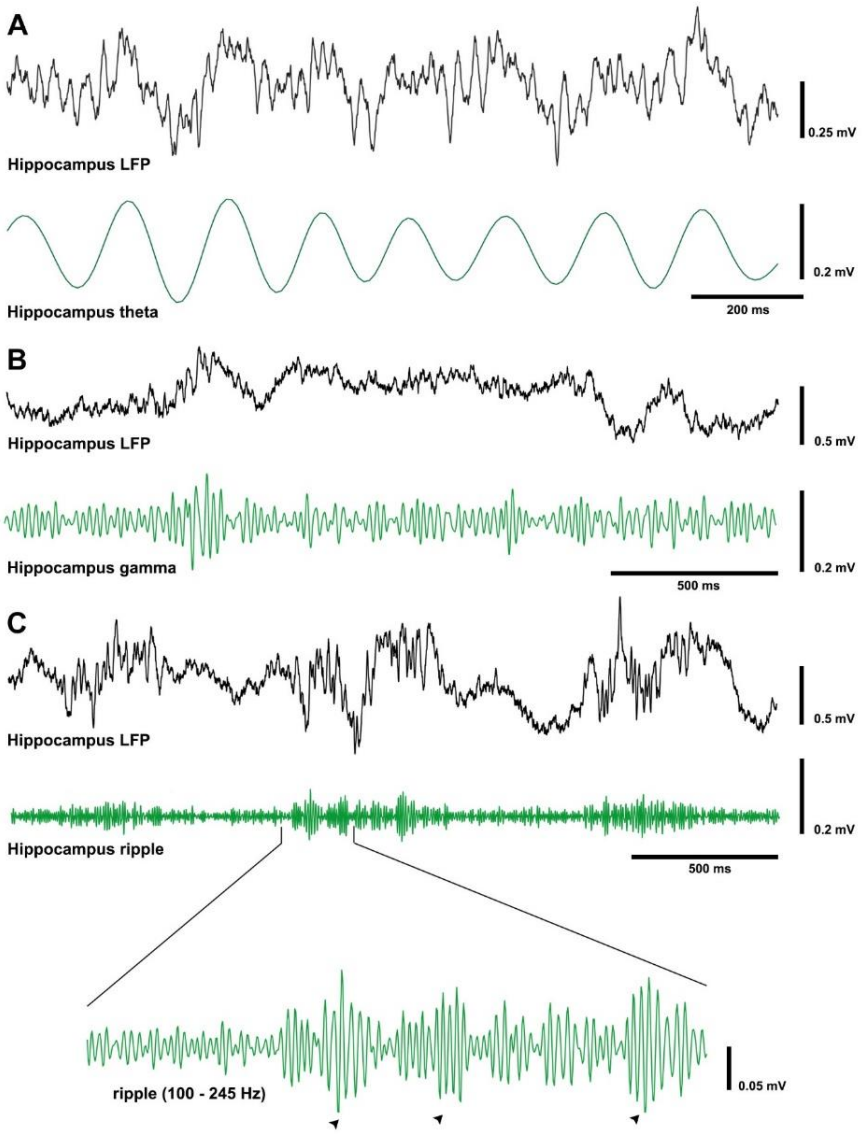

Figure S3. Representative recordings of local field potential (LFP, 0.3-2 kHz) and filtered traces*. (A) Acute theta recordings were acquired from the dorsal CA1 stratum pyramidale, note that filtered recording showed theta rhythm (green line). (B) Acute gamma recordings were acquired from the dorsal CA1 stratum pyramidale, note the filtered recording showed high-amplitude periods of gamma rhythm (green line). (C) Acute ripple recordings were acquired from the dorsal CA1 stratum pyramidale, note the filtered recording showed sharp-wave ripples (were evident in the hippocampal CA1 pyramidal layer (green lines in the inset at the bottom). All records are taken from the Laboratory of Neural Circuits database.*

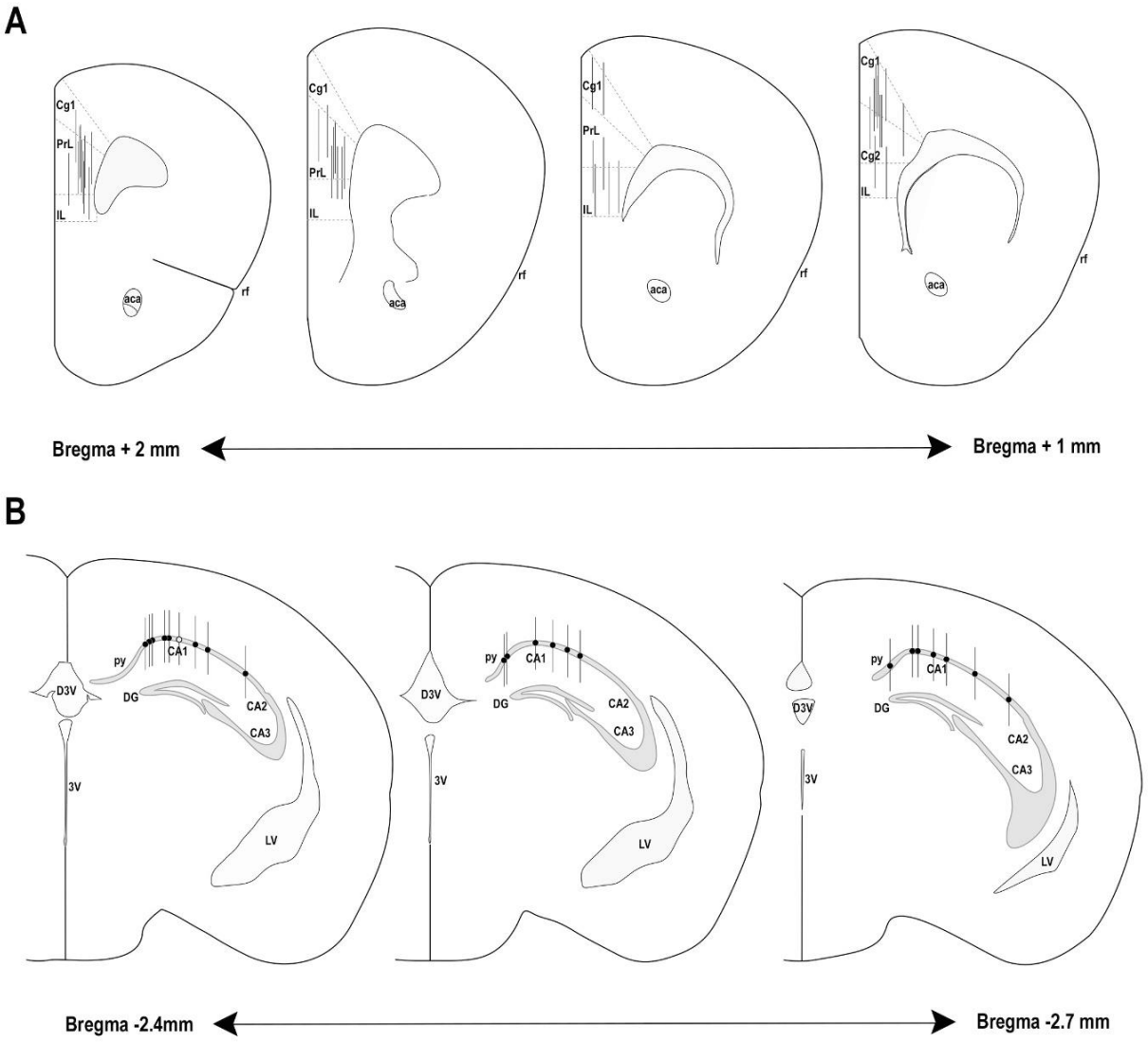

Figure S4. Schematic of coronal sections drawings made from the stereotaxic mouse brain atlas from Paxinos and Watson (1986) at the indicated distances (in millimeters) from the bregma*. Black lines represent the simultaneously recording sites in the PFC and CA1 hippocampus, respectively.*

SUPPLEMENTAL FIGURES

	perf ind	perf coll	lat ind	lat coll	thet a amp	theta fq	theta coh	ripple s amp	ripple s fq	cc peak-ripple	cc post-ripple	firin g fq	pyr fq	int fq	PP C	PSI
perf ind		e-5	0.01	e-3	0.16	0.14	0.64	0.85	0.97	0.39	0.03	0.68	0.65	0.50	0.53	0.18
perf coll	e-5		0.49	e-3	0.39	0.58	0.70	0.43	0.24	0.45	0.67	0.19	0.17	0.68	0.63	0.97
lat ind	0.01	0.49		e-5	0.05	0.01	0.99	0.94	0.93	0.58	e-3	0.39	0.48	e-3	0.78	0.07
lat coll	e-3	e-3	e-5		0.04	0.03	0.87	0.82	0.41	0.15	0.19	0.55	0.42	0.16	0.96	0.43
theta amp	0.16	0.39	0.05	0.04		0.29	0.16	0.02	0.22	0.71	0.14	0.71	0.76	0.05	0.56	0.84
theta fq	0.14	0.58	0.01	0.03	0.29		0.39	0.79	0.12	0.54	e-3	0.93	0.75	0.29	0.06	0.08
theta coh	0.64	0.70	0.99	0.87	0.16	0.39		0.59	0.03	0.86	0.63	0.53	0.81	0.06	0.49	0.74
ripples amp	0.85	0.43	0.94	0.82	0.02	0.79	0.59		0.03	0.77	0.67	0.82	0.42	0.82	0.83	0.62
ripples fq	0.97	0.24	0.93	0.41	0.22	0.12	0.03	0.03		0.46	0.95	0.89	0.37	0.78	0.68	0.92
cc pk-ripple	0.39	0.45	0.58	0.15	0.71	0.54	0.86	0.77	0.46		0.24	0.13	0.10	0.51	0.45	0.87
cc post-ripple	0.03	0.67	e-3	0.19	0.14	e-3	0.63	0.67	0.95	0.24		0.57	0.68	0.09	0.44	e-3
firing fq	0.68	0.19	0.39	0.55	0.71	0.93	0.53	0.82	0.89	0.13	0.57		e-15	e-3	0.63	0.08
pyr fq	0.65	0.17	0.48	0.42	0.76	0.75	0.81	0.42	0.37	0.10	0.68	e-15		0.01	0.78	0.78
int fq	0.50	0.68	e-3	0.16	0.05	0.29	0.06	0.82	0.78	0.51	0.09	e-3	0.01		0.51	0.09
PPC	0.53	0.63	0.78	0.96	0.56	0.06	0.49	0.83	0.68	0.45	0.44	0.63	0.78	0.51		0.13
PSI	0.18	0.97	0.07	0.43	0.84	0.08	0.74	0.62	0.92	0.87	e-3	0.08	0.78	0.09	0.13	

Table S1. P-values of linear regressions between pairs of neural and behavioral parameters*. Yellow squares show significant correlations, P < 0.05.* ***Abbreviations****: Performance in individual trials, perf ind; performance in collective trials, perf coll; latency in individual trials, lat ind; latency in collective trials, lat coll; theta oscillation amplitude, theta amp; theta oscillation frequency, theta fq; theta oscillation coherence, theta coh; sharp-wave ripples amplitude, ripple amp; sharp-wave ripples frequency, ripple fq; cross correlogram peak amplitude, cc pk-ripple; cross correlogram post-ripple amplitude, cc post-ripple; neuronal firing rate; firing fq; pyramidal neurons firing rate,*

pyr fq; interneurons firing rate; int fq; pairwise phase consistency, PPC; peer sensitivity index, PSI. 10e-3, e-3; 10e-5, e-5; 10e-15, e-15.

parameter	SS	F	p
Intercept	10187.48	1169.875	*0.000000*
PFC area	15.66	1.799	0.179932
neuron type	325.64	37.395	*0.000000*
hierarchy	93.78	3.590	*0.013127*
PFC area*neuron type	20.00	2.297	0.129738
PFC area* hierarchy	64.68	2.476	0.059632
neuron type* hierarchy	40.71	1.558	0.197450
PFC area*neuron type* hierarchy	64.79	2.480	0.059302

Table S2. Univariate tests of significance for firing rate *(n = 22 animals used for acute recordings).* ***Abbreviations:*** *SS, sum of squares; F, F-statistic; p, p-value; PFC area (dorsal or ventral prefrontal cortex); neuron type (fast spiking or regular spiking cells); hierarchy (dominant, first active subordinate , second active subordinate and submissive).*

Figure	Test	Condition	Statistic	P
4B	Wilcoxon signed rank test	performance	Zval = 5.5584	2.72E-08
5B	Wilcoxon signed rank test	latency	Zval = -5.0317	4.86E-07
6A	Spearman correlation	latency(diff.)/performance (diff.)	r2 = 0.642	6.80E-14
6B	Spearman correlation	latency (individual)/latency (collective)	r2 = 0.508	4.40E-11
7	Pearson correlation	performance (individual)/performance (collective)	r2 = 0.582	1.45E-14
8	Spearman correlation	animal density selected arm/collective performance	r2 = 0.252	1.60E-04
9	Spearman correlation	animal density opp. arm /collective performance	r2 = 0.019	0.293
10B	one-way ANOVA	time in tube	F(5,84) = 20.58	2.31E-13
12A	one-way ANOVA	initial body mass	F(3,56) = 0.31	0.8216
12B	one-way ANOVA	final body mass	F(3,56) = 0.54	0.6554
12C	one-way ANOVA	% of body weight change	F(3,56) = 0.01	0.983
14C	Kruskal-Wallis test	days to criterion	Chi-sq = 2.59	0.4585
14D	Kruskal-Wallis test	latency at criterion	Chi-sq = 0.3	0.9609
16A	one-way ANOVA	performance (coll.-ind.)	F(3,56) = 0.54	0.6552
16B	one-way ANOVA	latency (coll.-ind.)	F(3,56) = 0.68	0.5662
17A	one-way ANOVA	animal density (selected arm)	F(3,580) = 4.11	0.007
17B	one-way ANOVA	animal density (opposite arm)	F(3,56) = 0.89	0.4499

17C	one-way ANOVA	animal density (opposite+ selected arm)	F(3,56) = 1.7	0.1783
18	one-way ANOVA	Latency DP	F(3,56) =0.39	0.275
19	one-way ANOVA	PSI	F(3,56) = 4.3	0.0084
21B	one-way ANOVA	delta power	F(3,155) = 2.29	0.081
22C	one-way ANOVA	mean firing rate (fast spiking)	F(3,316) = 0.59	0.6243
22D	one-way ANOVA	mean firing rate (regular spiking)	F(3,3378) = 18.57	6.07E-12
23A	one-way ANOVA	mean firing rate (all neurons)	F(3,3698) = 17.03	5.56E-11
23B	Pearson correlation	latency (time in interaction tube)/diff firing rate	r2 = 0.226	0.0142
24A	Pearson correlation	latency (time in tube)/diff. fast spiking rate	r2 = 0.106	0.13
24B	Pearson correlation	latency (time in tube)/diff. regular spiking rate	r2 = 0.178	0.032
25C	one-way ANOVA	theta power	F(3,131) = 1.03	0.3811
25E	one-way ANOVA	theta coherence	F(3,139) = 1.1	0.35
25G	one-way ANOVA	PPC	F(3,73) = 1.89	0.1387
26A	one-way ANOVA	theta frequency	F(3,155) = 2.63	0.0524
26B	one-way ANOVA	theta periods	F(3,155) = 2.13	0.0987
27C	one-way ANOVA	ripple amplitude	F(3,18567) = 27.59	8.55E-18
27D	one-way ANOVA	duration of ripples	F(3,18567) = 2.4	0.0658
27E	one-way ANOVA	ripple frequency	F(3,18567) = 59.06	5.45E-38
28C	one-way ANOVA	Amplitude crosscrorr. Peak (shuff.)	F(3,654) = 4.92	0.002

28D	one-way ANOVA	Amplitude crosscrorr. Plateau (shuff.)	F(3,654) = 11.37	2.81E-07
30C	one-way ANOVA	Amplitude crosscrorr. Plateau (raw)	F(3,3698) = 74.59	7.71E-47
30D	one-way ANOVA	inter ripple interval	F(3,19992) = 0.59	0.6193
31A	Pearson correlation	amplitude peak/ ind. performance	r2 = 0.235	0.026
31B	Pearson correlation	amplitude peak/ ind. Latency	r2 = 0.404	0.0019
32	Pearson correlation	amplitude plateau/ PSI	r2 = 0.328	0.00666
33A	Pearson correlation	performance/rate	r2 = 0.116	0.121
33B	Pearson correlation	latency/rate	r2 = 0.246	0.019
34A	Pearson correlation	fast spiking/rate	r2 = 0.087	0.087
34B	Pearson correlation	regular spiking/rate	r2 = 0.269	0.013

Table S3. Summary of statistical tests per figure